UNIVERSITÀ
DI PARMA

DOCTORAL PROGRAMME IN CHEMICAL SCIENCES

XXXIII Cycle

Supported sulphonic acids as catalysts for eco-compatible syntheses and carbon utilization

Coordinator:
Prof. Alessia Bacchi

Supervisor:
Prof. Raimondo Maggi

PhD student: Francesco Pancrazzi

2017/2020

“All we have to decide is

what to do with the time that is given us.”

J.R.R Tolkien

Index

1) Green chemistry

1.1 Introduction

In order to prevent pollution production and according to increasing regulations for global warming, in recent years, a great revision of the older processes for fine chemical and pharmaceutical synthesis occurred in order to make them safer and cleaner. This global trend is known today as "Green Chemistry" [1-3] and involves a radical shift from the traditional concepts concerning chemical process based on chemical yield to something new, able to assign a new worth based on waste production prevention, economic value and avoid utilization of toxic and hazardous chemicals. High chemo-, regio- and stereoselectivity single step procedures and the solvent free reactions are achievements to reach for a novel process.

"Green Chemistry efficiently utilizes (preferably renewable) raw materials, eliminates waste and avoids the use of toxic and/or hazardous reagents and solvents in the manufacture and application of chemical products"

Sustainable technology is the synonym used by chemical industry and well represented by the following definition [4]:

"meeting the needs of the present generation without compromising the ability of future generations to meet their own needs"

Following the principles of Green Chemistry, organic chemists have to use and develop new methodologies. In this thesis the utilization of heterogeneous catalysis represents the main tool to follow the described pathway together with the use of green wastes such as CO and CO_2.

1.2 Heterogeneous catalysis

Catalysis represents undoubtedly a powerful means to reach good sustainability required for a chemical process [5] and the heterogeneous catalysis has undoubtedly some improvements over the homogenous one [6].
However, a heterogeneous catalyst should meet some requisites to be used practically:

- easy to prepare;
- comparable to his homogeneous homologue;
- easy to separate;
- should not leach;
- should be reusable;
- stable at operative temperature;

The heterogeneous catalyst action always passes through the following steps: (**Figure 1**):

1) The diffusion of reagents on the surface of the catalyst. The rate is dependent from viscosity and flow of the system. Surface is the real site where reagents come into contact with each other;
2) The diffusion inside the pores. The pore size becomes the main factor when working with large molecules;
3) The physical adsorption of reagents on the surface of the catalyst. Van der Waals forces established between the surface and the reagents that must be reversible, driven this step;
4) The chemical reagent adsorption on surface of the catalyst. It consists in bonds formation between reagents and the catalyst's surface; new bonds have to be strong enough to prevent desorption but not strong enough to inhibit the reaction;

6) Reaction. In this step, the real product formation takes place;
7) Desorption of products. This is the main step that allows the regeneration of the catalyst [7].

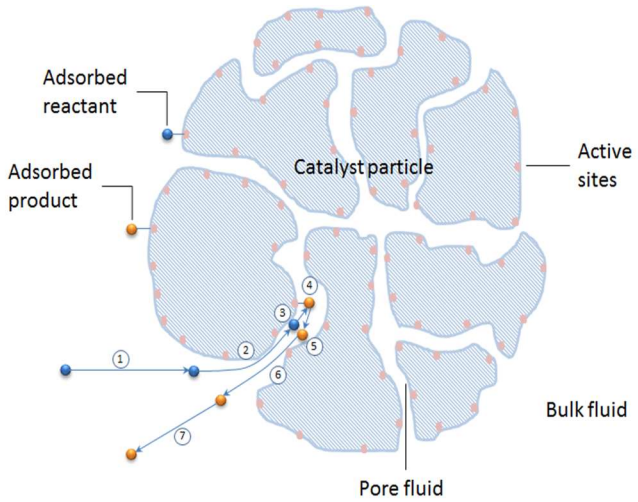

Figure 1.

In heterogeneous catalysis, the reagent diffusion through surface and product desorption from surface represent the determining step because they represent the rate of frequency contact. The catalyst's amount and its activity determine the rates of contacts. In recent years, two different strategies have been applied to prepare heterogeneous catalysts, namely the heterogenization of inorganic oxides and the preparation of polymer-supported catalysts [8-9]. It's worth to notice that, in recent years, the field of cross-linked polymer supports grew up together with the development of microporous materials with a rigid porous matrix [10]. Some molded mesoporous materials with attractive properties for catalysis as well for asymmetric synthesis are reported in literature. [11]

Conversely, inorganic oxides display some strong points: easier handling, higher mechanical resistance, and a broader range of tolerable solvents.
These characteristics gather selectivity and versatility of homogeneous catalysts together with the strengths of solid ones such as the easy catalyst recovery by filtration from reaction mixture, the possibility of recycling, and the tolerance to the utilization of a great variety of reaction parameters [12].
Nevertheless, the designing and crafting of the ideal support remains a great challenge for today processes due to difficulties that have to be overcome; practically speaking, the heterogenization always involves a decreasing in activity and stereoselectivity compared to the homogeneous catalyst; in addition, solid supporting limits the reactants diffusion leading to lower reaction rates. The main focus of this work is about the immobilization of homogeneous dispersion of perfluorinated sulphonic acid resin and sulphonic acid pendants onto solid supports and the synthesis of different supports and acid pendants to study the effect of Bronsted and Lewis acidity in flow process for dehydration of methanol to dimethyl ether (DME).

1.3 Supported catalysts

The researchers have taken different routes in recent year, to perform the catalyst heterogenization on different supports. There are many qualities that a supported catalyst should own to implement advantages of homogeneous catalysts and heterogeneous ones [13] in the same material.
Anyway, the aim to create the ideal support did not yet accomplish due to many problems related to this technology, *i.e.* the above-mentioned loss of activity shifting from a homogeneous catalyst to a heterogeneous one.

The matrix effect causes not only lower activity problems but lower selectivity too; the support surface, in fact, plays an important role and can have an effect on the outcome of a reaction. Silica represents a typical example of support: its polar groups present on the surface easily interact through hydrogen bonds formation with the most of organic polar functions or metal ions and this outcome can modify reactants orientation with respect to the catalyst.

Behind this, supports created with an organic polymer own a lower porosity, and this force the catalyst not to assume the optimal configuration.

Recyclability, of course, is one of the most important feature a solid supported catalyst should have but, nowadays, there are some problem as the damage that catalyst can suffer during a reaction or the possibility to suffer from a partial leaching of active species of the catalyst that could involve a partial deactivation of the catalyst. On other point of view, the supporting operation can improve characteristics of catalyst by eliminating aggregation and dimerization effect that represent the main causes of deactivations for homogeneous catalysts.

Indeed, the key concept for the better performing of heterogeneous catalysis is the "site isolation" that requires to graft catalyst onto a support so that catalytic sites aren't allowed to interact each other [14].

In order to overcome the described drawbacks a pondered catalyst design together with the choice of an appropriate support is undoubtedly required.

1.3.1 The anchoring methodologies

There are mostly three different approaches described in the literature, for catalyst heterogenization [15] (**Figure 2**)

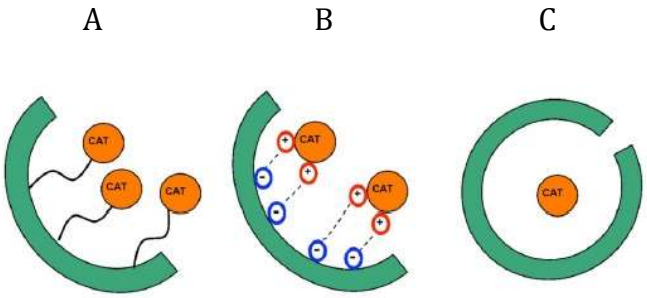

Figure 2. Grafting methodologies through: A) covalent bound; B) adsorption; C) entrapment

- *Covalent bound* (figure 2a)

Covalent binding represents undoubtedly the most utilized strategy; it can be done either by copolymerization of appropriate functionalized catalysts together with a suitable monomer, or anchoring catalysts and/or ligands bearing reactive groups to a premade surface [15]. Following the described paths, it is possible to synthesize organic/inorganic materials (mixed gels and organic moieties grafted onto inorganic supports) and organic materials (polymeric materials) [17- 18].

Some specific examples of covalent anchoring will be underlined in the following chapters.

The inner complexity of heterogeneous catalysts over the homogeneous ones makes that many additional parameters have to be evaluated to achieve a good catalytic performance such as. spacer length, spacer flexibility, support type, porosity and surface area.

- *Heterogenization via adsorption* (figure 2b)

  This approach is based on various absorptive interactions between carrier and catalyst (usually a metal complex) [19-20].
  This methodology has some practical limitations connected with the impossibility of avoid leaching of the active species in the solution phase with consequent impossibility to recycle the catalyst.

- *Heterogenization via entrapment* (figure 2c)

  In this kind of methodology, the size of catalyst plays the main role compared to a specific adsorptive interaction. Mainly, there are two different strategies:[21-22] the first strategy, the so called "ship in the bottle" approach, consists in building up catalysts in premade cages of porous supports; the other approach is about growing up an inorganic sol-gel or an organic polymeric network around a preformed catalyst. However, the entrapped catalysts obtained with this methodology are much less active than the homogeneous ones.

1.3.2 Solid supports

The interest in the role of the support for heterogeneous catalysts has increased through the years and many researchers all over the world have investigated a huge variety of solid supports that may be mainly divided in two different classes: organic polymers and inorganic materials.

- *Inorganic materials*

  Three are the main subclasses in which we can divide inorganic supports used for heterogeneous catalysts preparation: a) amorphous materials such as alumina and silica b) mesoporous materials such as MCM41 and various mesoporous silicas and c) crystalline materials such as zeolites

Amorphous silica

Amorphous silica is characterized by non-ordered structure due to irregular channels and pores that are different from a support to another; on the other side they are readily available and really cheap. Due to the irregular pore-size of the support, the active phase can penetrate into the smaller pores during supporting procedure and can make them harder to reach for reactants.

Synthetic mesoporous silicas (MCM-41)

Ordered mesoporous aluminosilicates are usually synthesized using a surfactant micelle template and for this reason they possess uniform channels with modular diameters. MCM-41[23-25] is the most known and widely used material among Mobil M41S family materials with tunable diameters (1.5-10 nm). M41S family is composed by three types of materials characterized by an high surface area (more than 700 m^2/g) and are different from each other due to the spatial mesoporous organization: MCM-41 in which a mono-dimensional scaffold of hexagonal channels is present, MCM-48 composed of a 3d scaffold of cubic channels and MCM-50 characterized by a lamellar organization of channels.

As already mentioned, MCM-41 is undoubtedly the most studied and used catalyst from the M41S family. MCM-41 has a high surface area and pore volume that allow reactants to easily diffuse into the catalyst to the catalytic sites; bulk catalyst lies in the mesopores (typically in the range of 3-6 nm depending on synthetic parameters) and well isolated catalytic site can be produced.
MCM-41 has a "so called" long range ordered structure even if, at microscopic level, does not have a short-range order and is amorphous.
Besides M41S family it is important to mention another class of mesoporous aluminosilicates material. Zeolites are all composed by a basic structure (aluminosilicate framework) comprising of a tetrahedral arrangement of siliceous Si^{4+} and aluminum Al^{3+} cations surrounded by four oxygen anion O^{2-}. Starting from natural zeolites these compounds exhibited a huge variety of different applications due to the possibility of modulate the inner surface of the material [26].

- *Organic Polymers*

There are three kind of organic polymers used as supports for heterogeneous catalysts for different applications (**table 1)** [27-28]: soluble polymers such as polyethers, cross-linked insoluble polymers like PEG and macro reticulated resins like styrene-divinylbenzene.

Polymeric support	Format	Loading level (mmol/g)	Applications
Poly (styrene-*co*-maleic anhydride)	soluble	1.0-1.5	solid-phase synthesis and catalyst immobilization
polyacrylate	soluble	02.-0.5	catalyst immobilization

polyacrylamide	linear	0.2	Pd catalyst and organo catalyst immobilization
Poly-(N-vinylimidazole)	soluble	10.6	Pd catalyst immobilization
polyglycerol	soluble	5.0-14.0	catalyst immobilization
Polystyrene	Insoluble large uniform beads	1.0-1.5	solid-phase synthesis
Polynorbornene	Insoluble monolith	0.7-1.5	metal catalyst immobilization
Poly (ethylene glycol)	Insoluble core-shell	0.1-0.4	solid-phase peptide synthesis

Table 1 utilization of different organic polymers used as support

1.4 PFSA

Sulphonic group came out to be a very active acid catalyst for organic reactions. Recent studies, starting from the need to avoid the use of mineral acid such as hydrochloric acid and sulphuric acid, developed several new eco-friendly materials.

Among these material, perfluorosulphonic resins bearing sulphonic acid groups on the main chain have a special role in development of supported acid catalysts. Several examples for this class of materials, commonly called (PerFluoroSulphonic Acids) PFSAs, are nowadays available on market.

The older one is Nafion that is commercialized since 1970 by DuPont; it is a random copolymer of a semicrystalline backbone and a randomly tethered chain with SO_3^- moiety and it's one of the so-called long side chain PFSA. On the contrary, Aquivion, a more recent PFSA produced by Solvay, is commonly classified as a short side chain PFSA.[29]

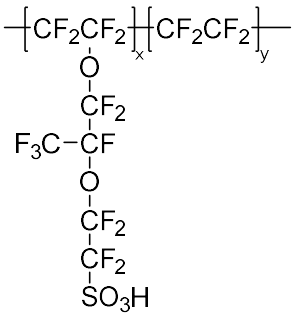

Nafion

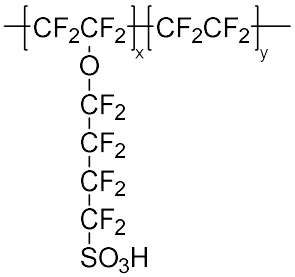

3M

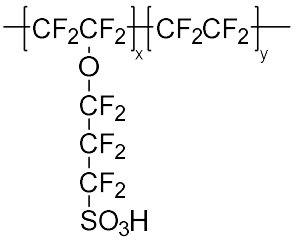

Ashai

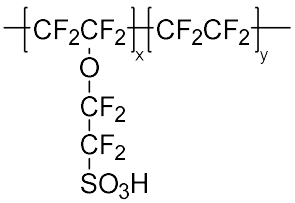

Aquivion

The applications of Nafion are as exchangeable membrane [30] in fuel cells but its catalytic properties as acid catalyst are well known and used in various reactions [31], moreover it is also used as metal support [32].

All these materials have a crystalline part (tetrafluoroethylene chain) and an amorphous part (sulphonic pendant).

Aquivion is the latest arrival on market and it is the PFSA with the shorter aliphatic chain (-O-CF_2-CF_2-), and it is mainly used in fuel cells as membrane exchanger.

Aquivion and Nafion are similar to each other but there are some differences, which cause a change in their performances; their acidity is about the same but, due to the shorter side chain, Aquivion has a higher loading in acidic sites (1.47 mmol/g for Aquivion PW66S *vs* 0.8mmol/g for Nafion).

Furthermore, Aquivion has a glass transition point higher than those of Nafion; this allows Aquivion to be used at higher temperature (T_g Aquivion is at 140 °C, 40% more than those of Nafion).

In addition, Aquivion has better mechanical and chemical properties due to the shorter chain with organic moieties (less solvent swelling, lower leaching of the active species and increased friction resistance).

1.5 Sol-Gel process

The sol-gel process is a powerful tool of "soft chemistry"; it has several technological applications [33-34] from culture media in biochemistry to hybrid organic/inorganic support material.
In this PhD thesis most of the catalysts have been prepared by employing this methodology for support synthesis.

1.5.1 General considerations about the Sol-Gel process

- *Basic chemical reactions*

In sol-gel process, at room or moderately low temperature a network made of an oxide is formed through inorganic polymerizations [35-36]. Both crystalline (quartz) and amorphous (glass) materials can be prepared regulating the macromolecular structures. The most used precursors as metal-organic components are the alkoxides $M(OR)_n$ (M is a metal and R is generically an alkyl group) and among those TEOS (tetraethyl orthosilicate) is widely used for synthesis of glasses and silicas with sol-gel methodology. The above-mentioned chemicals must usually be dispersed into water or an organic solvent and react following well-known polymerization steps:

- *Initiation*

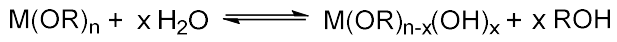

The principal reactive bond M-OH is formed in this step.

- *Propagation*

Hydrolyzed species start the condensation leading to the bridging oxygen formation following two possible paths:

<u>oxolation</u>, corresponding to a dehydration (H_2O is the leaving group)

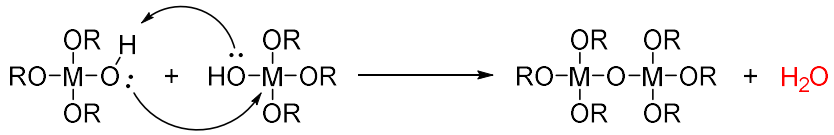

or <u>alcoxalation</u>, corresponding to a dealcoholation (ROH is the leaving group)

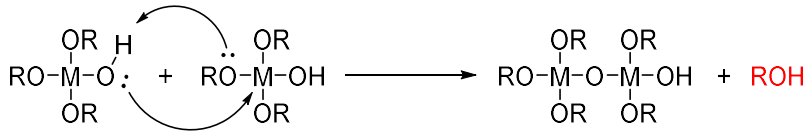

1.5.2 <u>Sol-Gel transition</u>

Starting from the initial solution to the final solid, several steps occur in which Sol (colloidal suspension of particles in liquid) or Gel (a semisolid system in which two phases, solid and liquid, are present) are formed.

The precursor polycondensation proceeds increasing the size of the Sol formed particles to form clusters. With the proceeding of reaction, the crude becomes a Gel in which the pores of the solid material are of colloidal size.

All the process comes with the increase of viscosity (η) during the reaction.

The obtained Gel hardens as residual isolated clusters encounter the increasing network (this phenomenon is called Aging).
The Aging step is necessary to obtain, for Gel, the feature to dry with lowest possible number of cracks.

1.5.3 Drying the Gel

The so formed alcoholgel still needs of a thermal treatment through which is possible to obtain various materials.
Solvent can be removed with two different methods:

1) *Evaporation*. Drying by evaporation of the liquids present in the pores rise to capillary pressure that involves shrinkage of the so formed Gel network; the resulting Gel is called Xerogel and its volume compared to the original wet Gel is from 5 to 10 times lower. The evaporation process usually destroys the monolithic body of the gel and thus obtain a powder.

2) *Supercritical evacuation*. The typical supercritical evacuation takes place in an autoclave placed with temperature and pressure higher than Tc and Pc. Under these conditions, it is possible to avoid capillary stresses, in presence of a supercritical fluid. After Critical Point is reached, temperature is maintained and supercritical fluid removed by decreasing of pressure.

In this PhD Thesis, the drying of solid phase involved the shrinkage of the material (Xerogel).

1.5.4 Applications of the Sol-Gel process

Due to high cost of the method, using Sol-Gel process should be always justified (a glass obtained with Sol-Gel methodology is more expensive compared to a classic one). Materials synthesized with Sol-Gel method due to their perfection at atomic scale and their high purity (easy to purify) are extremely interesting in optical material field.

It's worth to underline a few other utilizations: the coating, in which a ceramic thin film can be synthesized by soaking substrates into the alkoxides solution, the use to obtain hybrid organo-alkoxides materials with a polymerization and their use to control porosity of materials and fiber by adjusting the gel viscosity.

In this PhD Thesis work, several catalysts have been synthesized using Sol-Gel methodology and different methodology have been used to support organic moieties onto the so formed supports.

1.6 References

[1] P. Anastas, J. C. Warner (Eds.), *Green Chemistry: Theory and Practice*, Oxford University Press, Oxfrod, **1998**

[2] I. T. Horváth, P. T. Anastas, *Chem. Rev.*, **2007**, 107, 2169

[3] J. H. Clark (Ed.), *The Chemistry of Waste Minimization*, Blackie, London, **1995**

[4] C. G. Brundtland, Our common Future, *The World Commission on Environmental Development*, Oxford University Press, Oxford, **1987**

[5] R. A. Sheldon, H. van Bekkum, *Fine Chemicals through Heterogeneous Catalysis*, Wiley-VCH, Weinheim, **2001**

[6] R. Schlögl, *Angew. Chem. Int. Ed.*, **2015**, 54, 3465

[7] P. T. Anastas, M. M. Kirchhoff, T. C. Williamson, *Appl. Catal. A: Gen.*, **2001**, 221, 3

[8] D. E. De Vos, I. F. K. Vankelecom, P. A. Jacobs, *Chiral Catalyst Immobilization and Recycling*, Wiley-VCH, Wenheim, **2001**

[9] H. Fan, Y. M. Li, A. S. C. Chan, *Chem. Rev.*, **2002**, 102, 3385

[10] F. Svec, J. M. J. Frechet, *Chem. Mater.*, **1995**, 7, 707

[11] *Camilla Viklund, Frantisek Svec, and Jean M. J. Fre´chet* Chem. Mater. **1996,** 8, 744-750

[12] D. C. Sherrington, A. P. Kybett, *Supported Catalysts and their Applications*, RSC, Cambridge, **2001**

[13] P. Munnik, P. E. de Jongh, K. P. de Jongh, *Chem. Rev.*, **2015**, 125, 6687

[14] B. Pugin, *J. Mol. Catal. A: Chem.*, **1996**, 107, 275

[15] F. Hoffmann, M. Cornelius, J. Morell, M. Fröba, *Angew. Chem. Int. Ed.*, **2006**, 45, 3216

[16] C. Li, *Catal. Rev.*, **2004**, 46, 419

[17] J. T. Thomas, R. Raja, D. W. Lewis, *Angew. Chem. Int. Ed.*, **2005**, 44, 6456

[18] X. S. Zhao, G. Q. Lu, X. Hu, *Chem. Commun.*, **1999**, 1391

[19] P. McMorn, G. J. Hutchings, *Chem. Soc. Rev.*, **2004**, 33, 108

[20] R. Augustine, S. Tanyelian, S. Anderson, H. Yang, *Chem. Commun.*, **1999**, 1257

[21] T. Bein, *Curr. Opin. Solid State Mater Sci.*, **1999**, 4, 85

[22] S. B. Ogunwami, T. Bein, *Chem. Commun.*, **1997**, 901

[23] C. T. Kresge, M. E. Leonowicz, W. J. Roth, J. C. Vartuli, J. S. Beck, *Nature*, **1992**, 359, 710

[24] D. Zhao, Q. Huo, J. Feng, B. F. Chmelka, G. D. Stucky, *J. Am. Chem. Soc.*, **1998**, 120, 6024

[25] M. Benaglia, A. Puglisi, F. Cozzi, *Chem. Rev.*, **2003**, 103, 3401

[26] Mohau Moshoeshoe, Misael Silas Nadiye-Tabbiruka, Veronica Obuseng. A Review of theChemistry, Structure, Propertiesand Applications of Zeolites. American Journal of Materials Science 2017, 7(5): 196-221

[27] M. R. Buchmeiser, *Chem. Rev.*, **2009**, 109, 303

[28] M. A. Harner, W. E. Farneth, Q. Sun, *J. Am. Chem. Soc.*, **1996**, 118, 7708

[29] *Ahmet Kusoglu and Adam Z. Weber Chemical* ***reviews****, 2017 -* ***ACS*** *Publications*

[30] J. Lu, P. H. Toy, Chem. Rev., **2009**, 109, 815-838

[31] G. A. Olah, S. I. Pradeep, G. K. Prakash, *Synthesis*, **1986**, 513

[32] P. Barbaro, F. Liguori, *Chem. Rev.*, **2009**, 109, 515

[33] C. J. Brinker, G. W. Scherer, Sol-Gel Science, Academic: New York, 1990

[34] L. C. Klein (Ed.), Sol-Gel Technology for Thin Films, Fibers, Preforms, Electronics and Specialty Shapes, Noyes: Park Ridge, New York, 1988

[35] J. Livage, M. Henry, C. Sanchez, Prog. Solid State Chem., 1988, 18, 259

[36] L. L. Hench, J. K. West, Chem. Rev., 1990, 90, 33

2) Oxidative dearomatization of phenols and naphthalenes over Aquivion resin as catalyst

2.1 Introduction

Organic molecules controlled oxidation still represents a challenging task in today's chemistry. As a matter of fact, partially oxidized species are more suitable toward oxidation reaction respect to the corresponding precursor.
This factor involves a good selection over the oxidizing agents as well as a strict control over reaction conditions.
Arenes oxidation is obviously a typical example for the statements above described. The use of an appropriate oxidizing agent is fundamental in order to obtain more or less selectivity towards different intermediates possible in oxidation reaction.
Undoubtedly an efficient route to 1,4 quinones is represented by selective oxidation of arenes. There are several interests around quinone scaffolds in today society, technology and in synthesis [1-6]; 1,4-naphthoquinone is significant, from an industrial point of view, as intermediate for the anthraquinone synthesis according to Bayer or Kawasaki methodology [7-8] and has been studied as an hardener in photochemically obtained cross-linked polyesters [9] and as an efficient polymerization regulator [10]. It can react together with esters of cyclic phosphinic acid to give the 1,4-naphthalene diol that is used for synthesis of flame resistant and thermally stable polyesters [11-13]. The leading role in many biological processes are bounded with their extreme versatility in redox reactions[14]. Together with their involvement in the respiratory chain and photosynthesis, quinone based vitamins such as

menadione (vitamin K_3) and 2,3,5-trimethylbenzoquinone, a crucial intermediate for vitamin E [15-16] are fundamental additives in food.

Due to these factors several methodologies have been proposed through the years for the preparation of these compounds. One of the most applied method is represented undoubtedly by oxidative dearomatization of basic aromatics [1,17-18], in which phenols and naphthalenes occupy a place of honour [19-20] despite the difficulties connected with the inner challenge of removing aromaticity from the rings that often require complex catalytic systems or forced experimental condition. As always, Nature offers a good number of examples of oxidative dearomatizations to obtain reducted scaffolds completed by elaborated enzymes [21-24]. The presence of high cost transition metal or an organocatalyst are often required to carry out these transformations [25-31] that are well described by literature (naphthalenes and phenols oxidation are among the most studied [32]). Expensive oxidants such as NBS, organic peroxides and high valent Iodine reagents are often used to carry out the reactions according to literature, while, only a few examples are reported using hydrogen peroxide as oxidant often involving the use of a transition metal as catalyst [33-35]. At best of our knowledge the main exception is represented by a recent methodology report using 1,1,1,3,3,3-hexafluoroisopropanol [36].

Oxygen is indeed the greenest oxidant and its use should be preferred when possible; several procedures are reported in literature, usually involving the use of a metal catalyst and/or a pre oxidized substrate such as phenols or naphthols together with a strict control over the reaction conditions to tune oxidant power.[37-38]

Recently, our group of research developed and reported an efficient route for obtaining carbonyl derivates from aryl methylene groups through an oxidation reaction carried out over a perfluorinated sulphonic acid; Aquivion indeed

proved to be a metal free oxidation catalyst in presence of hydrogen peroxide (**figure 1**) [39].

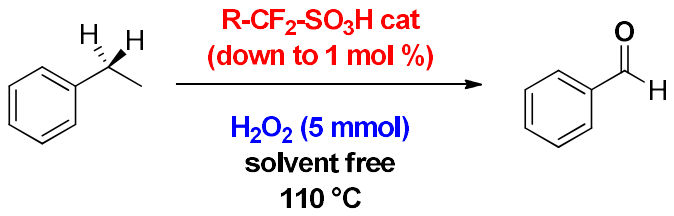

Figure 1

This approach shows the possibility af a simple and safe methodology for oxidation reactions under mild conditions together with the use of hydrogen peroxide that is a cheap and sustainable reagent. During the first part of my PhD period my activity was focused on the possibility to apply our Aquivion based methodology for oxidative dearomatization of phenols and naphthalenes.

2.2 ***Results and discussion***

A preliminary study was then performed making two mmol of phenol react with a 33% solution of hydrogen peroxide in acetic acid at 80 °C, over an acid catalyst, for 24h. Table 1 summarizes the different results obtained with different acid catalysts.

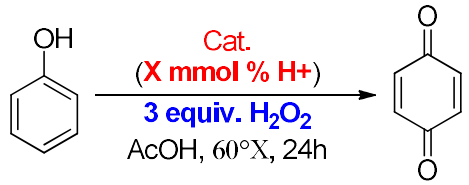

1a **2a**

Entry	Catalyst	Yield % (2a)[b]	Selectivity % (2a)[c]
1	H_2SO_4	28%	41%
2	CF_3SO_3H	61%	87%
3	Aquivion® PW66S	29%	53%
4	Nafion NR50	26%	100%
5	Amberlite IR-120	8.6%	24%
6	Acid Al_2O_3	32%	87%
7	TiO_2	12.6%	55%
8	Aquivion®@NP-SiO_2	10%	100%
9	Nafion@NP-SiO_2	22%	88%
10	-	-	-
11	Aquivion®@AM-SiO_2	69%	96%

Table 1 Reaction condition: 2 mmol phenol, 12 mmol H_2O_2 (3 equiv), 5 ml acetic acid and measured amount of acid catalyst, 60 °C for 24h; [b]by GC upon calibration with an authentic sample and using dodecane as internal standard, [c] selectivity measured as yield/conversion ratio

The reaction carried out with sulphuric acid (entry 1) demonstrated that the approach was possible; high conversion was observed on substrate **1a** together with 28% of desired quinone and several by-products present at trace level. We proceeded with testing another homogeneous acid catalyst (trifluoromethanesulfonic acid, entry 2) that provided quinone **2a** in higher yield with a greater selectivity despite the same conversion value observed in the previous case. This result indeed confirmed that fluorinated sulphonic acids could have been more selective catalyst over this reaction. Comparable outcomes were obtained testing Aquivion and Nafion in their commercial form even if Nafion exhibited a greater selectivity toward product **2a**. Well known acid catalysts such as Amberlite, alumina and titanium oxide provided quinone 2a in low yield. Encouraged by comparison we tested the perfluorinated polymers bearing the sulphonic acid groups differently grafted on silica. Aquivion and Nafion trapped on silica nanoparticles gave low yields toward quinone **2a** despite the great selectivity exhibited by the so-supported Aquivion (entry 8). Quinone **2a** was obtained in good yields carrying out the reaction over the amorphous silica supported Aquivion based catalyst with an excellent selectivity (entry 11).

We then proceeded to optimize the reaction parameters for our standard reaction (**1a** to **2a**)

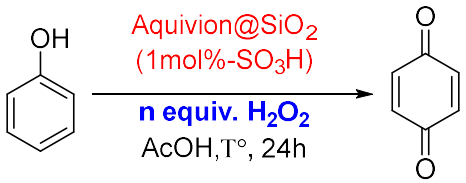

1a **2a**

Entry	T °C	Cat. (-SO_3H %)	1a/H_2O_2	Solvent	Yield % (2a)[b]	Sel.[c] % (2a)[b]
1	60	1.5 mol %	1:6	hexane	-	-
2	60	1.5 mol %	1:6	acetonitrile	29%	71%
3	60	1.5 mol %	1:6	DMSO	46.5%	75%
4	80	1.5 mol %	1:6	Acetic acid	14.2%	15%
5	40	1.5 mol %	1:6	Acetic acid	65%	87%
6	40	1.5 mol %	1:4	Acetic acid	58%	72%
7	40	3 mol %	1:4	Acetic acid	12%	14%
8	40	1 mol %	1:4	Acetic acid	74%	92%
9	40	1 mol %	1:2	Acetic acid	54%	93%

Table 2: Reaction condition: 2 mmol of phenol, 24h; [b]by GC upon calibration with an authentic sample and using dodecane as internal standard, [c] selectivity measured as yield/conversion ratio

The initial screening on solvent revealed that increasing the polarity of the solvent involved undoubtedly an increase in the yield of benzoquinone (entry

1-2-3-4); a polar and water-soluble species is thus required. It's worth to notice that no improvement was observed carrying the reaction at 80 °C due to the total loss of selectivity towards 2a product (entry 4); on the contrary we noticed that the decreasing of temperature was beneficial to our reactivity (entry 5) affording product 2a in 65% yield. The amount of oxidant was also investigated: the decreasing of the substrate-oxidant molar ratio did not involve a consistent drop in terms of yield (entry 6) even if a stoichiometric amount of oxidant gave worst results in terms of yield (entry 9). The optimum catalyst amount was found to be 1% providing benzoquinone in 74% yield (entry 8).

Thanks to our optimized conditions we were able to provide a few examples of different substituted benzoquinones and naphthoquinones starting from the respective lightly oxidized substrates in good to excellent yield.

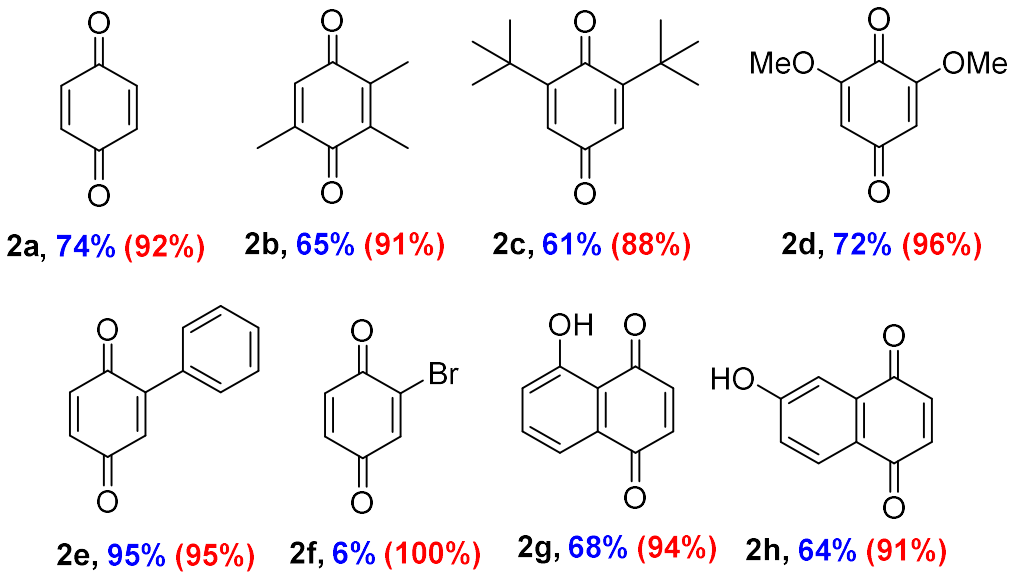

Scheme 1 reaction scope, isolated yields

As it can be seen phenols bearing electron donating groups are well tolerated in this transformation; in particular, it's worth to notice that steric hindrance of 2,3,5 trimethylphenol and 2,6-ditertbutyl phenol was tolerated providing the two corresponding quinones in good yield (2b, 2c). Phenols bearing alkoxy group and phenyl group are indeed well transformed to the corresponding benzoquinones (2d and 2e); the reaction was then extended to polycyclic phenols and we were able to obtain compound 2g and 2h in a shorter reaction time (2h) compared to phenols in good yields. As expected, a great limitation was observed studying reactivity of phenols bearing electron withdrawing groups here represented from 2-bromo phenol (2f) that was, for a minimal part, transformed in the corresponding quinone.

It is worth to know that ,encouraged by these results, we tried to carry out the oxidative dearomatization of basic arenes, but a few attempts to oxidize benzene failed, suggesting that the energetic barrier due to aromaticity represents a too deep hurdle to overcame in this case.

On the contrary, traces of naphthoquinones 4a were detected carrying out the reaction in the optimized condition previous reported and a good shift in terms of yield was observed with increasing the reaction temperatures to 80°C starting from naphthalene. We decided to investigate the best reaction condition for oxidative dearomatization of naphthalenes (table 3).

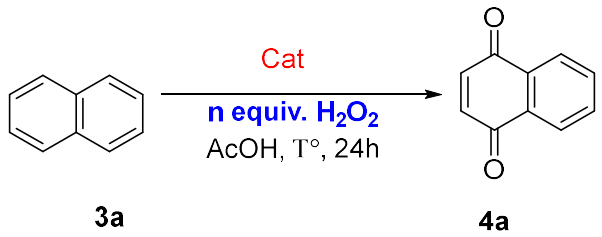

3a **4a**

Entry	Catalyst (mol% H^+)	Temp. (°C)	Yield of **4a** (%)[b]	Sel. of **4a** (%)[c]
1	Aquivion @ SiO_2 (1.5)	80	47	68
2	-$(CH_2)_3$-SO_3H @ SiO_2 (1.5)	80	33	54
3	SiO_2	80	1	10
4	Aquivion PW66S (1.5)	80	44	94
5	Aquivion PW66S (7)	80	50	98
6	Aquivion PW66S (13)	80	58	70
7	Aquivion PW66S (1.5)	100	52	63
8[d]	Aquivion PW66S (1.5)	80	45	44
9[e]	Aquivion PW66S (1.5)	80	88	97

Table 3: [a] Reaction conditions: **3a** (2 mmol), 33% aqueous H_2O_2 (6 mmol, 1 equiv.), acid catalyst, 5 mL of AcOH, for 24 hours; [b] by GC upon calibration with an authentic sample and using dodecane as internal standard; [c] selectivity measured as yield/conversion ratio; [d] with 18 mmol of H_2O_2; [e] with 12 mmol (2 equiv.) of H_2O_2.

The propyl sulphonic acid grafted on silica exhibited an encouraging activity providing naphthoquinone in 33% yield (entry2). It's evident by the reaction carried out in the presence of supported Aquivion and by the results obtained carrying out the reaction with inorganic support only (entry 1 and entry 3) that support wasn't beneficial to our reaction. The selectivity of the reaction increased using the unsupported Aquivion PW66s (powder form) directly provided by Solvay (entry 4). We were able to achieve the yield of 88% in naphthoquinone 4a optimizing the substrate to hydrogen peroxide ratio and the catalyst amount (1.5%, entry 9). Thanks to the so-optimized condition we were able to complete the reaction scope (scheme 2).

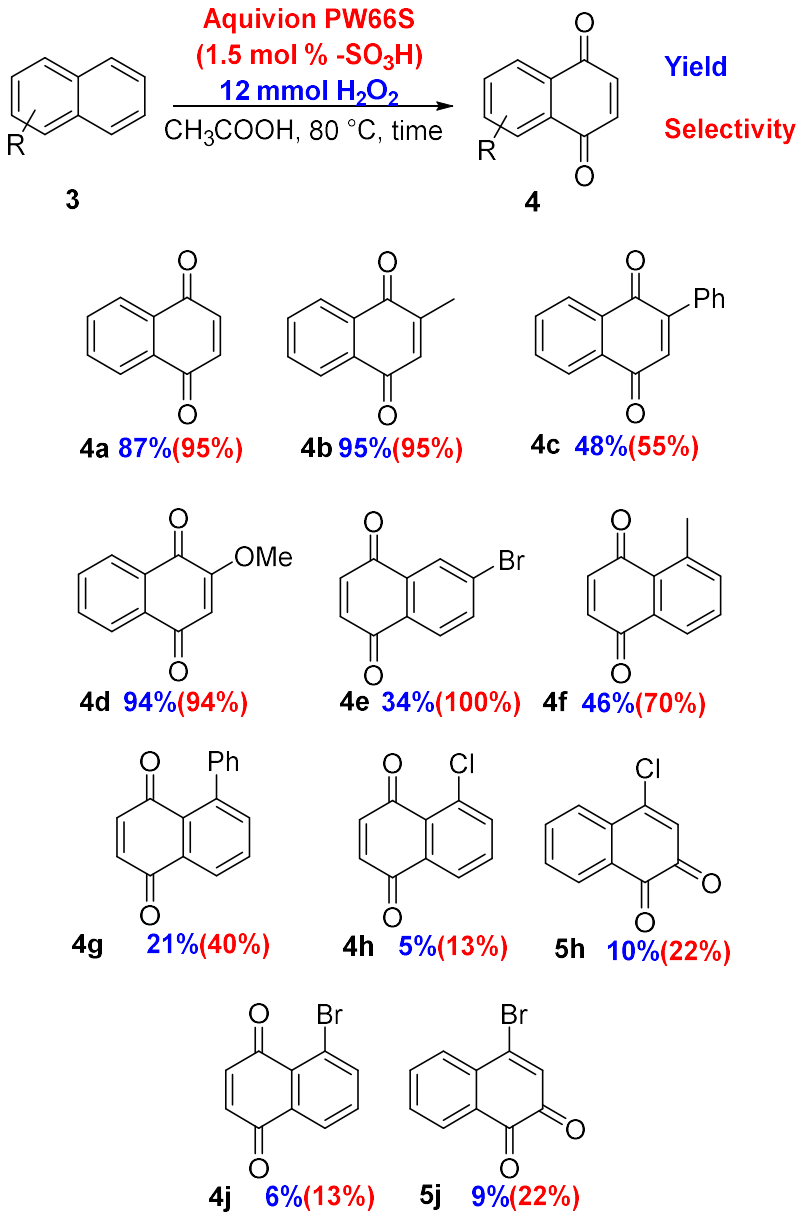

Scheme 2 scope of the reaction of dearomatization of naphthalenes

As it can be seen the dearomatization occurred selectively on the most electron rich ring; indeed 2-methyl naphthalene oxidation provided menadione in 95% yield and good to excellent yield were achieved using electron donating groups. A different reactivity was observed for naphthalenes bearing electron withdrawing groups providing products oxidized on the less substituted ring

(4e). Oxidation of naphthalenes bearing halogen group in 1 position afforded two different quinones oxidized in different rings in low yields. Again, the presence of an EWG group came out to be a strong limitation for our catalytic system.

The methodology has been extended to heavier arenes and a few examples were reported in decent to excellent yield (scheme 3):

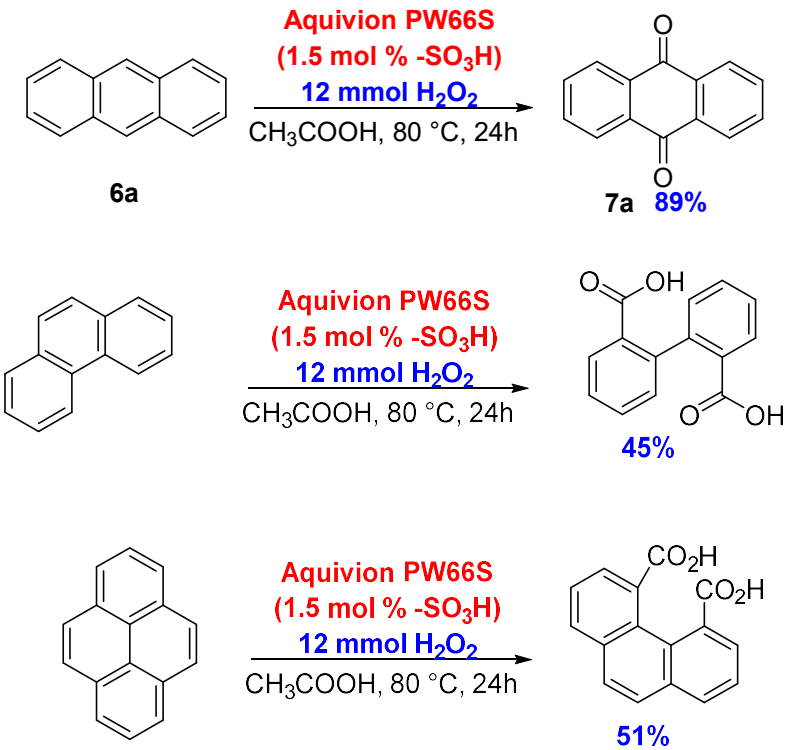

Scheme 3

Anthraquinone was indeed provided from anthracene oxidation in 89% yield while the dicarboxylic acid formation occurred in case of pyrene and phenanthrene together with 1,2 quinones formation in traces.

2.3 Conclusion

We were able to adapt our Aquivion based oxidizing methodology for the oxidation of phenols, naphthalenes and a few heavier polycyclic aromatic compounds providing corresponding products generally in good yield. The transformations are carried out under mild condition in a single step process using hydrogen peroxide as oxidant over a small catalyst amount; this allows to diminish the amount of wastes generated. A possible limitation of the reaction could be represented by the use of two equivalent of hydrogen peroxide which could affect the cost-effectiveness of the process.

2.4 Experimental section

2.4.1 Synthesis of catalysts

General procedure for synthesis of -$(CH_2)_3$-SO_3H @ SiO_2 [40]

The catalyst was prepared according to previews literature procedure. Silica support (2 g) (amorphous silica) has been mixed together under stirring with MPTS ((3-mercaptopropyl) trimethoxysilane) (0.1875 ml; 0.7625 mmol) for 24 h in toluene (20 ml) under reflux. The obtained supported propylmercaptane has been then oxidized to sulphonic acid by using 30% aq H_2O_2 (0.2 mol, 20 ml) at room temperature for 24 h under stirring, adding concentrated sulphuric acid (few drops).

Surface acidity of the obtained catalyst was measured by titration method and was found to be 0.20 mmol H^+/g

General procedure for synthesis Aquivion @ SiO_2[41]

The catalyst was prepared adapting a procedure found in literature. Typically, in a two necked flask, Aquivion D98-20BS–water dispersion (11 g) was slowly added to a TEOS (15 g) solution. The mixed solution has been stirred for 2 hours at room temperature and further refluxed at 100 °C for 20 h. Final solid was centrifuged and washed with excessive deionized water until the supernatant fluid is of a neutral pH. The solid was finally dried at 120 °C for 15 h. Surface acidity of the so obtained catalyst was measured by titration method and was found to be 0.47 mmol H^+/g

General procedure for surface acidity determination [42]

The surface acidity was measured by a well-known titration method: 0.5 g of the synthesized catalyst sample were added to a solution of NaCl (200 g/L, 50 mL) and placed under stirring at room temperature for 24h. Residual catalyst was filtered and the aqueous solution has been titrated with NaOH solution (0.01 N) in presence of phenolphthalein used as pH indicator.

2.4.2 Synthesis of products

General procedure A for oxidative dearomatization of phenols

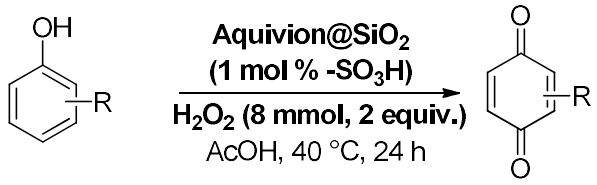

In a glass tailed test tube, acetic acid (5 ml), H_2O_2 (8 mmol) and aquivion supported on amorphous silica are mixed under stirring. The resulting mixture was stirred in an oil bath at 40 °C for 1 hour to promote peracetic acid formation after which the phenolic substrate (2 mmol) is added to the solution. The obtained mixture has been heated at 40 °C, under stirring, for further 20 hours. The catalyst was separated by filtration and the reaction crude was diluted with ethyl acetate and washed with abundant water. Organic phase was dried over Na_2SO_4, filtered and concentrated under reduced pressure. The resulting crude was then analyzed by GC-MS and finally purified by flash column chromatography on silica gel using mixture of hexane-ethyl acetate as eluent.

General procedure B for oxidative dearomatization of naphthols

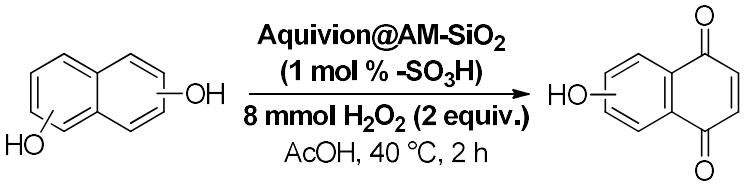

In a glass tailed test tube, acetic acid (5 ml), H_2O_2 (8 mmol) and aquivion supported on amorphous silica are mixed together under stirring. The resulting mixture was stirred in a pre-heated oil bath at 40 °C for 1 hour to promote peracetic acid formation after which the naphtholic substrate (2 mmol) is added to the mixture. The obtained mixture was stirred at 40 °C for further 20 hours. The catalyst was filtered off and the reaction mixture diluted with ethyl acetate and washed with abundant water. The organic layer was dried over Na_2SO_4, filtered and concentrated under reduced pressure. The resulting crude was then analyzed by GC-MS and finally purified by flash column chromatography on silica gel using hexane-ethyl acetate (8-2 respectively) as eluent.

General procedure C for oxidative dearomatization of naphthalenes

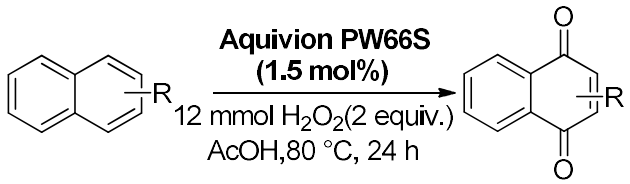

In a glass tailed test tube the naphthalenic substrate (2 mmol) have been solved in acetic acid at 80 °C under stirring. When substrate is totally solved Aquivion PW66S is added to the reaction mixture (1.5 mol %) and H_2O_2 (1.11 ml, 12 mmol) is slowly added using a syringe. Reaction mixture was kept to 80 °C for further 20 hours. The catalyst was filtered off and the reaction mixture was diluted with ethyl acetate and washed with abundant water. The organic layer was dried over Na_2SO_4, filtered and concentrated under reduced pressure. The resulting crude was then analyzed by GC-MS and finally purified by flash column chromatography on silica gel using mixture of hexane-ethyl acetate as eluent.

2.4.3 Characterization of products

cyclohexa-2,5-diene-1,4-dione 2a

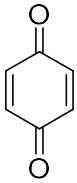

The general procedure **A** was followed using the correspondent phenol (188 mg, 2 mmol). Purification by chromatography on silica gel yielded **2a** (160 mg, 74 %) as yellow solid.
^{1}H-NMR: δ 6.74 (s);^{13}C-NMR: δ 187.12, δ 136.41; MS calcd for $C_6H_4O_2$ =108.02 EI-MS m/z found= 108

2,3,5-trimethylcyclohexa-2,5-diene-1,4-dione 2b

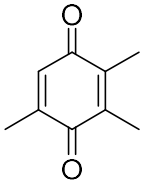

The general procedure **A** was followed using the correspondent phenol (272 mg, 2 mmol). Purification by chromatography on silica gel yielded **2b** (195 mg, 65 %) as yellow solid.
^{1}H-NMR: δ 6.50 (q, J=1.5Hz, 1H), δ 1.97 (m, 10H); ^{13}C-NMR: δ 187.7, δ 187.3, δ 145.2, δ 140.8, δ 140.6, δ 132.9, δ 15.7, δ 12.2, δ 11.9; MS calcd. for $C_9H_{10}O_2$= 150.07; EI-MS m/z found= 150

2,6-di-tert-butylcyclohexa-2,5-diene-1,4-dione 2c

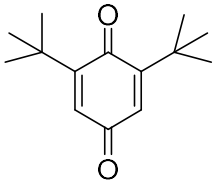

The general procedure **A** was followed using the correspondent phenol (512 mg, 2 mmol). Purification by chromatography on silica gel yielded **2c** (268 mg, 61 %) as yellow solid.

^{1}H-NMR: δ 6.45 (s, 2H), δ 1.23 (s, 18H) ;^{13}C-NMR: δ 188.9, δ 187.7, δ 157.8, δ 130, δ 35.5, δ 29.3; MS calcd. for $C_{14}H_{20}O_2$= 220.15; EI-MS *m/z* found : 220

2-bromocyclohexa-2,5-diene-1,4-dione 2d

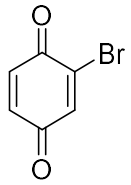

The general procedure **A** was followed using the correspondent phenol (344 mg, 2 mmol). Purification by chromatography on silica gel yielded **2d** (22 mg, 6 %) as a pale yellow solid.
^{1}H-NMR: δ 7.30 (d, j=2.3 Hz, 1H), δ 6.96 (d, J=10.1 Hz, 1H), δ 6.82 (dd, J=10.1 Hz, 1H);^{13}C-NMR: δ 187.6, δ 186.6, δ 145.9, δ 137, δ 136.2, δ 132.6, δ 130.1, δ 129.2, δ 128.5; MS calcd. for $C_6H_3BrO_2$= 185.93; EI-MS *m/z* found: 186

2,6-dimethoxycyclohexa-2,5-diene-1,4-dione 2e

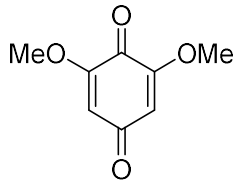

The general procedure **A** was followed using the correspondent phenol (308 mg, 2 mmol). Purification by chromatography on silica gel yielded **2e** (242 mg, 72 %) as a yellow solid.
^{1}H-NMR: δ 5.84 (s, 2H), δ 3.81 (s, 6H) ; ^{13}C-NMR: δ 186.8, δ 176.6, δ 157.3, δ 107.4, δ 56.5; MS calcd. for $C_8H_8O_4$= 168.04; EI-MS *m/z* : 168

2-phenylcyclohexa-2,5-diene-1,4-dione 2f

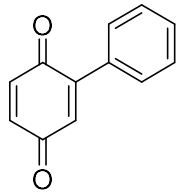

The general procedure **A** was followed using the correspondent phenol (340 mg, 2 mmol). Purification by chromatography on silica gel yielded **2f** (349 mg, 95 %) as a yellow solid.
^{1}H-NMR: δ 7.46 (s, 5H), δ 6.96 (d, J=10.1Hz, 1H); ^{13}C-NMR: δ 187.6, δ 186.6, δ 145.9, δ 137, δ 136.2, δ 132.6, δ 130.1, δ 129.2, δ 128.5; MS calcd. for $C_{12}H_8O_2$= 184.05; EI-MS *m/z* found: 184

5-hydroxynaphthalene-1,4-dione 2g

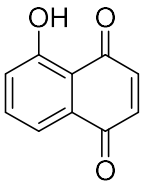

The general procedure **B** was followed using the correspondent naphtol (320 mg, 2 mmol). Purification by chromatography on silica gel yielded **2g** (237 mg, 68 %) as an orange solid.
^{1}H-NMR: δ 11.9 (s, 1H), δ 7.68-7.58 (m, 2H), δ 7.30-7.25 (m, 1H), δ 6.95 (s, 2H); ^{13}C-NMR: δ 190.3, δ 184.2, δ 161.2, δ 139.6, δ 138.6, δ 136.6, δ 131.7, δ 124.5, δ 119.2, δ 114.9; MS calcd. for $C_{10}H_6O_3$= 174.03; EI-MS *m/z* : 174

6-hydroxynaphthalene-1,4-dione 2h

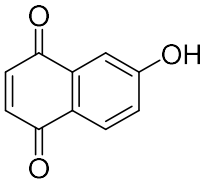

The general procedure **B** was followed using the correspondent naphtol (320 mg, 2 mmol). Purification by chromatography on silica gel yielded **2h** (223 mg, 64 %) as an orange solid.
^{1}H-NMR: δ 11.9 (s, 1H), δ 7.68-7.58 (m, 2H), δ 7.30-7.25 (m, 1H), δ 6.95 (s, 2H)
^{13}C-NMR: δ 186.8, δ 185.8, δ 164.7, δ 140.4, δ 139.6, δ 135.8, δ 130.4, δ 125.9, δ 122.0, δ 113.3; MS calcd. for $C_{10}H_6O_3$= 174.03; EI-MS *m/z*: 174

naphthalene-1,4-dione 4a

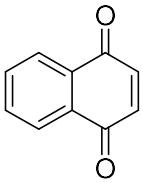

The general procedure **C** was followed using the correspondent naphthalene (256 mg, 2 mmol). Purification by chromatography on silica gel yielded **4a** (275 mg, 87%) as a yellow solid.
^{1}H-NMR: δ 8.08 (dd, J = 5.7, 3.3 Hz, 2H), 7.76 (dd, J = 5.7, 3.4 Hz, 2H), 6.98 (s, 2H); ^{13}C-NMR: δ 185.0, 138.6, 133.9, 131.9, 126.4; MS calcd. for $C_{10}H_6O_2$= 158.04; EI-MS m/z : 158

2-methylnaphthalene-1,4-dione 4b

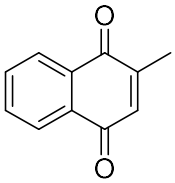

The general procedure **C** was followed using the correspondent naphthalene (284 mg, 2 mmol). Purification by chromatography on silica gel yielded **4b** (327 mg, 95%) as a ligh orange solid.
^{1}H-NMR: δ 8.04 (ddd, J = 3.2, 5.8, 11.5 Hz, 2H), 7.69 (dd, J = 3.3, 5.7 Hz, 2H), 6.81 (s, 1H), 2.17 (s, 3H); ^{13}C-NMR: δ 185.4, 184.9, 148.1, 135.6, 133.5, 132.1, 126.4, 126.0, 16.4; MS calcd. for $C_{11}H_8O_2$= 172.05; EI-MS m/z :172

2-phenylnaphthalene-1,4-dione 4c

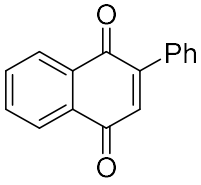

The general procedure **C** was followed using the correspondent naphthalene (408 mg, 2 mmol). Purification by chromatography on silica gel yielded **4c** (225 mg, 48%) as a yellow solid.

^{1}H-NMR: δ 8.20-8.10 (m, 2H), 7.78-7.75 (m, 2H), 7.59-7.56 (m, 2H), 7.50-7.45 (m, 2H), 7.07 (s, 1H); ^{13}C-NMR: δ 185.1, 184.3, 148.1, 135.2, 133.8, 133.8, 133.4, 132.5, 132.1, 130.0, 129.4, 128.4, 127.0, 125.9; MS calcd. for $C_{16}H_{10}O_2$= 234.07; EI-MS m/z :234

2-methoxynaphthalene-1,4-dione 4d

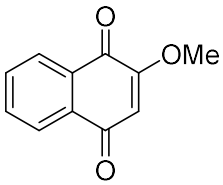

The general procedure **C** was followed using the correspondent naphthalene (316 mg, 2 mmol). Purification by chromatography on silica gel yielded **4d** (353 mg, 94%) as an orange solid.
^{1}H-NMR: δ 8.03-7.96 (m, 2H), 7.69-7.60 (m, 2H), 6.10 (s, 1H), 3.84 (s, 3H);
^{13}C-NMR: δ 184.7, 180.0, 160.3, 134.3, 133.3, 131.9, 131.0, 126.6, 126.1, 109.8, 56.4; MS calcd. for $C_{11}H_8O_3$= 188.05; EI-MS m/z found:188

6-bromonaphthalene-1,4-dione 4e

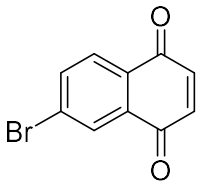

The general procedure **C** was followed using the correspondent naphthalene (410 mg, 2 mmol). Purification by chromatography on silica gel yielded **4e** (353 mg, 34%) as an orange solid.
^{1}H-NMR: δ 8.21 (d, J = 1.8 Hz, 1H), 7.91 (dt, J = 5.1, 8.3 Hz, 2H), 6.99 (s, 2H); ^{13}C-NMR: δ 184.2, 183.8, 138.8, 138.4, 137.0, 132.9, 129.5, 128.2; MS calcd. for $C_{10}H_5BrO_2$= 235.95; EI-MS m/z : 235

5-methylnaphthalene-1,4-dione 4f

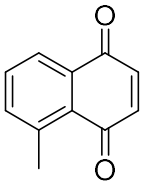

The general procedure **C** was followed using the correspondent naphthalene (284 mg, 2 mmol). Purification by chromatography on silica gel yielded **4f** (158 mg, 46%) as a dark yellow solid.
^{1}H-NMR: δ 7.99 (dd, J = 4.3, 8.4 Hz, 1H), 7.84-7.70 (m, 1H), 7.63-7.46 (m, 2H), 6.90 (s, 1H), 2.75 (s, 3H); ^{13}C-NMR: δ 187.0, 185.4, 141.3, 140.4, 137.9, 136.9, 133.3, 130.0, 125.3, 22.6; MS calcd. for $C_{11}H_8O_2$= 172.05; EI-MS m/z : 172

5-phenylnaphthalene-1,4-dione 4g

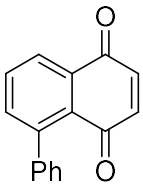

The general procedure **C** was followed using the correspondent naphthalene (408 mg, 2 mmol). Purification by chromatography on silica gel yielded **4e** (98 mg, 21%) as a yellow solid
^{1}H-NMR: δ 8.18 (dd, J=1.35, 7.72 Hz, 1H), 7.74 (t, J=7.69 Hz, 1H), 7.57 (dd, J=1.34, 7.66 Hz, 1H), 7.44-7.42 (m, 3H), 7.29-7.24 (m, 2H), 6.95 (d, J=10.27 Hz, 1H), 6.83 (d, J=10.27 Hz, 1H); ^{13}C-NMR: δ 185.1, 185.0, 143.6, 140.9, 140.2, 137.4, 136.9, 133.2, 132.7, 129.0, 128.0, 127.3, 126.3; MS calcd. for $C_{16}H_{10}O_2$= 234.07; EI-MS m/z : 234

5-chloronaphthalene-1,4-dione 4h

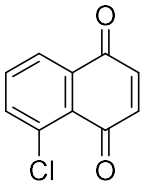

The general procedure **C** was followed using the correspondent naphthalene (324 mg, 2 mmol). Purification by chromatography on silica gel yielded **4h** (19 mg, 5%) as a yellow solid
^{1}H-NMR: δ 8.07 (dd, J=1.35, 7.63 Hz, 1H), 7.75 (dd, J=1.35, 8.07 Hz, 1H), 7.66-7.61 (m, 1H), 6.96 (d, J=6.24 Hz, 2H); ^{13}C-NMR: δ 183.8, 183.3, 176.7, 140.3, 137.5, 136.7, 134,4, 126.0; MS calcd. for $C_{10}H_5ClO_2$= 192.00; EI-MS m/z : 192

5-bromonaphthalene-1,4-dione 4j

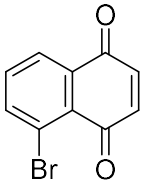

The general procedure **C** was followed using the correspondent naphthalene (410 mg, 2 mmol). Purification by chromatography on silica gel yielded **4j** (28 mg, 6%) as a yellow solid
^{1}H-NMR: δ 8.13 (dd, J=1.19, 7.70 Hz, 1H), 8.00 (dd, J=1.19, 8.02 Hz, 1H), 7.55 (t, J=7.88 Hz, 1H), 7.00 (d, J=10.34, 1H), 6.95 (d, J=10.31, 1H); ^{13}C-NMR: δ 183.7, 183.3, 141.0, 140.2, 136.8, 134.6, 133.7, 129.0, 126.7, 122.0; MS calcd. for $C_{10}H_5BrO_2$= 235.95; EI-MS m/z : 236

4-chloronaphthalene-1,2-dione 5h

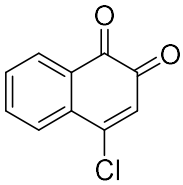

The general procedure **C** was followed using the correspondent naphthalene (324 mg, 2 mmol). Purification by chromatography on silica gel yielded **5h** (38 mg, 10%) as a yellow solid
^{1}H-NMR: δ 8.17-8.06 (m, 2H), 7.80-7.76 (m, 2H), 7.20 (d, J=4.49 Hz, 1H); ^{13}C-NMR: δ 182.6, 177.9, 146.3, 138.0, 135.9, 134.5, 134.1, 133.7, 127.5, 126.7; MS calcd. for $C_{10}H_5ClO_2$= 192.00; EI-MS m/z : 192

4-bromonaphthalene-1,2-dione 5j

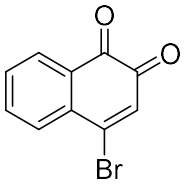

The general procedure **C** was followed using the correspondent naphthalene (410 mg, 2 mmol). Purification by chromatography on silica gel yielded **5j** (42.5 mg, 9%) as a yellow solid
^{1}H-NMR: δ 8.23-8.00 (m, 2H), 7.81-7.75 (m, 2H), 7.53-7.51 (m, 1H); ^{13}C-NMR: δ 182.4, 177.9, 141.6, 140.4, 134.4, 134.1, 133.7, 127.8, 126.9; MS calcd. for $C_{10}H_5BrO_2$= 235.95; EI-MS m/z : 236

anthracene-9,10-dione 4k

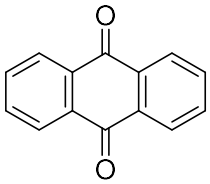

The general procedure **C** was followed using anthracene (356 mg, 2 mmol). Purification by chromatography on silica gel yielded **4k** (370 mg, 89%) as a pale-yellow solid
^{1}H-NMR: δ 8.31 (m, 4H), 7.80 (m, 4H); ^{13}C-NMR: δ 183.1, 134.1, 133.5, 127.2
MS calcd. for $C_{14}H_8O_2$= 208.05; EI-MS m/z :208

diphenic acid

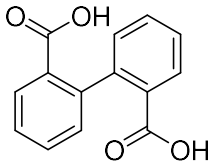

The general procedure **C** was followed using phenanthrene (356 mg, 2 mmol). Precipitation yielded diphenic acid (217 mg, 45%) as a white solid.

^{1}H-NMR: δ 12.50 (s, 2H), 7.95 (d, J = 7.7 Hz, 2H), 7.58 (t, J = 7.5 Hz, 2H), 7.47 (t, J = 7.5 Hz, 2H), 7.21 (d, J = 7.5 Hz, 2H); ^{13}C-NMR: δ 168.9, 144.1, 132.1, 131.4, 131.4, 130.6, 128.0
MS calcd. for $C_{14}H_{10}O_4$= 242.06; EI-MS *m/z :*224

phenanthrene-4,5-dicarboxylic acid

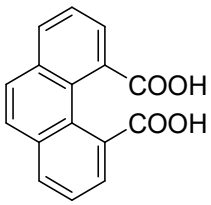

The general procedure **C** was followed using phenanthrene (356 mg, 2 mmol). Precipitation yielded phenanthrene-4,5-dicarboxylic acid (265 mg, 50%) as a dark brown solid.
^{1}H-NMR: δ 8.03 (d, J = 7.8 Hz, 2H), 7.94 (d, J = 7.2 Hz, 2H), 7.82 (s, 2H), 7.60 (t, J = 7.6 Hz, 2H); ^{13}C-NMR: δ 170.3, 135.0, 134.7, 132.2, 128.9, 128.3, 128.1, 127.3
MS calcd. for $C_{16}H_{10}O_4$= 266.06; EI-MS *m/z :*248

2.5 References

[1] Roche, S. P.; Porco, J. A. *Angew. Chem., Int. Ed.* **2011**, *50*, 4068-4093.

[2] Shiao, H. Y.; Hsieh, H. P.; Liao, C. C. *Org. Lett.* **2008**, *10*, 449-452.

[3] Yang, Q.; Draghici, C.; Njardarson, J. T.; Li, F.; Smith, B. R.; Das, P. *Org. Biomol. Chem.* **2014**, *12*, 330-344

[4] Krohn, K.; Zimmermann, G. *J. Org. Chem.* **1998**, *63*, 4140-4142.

[5] Ahn, J. H.; Cho, S. Y.; Ha, J. Du; Chu, S. Y.; Jung, S. H.; Jung, Y. S.; Baek, J. Y.; Choi, I. K.; Shin, E. Y.; Kang, S. K.; Kim, S. S.; Cheon, H. G.; Yang, S. D.; Choi, J. K. *Bioorg. Med. Chem. Lett.* **2002**, *12*, 1941-1946.

[6] Shukla, S.; Srivastava, R. S.; Shrivastava, S. K.; Sodhi, A.; Kumar, P. *Appl. Biochem. Biotechnol.* **2012**, *167*, 1430-1445.

[7] Kawasaki, US 4412954, **1981** (T. Kamatsu, K. Usui)

[8] Bayer, DE-OS 2532450, **1975** (J. Priemer, N. Schenk, M. Martin, W. Swodenik)

[9] AKzo GmbH, DE-OS 2325179, **1972** (L. Roskott, M. A. A. Groenendaal)

[10] F. A. Bovey, J. M. Kolthoff, *Chem. Rev.*, **1948**, 42, 491

[11] Rohm&Haas, US 3960671, **1974** (J. S. Clovis, J. Dohling)

[12] S. N. Litvinenko, L. K. Mushkalo, A. V. Stetsenko, A. K. Tyltin, *Khim. Tekhnol. Topl. Masel 18*, **1973**, no.8, 41

[13] Japan Exlan Co., JP 86261320A2, **1985** (T. Imamura *et al.*)

[14] H. Sies, L. Packer, *Method Enzymol.*, **2004**, 378, preface

[15] D. W. Stafford, *J. Thromb. Haemostasis*, **2005**, 3, 1873-1878

[16] C. K. Chow, in: *Handbook of Vitamins*, (Eds.: R. B. Rucker, J. W. Suttie, D. B. McCormick, L. J. Machlin), 3rd edn., Marcel Dekker, New York, **2001**, 165-198

[17] Zheng, C.; You, S.-L. *Chem.* **2016**, *1*, 830-857.

[18] Wertjes, W. C ; Southgate, E. H.; Sarlah, D. *Chem. Soc. Rev.* **2018**, *47*, 7996-8017

[19] Sun, W.; Li, G.; Hong, L.; Wang, R. *Org. Biomol. Chem.* **2016**, *14*, 2164-2176.

[20] Baker Dockrey, S. A.; Lukowski, A. L.; Becker, M. R.; Narayan, A. R. H. *Nat. Chem.* **2017**, *10*, 119-125.

[21] Sib, A. ; Gulder, T. A. M. *Angew. Chem., Int. Ed.* **2017**, *56*, 12888-12891.

[22] Murray, L. A. M.; McKinnie, S. M. K.; Pepper, H. P.; Erni, R.; Miles, Z. D.; Cruickshank, M. C.; López-Pérez, B.; Moore, B. S.; George, J. H. *Angew. Chem., Int. Ed.* **2015**, *54*, 11009-11014.

[23] Dockrey, S. A. M.; Doyon, T. J.; Perkins, J. C.; Narayan, A. R. H. *Chem Biol Drug Des*. **2018**, *93*, 1207-1213.

[24] Zhang, Z. A.; Gong, Y. K.; Zhou, Q.; Hu, Y.; Ma, H. M.; Chen, Y. S.; Igarashi, Y.; Pan, L. F.; Tang, G. L. *PNAS* **2017**, *114*, 1554-1559.

[25] Bosset, C.; Coffinier, R.; Peixoto, P. A.; El Assal, M.; Miqueu, K.; Sotiropoulos, J. M.; Pouységu, L.; Quideau, S. *Angew. Chem., Int. Ed.* **2014**, *53*, 9860-9864.

[26] Yin, Q.; Wang, S.-G.; Liang, X.-W.; Gao, D.-W.; Zheng, J.; You, S.-L. *Chem. Sci.* **2015**, *6*, 4179-4183.

[27] Nan, J.; Liu, J.; Zheng, H.; Zuo, Z.; Hou, L.; Hu, H.; Wang, Y.; Luan, X. *Angew. Chem., Int. Ed.* **2015**, *54*, 2356-2360.

[28] Wang, S. G.; Liu, X. J.; Zhao, Q. C.; Zheng, C.; Wang, S. B.; You, S. L. *Angew. Chem., Int. Ed.* **2015**, *54*, 14929-14932.

[29] Wu, D. Q.; Guan, Z. Y.; Peng, Y.; Sun, J.; Zhong, C.; Deng, Q. H. *Adv. Synth. Catal.* **2018**, *360*, 4720-4725.

[30] Liu, X.; Zhang, J.; Bai, L.; Wang, L.; Yang, D.; Wang, R. *Chem. Sci.* **2020**, *11*, 671-676.

[31] An, J.; Lombardi, L.; Grilli, S.; Bandini, M. *Org. Lett.* **2018**, *20*, 7380-7383

[32] Yang, W.; Huang, L.; Yu, Y.; Pflästerer, D.; Rominger, F.; Hashmi, A. S. K. *Chem. - Eur. J.* **2014**, *20*, 3927-3930.

[33] de Carvalho, R. L.; Jardim, G. A. M.; Santos, A. C. C. ; Araujo, M. H.; Oliveira, W. X. C.; Bombaça, A. C. S.; Menna-Barreto, R. F. S.; Gopi, E.; Gravel, E.; Doris, E.; da Silva Júnior, E. N. *Chem. Eur. J.* **2018**, *24*, 15227-15235.

[34] Egusquiza, M. G.; Romanelli, G. P.; Cabello, C. I.; Botto, I. L.; Thomas, H. J. *Catal. Commun.* **2008**, *9*, 45-50.

[35] Romanelli, G. P.; Villabrille, P. I.; Vasquez, P. G.; Caceres, C. V.; Tundo, P. *Lett. Org. Chem.* **2008**, *5*, 332-335.

[36] Lloplis, N.; Baeza, A. *J. Org. Chem.* **2020**, *85*, 6159-6161.

[37] *Didier Villemin a, Mohamed Hammadi b & Messaoud Hachemi Synthetic comm. Volume 32, **2002**, 1501-1515.*

[38] *Robert J. Radel, * Jack M. Sullivan, and John. D. Hatfield, Ind. Eng. Chem. Prod. Res. Dev. 1982, 21, 566-570.*

[39] *Emanuele Paris, Claudio Oldani, Antonio S. Arico, Claudia D' Urso, Franca Bigi, Giovanni Maestri, Francesco Pancrazzi and Raimondo Maggi ACS Sustainable Chem. Eng. 2019, 7, 6, 5886–5891*

[40] R. D. Badley, W. T. Ford, *J. Org. Chem.* **1989**, 54, 5437.

[41] Fang, Wenhao; Wang, Sheng; Liebens, Armin; De Campo, Floryan; Xu, Hualong; Shen, Wei; Pera-Titus, Marc; Clacens, Jean-Marc, Catalysis Science & Technology (2015), 5(8), 3980-3990

[42] S. Leveneur, D. Y. Murzin, T. Salmi, *J. Mol. Cat. A: Chem*., **2009**, 303, 148

3) Methanol dehydration to dimethyl ether over supported sulphonic acids

3.1 Introduction

Carbon dioxide is the most abundant carbon containing compound gas on Earth and it's produced by any human activity; in last centuries, carbon dioxide concentration increased by 90 ppm for the huge amount of 480 billion tons while in very recent years the amount further increased to 1.5 ppm per year (8 billion tons) [1]. Unfortunately, carbon dioxide results to be a very stable and not reactive compound due to its high oxidation state, that requires a huge amount of energy to be overcome. Only 0.2 billion tons for year are used for synthesis of bulk chemicals such as Urea, alkylene carbonates, salicylic acids and its derivatives, formic acid and its esters [2]. The increasing global warming and the consequent need to reduce CO_2 emissions prompted both Industry and Academia to research and develop new strategies for the capture and utilization of CO_2; this global trend can be ascribe in the major concept of CCU and CCUS, both required to reach the Carbon Neutrality [3]. Nowadays a huge amount of alternative fuels has been considered for portable and more complex applications. Among those, new alternatives that have captivated a more and more attention are above all dimethyl ether (DME), formic acid, and alcohols [4]. Most of these alternative fuels can be easily stored and feed many energy systems with high efficiency and low pollutant emissions due to the possibility to have a very pure feedstock [5]. Compared to some other leading alternative fuel candidates, dimethyl ether appears to have the potential major impact on our society (Table1).

Table 1. Physical properties of DME and other alternative fuels

	DME	Methane	Methanol	Ethanol	FTD	LPG	Gasoline	Diesel	Hydrogen
Molecular Weight (g mol^{-1})	46.07	16.04	32.04	46.07		44.1	114	198.4	2.016
Density (g cm^{-3})	0.67[c]	0.00072[b]	0.792[b]	0.785[b]	0.76-0.79[e]	0.54[e]	0.71-0.77[e]	0.80-0.86[b]	0.00089[e]
Normal boiling point (°C)	-24.9	-162	64	78	180-320[e]	-30[e]	0-210[e]	125-400	-253[e]
Octane Number (RON)	-	122	110	110	-	90-96	90-100	-	>125
Cetane Number	55-60	-	5	-	55-75	-	-	40-55	-
Energy content[e] (MJ/kg)	28,43	50	19.5	28,4	44	46.3	42.7	43.1	119.9
Carbon Content[f] (wt%)	52.2	74	37.5	52.2	85[e]	82[e]	85.5	87	0
Sulfur Content[f] (ppm[g])	0	~7-25	0	0		10-50	~200	~250	0

Many DME properties, such as boiling point and vapor pressure, are similar to those of propane and butane and their commercial mixture liquefied petroleum gases (LPG). DME combustion shows undoubtedly lower NO_x, HC, and CO emissions due to aforementioned pure feedstock; in addition, PM emission for DME combustion is adequately low due to its molecular structure. These advantages have been confirmed by testing DME appropriately modified vehicles in Europe and North America, with one running for 750,000 miles [6]. Additionally, it is known that DME is an important starting material for chemical industry [7]; it is used as an eco-friendly aerosol propellant and as building block in the production of chemicals (e.g. olefins and dimethyl sulfate).

Nowadays there are two different methods to obtain DME based on coal or natural gas as feedstock: the so called direct process and the indirect one. The indirect process is divided into two different steps, where, in the first step, methanol is produced from syngas and, in the second one, methanol is converted through dehydration into DME over a solid-acid catalyst. In the direct synthesis, meanwhile, syngas is primarily converted to methanol over multifunctional catalysts, followed by dehydration to DME [8]. The second process is more attractive in terms of thermodynamics and atom economy [9].

The “one-step” route is more efficient than the “double-step” one, due to thermodynamic advantages related to the equilibrium shift of simultaneous reactions (methanol dehydration to DME obviously promotes the syngas conversion, scheme 1) and for a lower overall process cost due to the presence of a single reactor.

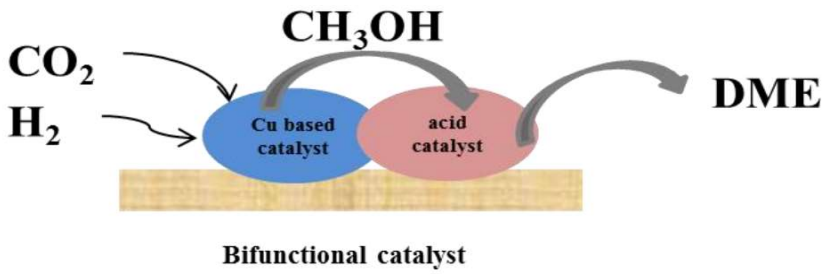

Scheme 1. Single step process

A good variety of solid acid catalysts were synthesized and used for methanol dehydration reaction to DME: acidic zeolites, especially MFI (HZSM-5), γ-alumina and heteropoly acids (HPAs) represent undoubtedly the most studied materials for this reaction. These indeed show higher catalytic activity but, by fact, are easily deactivated compared to γ-alumina [10-12]. HZSM-5 is known to be a valid catalyst for methanol dehydration, but, coke deposition due to hydrocarbon formation on its surface obviously involves a decrease in activity (poisoning). As a matter of fact, the major acid strength of HZSM-5 is able to catalyze not only methanol conversion to DME but methanol conversion to coke too. In order to enhance catalytic stability of HZSM-5-zeolite, its acidity was modified allowing the inhibition of deactivation of the catalyst. It has been recently reported by Fei et al that HZSM-5 modified with AlF_3 exhibited a good stability and a higher activity than basic zeolite due to the elimination of a great part of strong acid sites [13] involving a good switch in selectivity toward DME. Vapor phase process for methanol transformation to DME causes a huge

quantity of water to be formed together with product. In the reactor, so-formed water and methanol both attack acid sites of the acid catalyst competing each other; this factor is fundamental for γ-alumina that easily absorb water on its surface involving a decrease in the amount of catalytic sites and a consequent decrease in activity and selectivity towards DME [14]. It is evident that, for transformation of methanol to form DME, several parameters for the developing of the ideal catalyst must be considered: thermal stability, cooking resistance and toxicity are undoubtedly fundamental properties together with pores dimension and acid strength. Polymeric acid resins, nowadays used as ion-exchange, as Nafion appear to be valid candidates for the described reaction [15] due to the strengths of acid sites comparable to that of sulphuric acid. Unfortunately, Nafion owns a small surface area that caps the possible amount of acid sites, particularly in a gas phase process, active sites result to be anchored deep in the material and consequently not accessible for reagents involving a low catalytic activity for the catalyst. Recently, our group of research study has been focused on supported sulphonic acids and, thanks to a collaboration between our laboratory and ENEA - Casaccia research center, their application in methanol dehydration reaction to form DME [16]. The preliminary study demonstrated how small differences in Bronsted surface acidity involved a significant different behavior in terms of selectivity towards DME and activity of catalyst. In particular, MCM41, a well-known mesoporous silica, functionalized with propyl-sulphonic acid moiety exhibited a comparable to commercial used catalyst ($\gamma-Al_2O_3$ and Al-MCM-41) activity. It's worth to notice that sulfonated catalysts have several advantages such as the possibility to adjust acid strength due to the amount of sulphonic pendant, low cost, the operational safety and, overall, the possibility to be recycled. Considering the fascinating properties of the mentioned above materials, my work was centered on elucidating the solid acid catalyst's role and to design and synthesize a high

performance catalyst, (in terms of both activity and selectivity). For this purpose, a series of different functionalized catalysts bearing different sulphonic acid pendant grafted on silica or modified silica-alumina were synthesized, used and examined for the methanol dehydration reaction to form DME in the same operative conditions. With that in mind, I synthesized and then tested a broad range of supported acids with various SAR (silica/alumina Ratio) and different acidities some of which are still under investigation. It is expected that both Bronsted and Lewis acid functionalities will work cooperatively interacting with methanol and this will lead to increase the activity of the catalyst. In addition, the presence of aluminum might affect the structure of the support, modifying the evolution of the dehydration process, and thereby, the attained activities. The solid-acid catalysts presented in this chapter were also characterized by BET, TGA, XPS, ICP-OES and SEM methods. Furthermore, the deactivation effect of water in the stream on the activity, selectivity and yield has been investigated.

3.2 Results and discussion

3.2.1 Catalyst characterization

In Table 2 some structural properties of catalysts discussed in this chapter are underlined; all the catalysts have been synthesized according to well-known literature procedures described in the following part of this chapter. We indicated the silicoaluminate catalyst and silicas functionalized with propyl-sulphonic acid pendant respectively SiO_2-Al_2O_3-PropSO_3H_*x* and SO_3H*x*-SiO_2 where x represents the calculated surface acidity in mmol H^+/g. Synthesized catalyst exhibited a good surface area, a large pore size and volumes.

Table 2. Textural properties of materials

Catalysts	Surface Area (m^2/g)	Pore volume (cm^3/g)	D_p (nm)	D_a (nm)
SiO_2	540	0.80	5.1	5,3
SO_3H0.23 SiO_2	510	0.67	4.7	4.8
SO_3H0.37 SiO_2	506	0.61	4.7	4.6
SO_3H0.51 SiO_2	487	0.56	4.0	3.9
SiO_2/Al_2O_3	410	0.63	4.9	5.0
SiO_2/Al_2O_3-PropSO_3H_0.25	405	0.62	4.7	4.9
SiO_2/Al_2O_3-PropSO_3H_0.79	390	0.61	4.8	4.8
SiO_2/Al_2O_3-PhSO_3H	371	0.55	4.5	4.7

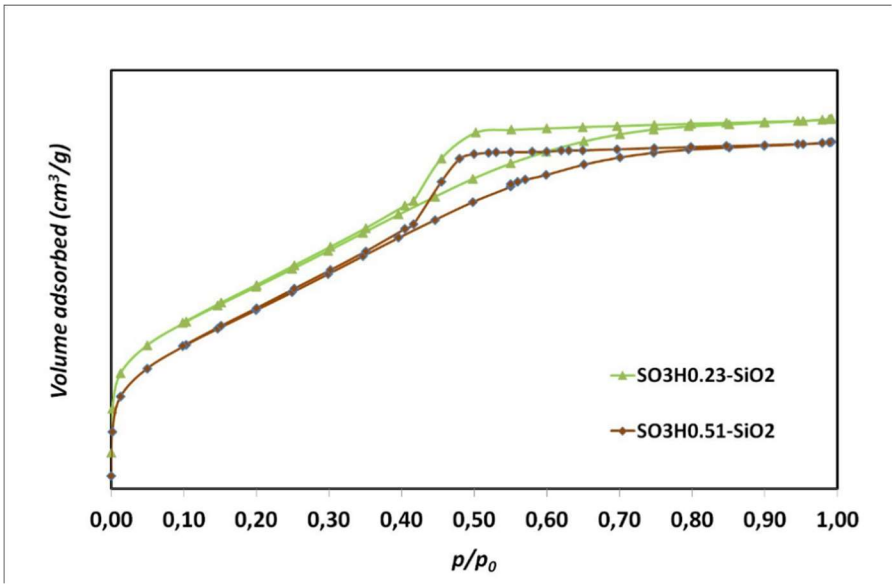

Figure 1. N_2 adsorption – desorption isotherms of the $SO_3H0.23$-SiO_2 and $SO_3H0.51$-SiO_2 catalysts.

The isotherms of these materials are of type IV characteristic of the mesoporous materials. The adsorption–desorption hysteresis of the propyl sulfonic acid functionalized silica catalysts (**figure 1**) takes place in the p/p_0 range of 0.40–0.55, demonstrating that the materials contain mesopores with a relatively uniform pore size. It's worth to notice that D_a (BJH pore diameters) and D_p (BJH peak pore diameter) are similar, this is due to a uniform mesoporous structure. As expected[17], commercial silica support exhibited an high surface area (540 m^2/g) that decreased with further functionalization with the organo-sulphonic moiety (510 m^2/g for $SO_3H0.23$-SiO_2, 506 and 490 m^2/g for $SO_3H0.37$-SiO_2 and $SO_3H0.51$-SiO_2 respectively)[15]. Medium pore volume was gradually decreased too passing from 0.80 of commercial silica to 0.57 cm^3/g of propyl-sulphonic functionalized one; this factor together with the decrease of the surface area pointed out that functional organic groups were located both in outer surface and inside mesoporous channel of the catalysts. Moreover, acid sites amount was gradually increased with the increasing amount of sulphonic acid groups

(Table 3); this clearly suggested the possibility to modify acid properties of the material by content and occurrence of sulphonic acid moieties. The contents of acid groups in the functionalized materials were measured by Sulfur elemental analysis technique and the results are given in Table 3. The accessibility to acid catalytic sites has been measured via titration methodology with a solution of NaOH after the ion exchanges with various size cations (Table 3) [18]. The measured amount of acid sites was very similar to the amount measured via Sulfur EA when sodium chloride was utilized to exchange the cation. In presence of a larger cation (TBA+) all the materials exhibited quite the same acid properties; this lead us to suppose that the major concentration of acid sites was located in the outer part of the catalyst that results to be easily accessible by cations. As for the SiO_2/Al_2O_3-$PhSO_3H$ sample, the acid capacities of the samples decreased slightly as the size of the cation increases, indicating that a portion of the phenyl-sulphonic acid groups in this sample was embedded in the silica-alumina networks.

Table 3. Acid capacities and sulfur contents of the catalysts

Samples	**S content (mmol/g)**	**NaCl Titration (mmol H^+/g)**	**TBAC Titration (mmol H+/g)**
SO_3H0.23-SiO_2	0.22	0.23	0.22
SO_3H0.37-SiO_2	0.36	0.37	0.36
SO_3H0.51-SiO_2	0.51	0.51	0.49
SiO_2/Al_2O_3-$PhSO_3H$	0.88	0.90	0.88
SiO_2/Al_2O_3-PropSO_3H_0.25	0.25	0.25	0.25
SiO_2/Al_2O_3-PropSO_3H_0.79	0.80	0.79	0.79

The thermal stability of organic pendant supported in the material has been evaluated through TGA (thermogravimetric analysis). Thermal profiles of aluminosilicate and of aluminosilicate bearing the phenyl-sulphonic organic functional group are shown in **figure 2.**

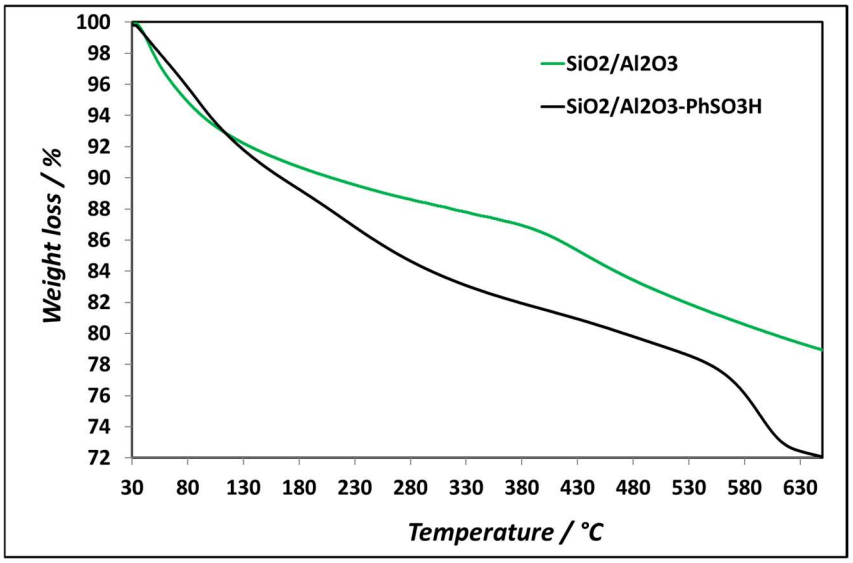

Figure 2. TGA comparison of silica-alumina and phenyl-sulphonic acid grafted on silica-alumina catalysts.

It can be observed in the range of 80-110° C the loss due to physically retained water resulting in a drop of 8 wt % in the silico-aluminate material. The weight loss due to the organic moiety covalently bonded onto the material was observed in the range of 500-600 °C in the functionalized aluminosilicate [19]. Clearly the weight loss attributed to water desorption results lowered by 2% in the functionalized aluminosilicate.

On the other side the thermal profile resulting from the analysis of functionalized propyl-sulphonic silica can be divided into three different regions (**figure 3**).

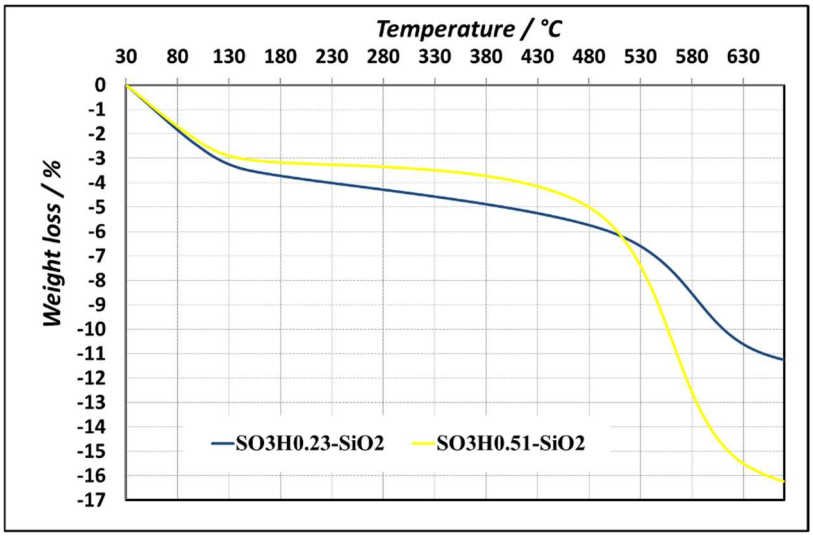

Figure 3. TGA comparison of different supported propyl-sulphonic acids.

The small weight loss at around 100°C is assigned, even in this case, to the adsorbed water; in the range of 200-400°C the weight loss is ascribed to mercaptopropyl decomposition, this was indeed confirmed by XPS spectra and then, by the TGA performed onto the unoxidized organic functionalized silica

(**figure 4 and 5**). A further weight loss is observed in the 400-600 °C that is referred to the decomposition of acid propyl-sulphonic groups anchored onto the material; the amount of the loss is clearly proportional to the amount of acid pendant and increases from 6 to 12 wt % passing from the lower acid material to the most acid one. Moreover, decomposition temperature range decreases from 510 to 480 °C with the increasing of acid loading [20].

Sulphonic acid group presence was also confirmed by XPS analysis (**figure 5**): functionalized silica-alumina exhibited only the peak assigned to sulfur in the sulphonic form at 169 eV while the SO_3H0.23-SiO_2 catalyst spectra presented another peak at 164 eV indicating that only partial oxidation of S-H occurred in this material [21].

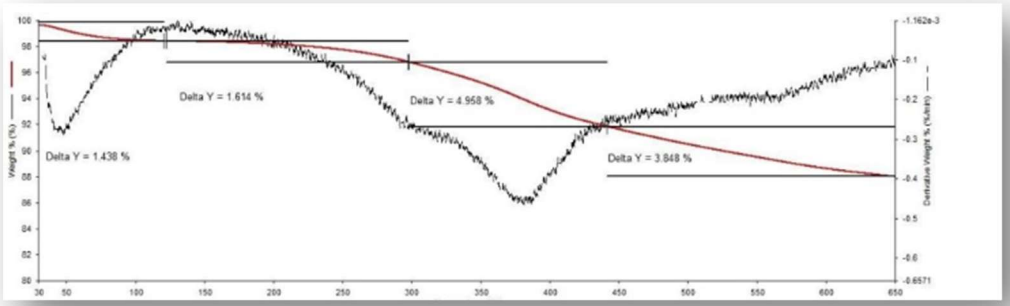

Figure 4. TG analysis on SiO_2-SH material.

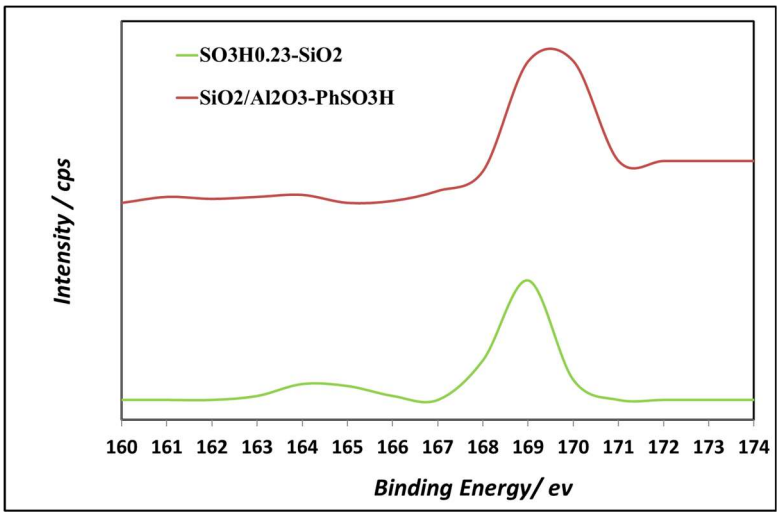

Figure 5. XPS spectra for propyl-sulphonic acid supported on silica and phenyl-sulphonic acid grafted on silica-alumina catalysts.

3.2.2 Catalytic activity results

Various aspects of catalyst such as acid site amount, typology (Bronsted and/or Lewis), location and strength are fundamental characteristics able to influence distribution of products and catalytic activity; this appears evident in the methanol dehydration reaction to give DME, where yield and selectivity towards DME are more important than methanol conversion. The first factor we considered was Bronsted acidity; for this purpose, we plotted the acidity of three different propyl functionalized silica (from 0.23 to 0.51 mmol H^+/g) with normalized (on catalyst amount) yield of DME at different temperatures (**figure 6**).

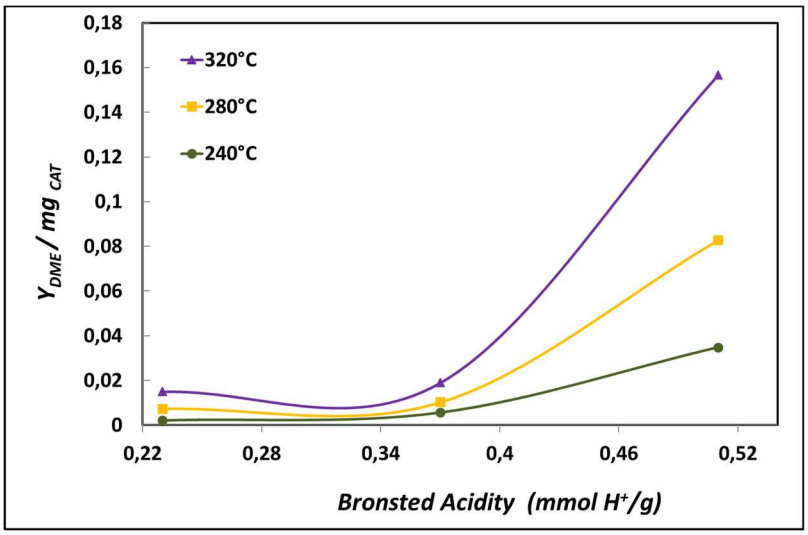

Figure 6. Catalytic results for three different supported propyl-sulphonic acids at three different temperatures, P = 1 bar and WHSW = 500 $g_{methanol} \cdot g_{cat}^{-1} \cdot h^{-1}$.

Undoubtedly the normalized conversion increases along with acidity increase; it appears evident that, considering the comparable surface area, the difference in the behavior can be ascribed to the different surface acidity. Light hydrocarbons and higher oxygenated compounds were not observed up to 320 °C. Various mechanism are nowadays proposed for the dehydration reaction performed over supported solid acid catalysts. Naccache e Bandiera [22] proposed that the reaction occurs at the Lewis basic site and its nearest Bronsted acid site passing through the formation of the surface species $[CH_3O]^-$ and $[CH_3OH_2]^+$ that can condense to form DME and water. A different reaction pathway has been suggested from Knozinger et al. [23] in which DME is basically formed through a surface reaction between methoxy anion adsorbed on the basic site and methanol adsorbed on the acid one.

Nowadays both Bronsted and Lewis acid sites role remains still unclear due to the lack of research about control of the amount of both types of acid sites loaded in the catalyst.

To better examine the role of surface acidity on the reaction, the supported sulphonic acids were modified adding alumina. Starting from the study proposed by Jiang et al. [8], in which is demonstrated that methanol conversion to DME increased with the decreasing of SAR (silica-alumina molar ratio) we selected the SAR of 3.2. The modification of propyl-sulphonic acid silica with alumina involved a good shift in terms of methanol conversion at significantly lower temperature (**figure 7**).

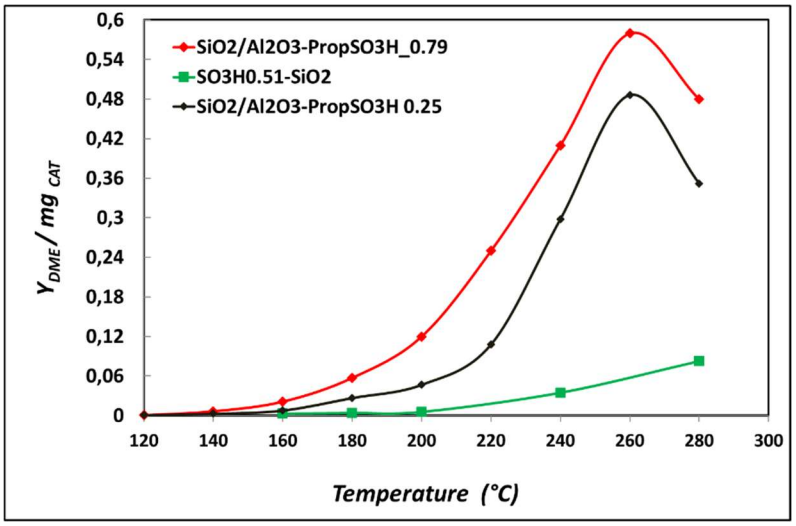

Figure 7. Catalytic comparison between silica-alumina supported acids and silica supported acid at P = 1 bar, time on stream = 2 h and WHSW = 500 $g_{methanol} \cdot g_{cat}^{-1} \cdot h^{-1}$.

Briefly, the activities followed the order of SiO_2 /Al_2O_3PropSO_3H_0.79 > SiO_2 /Al_2O_3PropSO_3H_0.25 > SO_3H0.51-SiO_2. It is seen that the SiO_2 /Al_2O_3PropSO_3H_0.79 demonstrated higher activity even at the temperature below 220 °C. At 260 °C, the activity reached maximum and then decreased proportionally with the increase of temperature. This is due to the equilibrium limitation since the reaction is exothermic. The much higher activity of propyl-sulphonic acid grafted on silica-alumina vs the one grafted on silica was not due to the much higher density of propane-sulphonic acid groups on silica-alumina. The sample prepared with a lower loading of propane-sulphonic acid groups on silica-alumina was more active than that with a higher loading of propane-sulphonic acid groups on silica so that it can be conclude univocally that the much higher activity was solely due to the acid properties of the support.

Grafting phenyl-sulphonic pendant on SiO_2 /Al_2O_3 (**figure 8**) involved a great improvement in catalyst activity for methanol dehydration reaction.

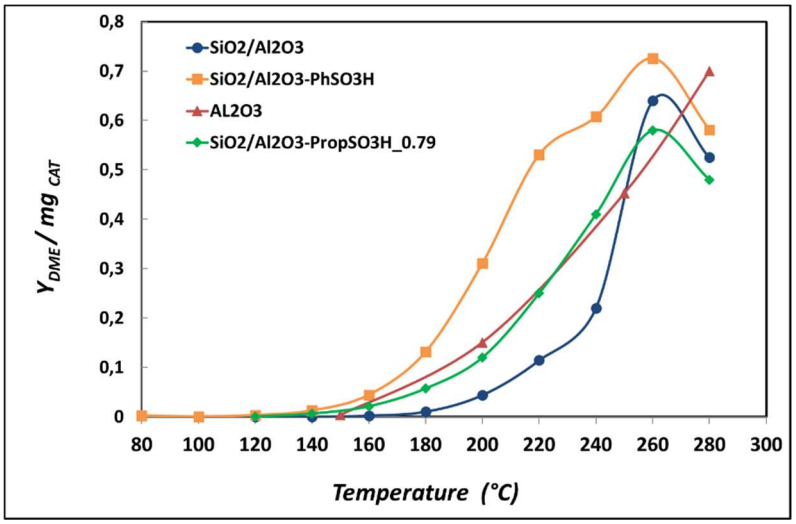

Figure 8. Catalytic comparison between different supported sulphonic acids on silica-alumina and commercial γ-Al_2O_3 catalysts at P = 1 bar, time on stream = 2 h and WHSW = 500 $g_{methanol} \cdot g_{cat}^{-1} \cdot h^{-1}$. Y_{DME} (pag 75)

In **figure 8**, it is possible to compare our synthesized catalysts with commercial γ-alumina under identical condition; our outcomes suggested a sort of synergism between Lewis and Bronsted acidity for methanol dehydration reaction. Higher activity of SiO_2-Al_2O_3-Ph-SO_3H in front of SiO_2-Al_2O_3-Prop-SO_3H could be correlated to higher value of pK_a of benzene sulphonic acid compared with that of propane-sulphonic one. The phenyl-sulphonic functionalized aluminosilicate exhibited high activity already below 200 °C. Charted achievements indicated that functionalization with sulphonic acids indeed increased the activity of the functionalized silico-aluminate and its activity in methanol dehydration reaction was indeed better than that of γ-alumina one at lower temperature. Bronsted acidity seemed to have a more crucial role compared to Lewis acidity from our results. The maximum of

catalysts activity for DME production was reached at 260 °C and then activity decreased with increasing temperature due to the loss of selectivity towards DME. In fact, it is well-known that dehydration of methanol, catalyzed by acid catalysts, represents the first step for transformation of methanol into olefins and hydrocarbons (**table 4**).

Table 4. Conversion, selectivity and yield at different temperatures for SiO_2/Al_2O_3, SiO_2/Al_2O_3-$PhSO_3H$ and γ–Al_2O_3 catalysts.

Catalyst	**Reaction Temperature[a] (°C)**	**X_{MeOH}[b] (wt %)**	**Selectivity (wt %) [c]**		**Y_{DME}[d] (wt %)**
			DME	**HCs**	
SiO_2/Al_2O_3	240	29	100	-	29
	260	86	98	2	84
	280	87	85	15	74
SiO_2/Al_2O_3-$PhSO_3H$	240	83	100	-	83
	260	92	100	-	92
	280	90	95	5	86
γ–Al_2O_3	240	61	100	-	61
	260	73	100	-	73
	280	89	100	-	89

[a] reaction temperature (°C); [b] Average conversion; TOS = 2h, 1bar and WHSW = 500 $g_{methanol}\cdot g_{cat}^{-1}\cdot h^{-1}$; [c] Average selectivity; TOS = 2h and WHSW = 500 $g_{methanol}\cdot g_{cat}^{-1}\cdot h^{-1}$; [d] Average yield; time on stream = 2h and WHSW = 500 $g_{methanol}\cdot g_{cat}^{-1}\cdot h^{-1}$.

No significant contribution for the formation of olefins and for higher oxygenated compounds was observed till 260°C; selectivity towards light hydrocarbons increased from 2% to 15% passing from 260°C to 280°C and this behavior of silica-alumina catalyst was comparable with reported literature

data [24]. High stability in front of hydrocarbons formation was also confirmed with the stability test (**figure 9**).

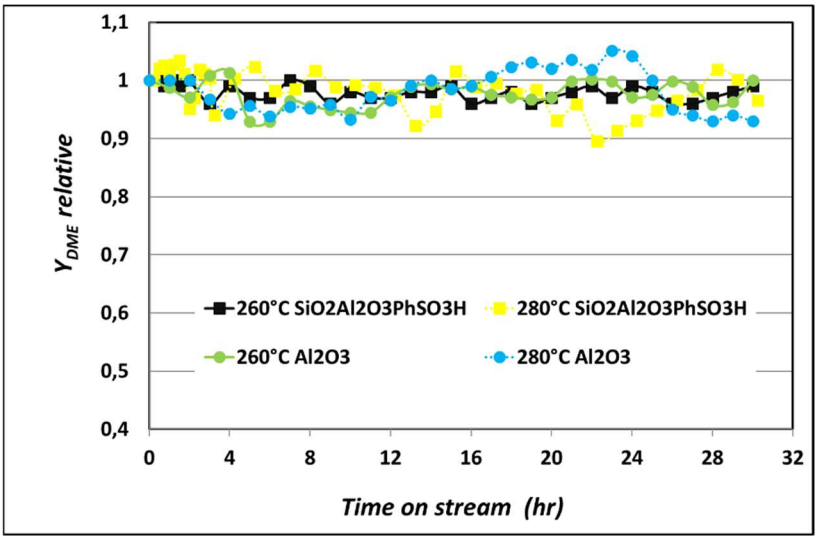

Figure 9. Normalized yield to DME of SiO_2/Al_2O_3-$PhSO_3H$ and γ-Al_2O_3 at different temperatures and WHSW = 500 $g_{methanol} \cdot g_{cat}^{-1} \cdot h^{-1}$.

The impossibility to regenerate the catalyst *in situ* clearly involves the fundamental aspect of having an high long-term stability of the catalyst and, as it can be seen, the material exhibited negligible changes for over 30 h of time on stream at 260 and 280 °C; stability was compared to that of γ-alumina, the commercial catalyst in this reaction. Activity showed a slight decrease with TOS at 280 °C due to the inhibition of acid sites by formation of water and also to hydrocarbon formation. No peaks relative to hydrocarbon formation was observed on GC at 260 °C, while a not very intense peak was observed at 280 °C; to verify the amount detected in GC, EDX analysis were performed on the spent catalyst measuring a weight increase in Carbon of only 1.7% corroborating the GC data.

SEM analysis confirmed the high thermal stability of all catalysts prepared and tested (**figure 10**).

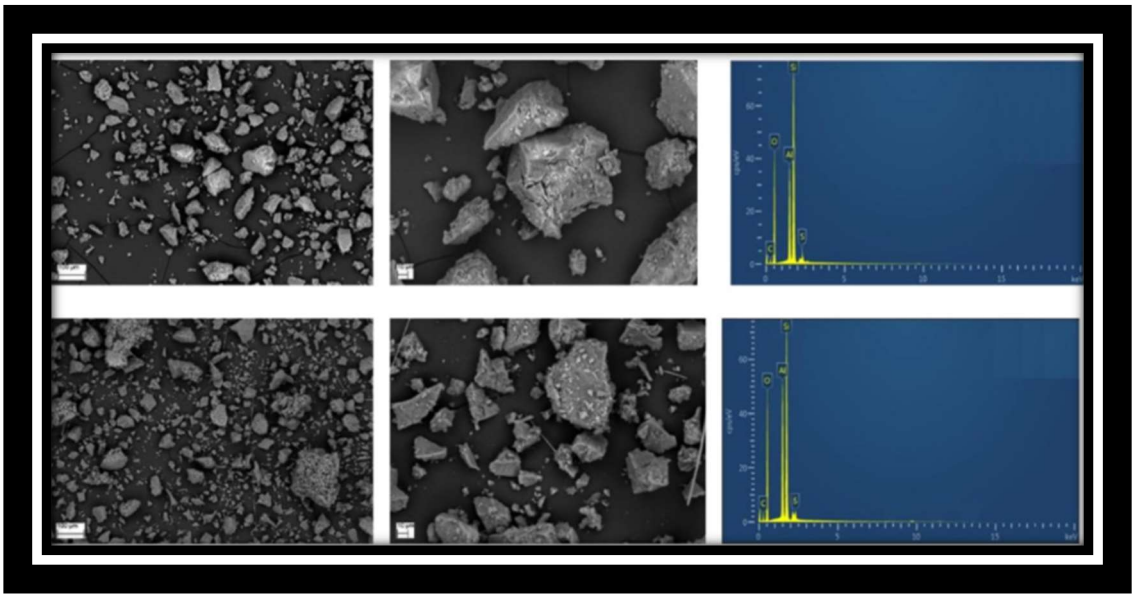

Figure 10. SEM images and EDS spectra of fresh (top) and spent (bottom) SiO_2/Al_2O_3-$PhSO_3H$ as catalyst in methanol dehydration reaction at 280 °C.

It was possible with this analysis, in a microstructural point of view, to prove that all catalysts exhibited a comparable aggregate size (from 2-3 up to 200 microns) in form of faceted particles. EDS analysis confirmed sulfur presence in the spent catalyst, suggesting that catalytic process did not involve a decrease in acid groups of the catalyst. SiO_2/Al_2O_3-$PhSO_3H$ was chosen as model to examine microstructure changes before and after catalytic reaction.

It is well known that water represent an inhibitor for the reaction due to the possibility of compete with methanol for catalytic sites [25]. For this reason, we investigated water effect adding water at a 3 Torr partial pressure into the reactant (**figure 11**).

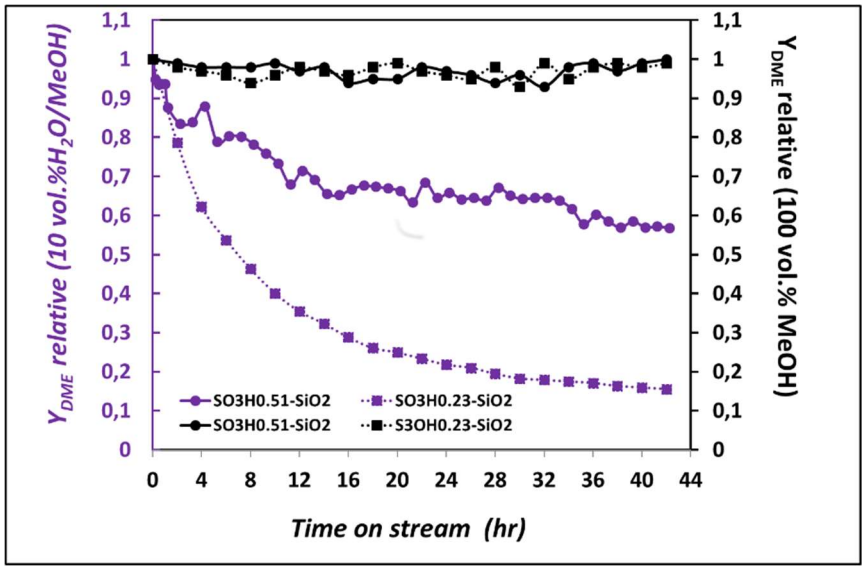

Figure 11. Normalized to its initial value yield to DME of $SO_3H0.51$-SiO_2 and $SO_3H0.23$-SiO_2 catalysts (black: without water, violet: with water) at 280 °C.

It's worth to notice that $SO_3H0.23$-SiO_2 and $SO_3H0.51$-SiO_2 catalysts showed an high thermal stability with only methanol in feed while for lower Bronsted acidity water deactivation process occurred more rapidly comparable to that of the higher acid catalyst after 42 hours at 280 °C. This result was indeed expected by TGA measurements (**figure 3**) because, in the temperature range relative to water desorption, $SO_3H0.51$-SiO_2 performed the lowest weight loss, suggesting a more hydrophobic behavior compared to the $SO_3H0.23$-SiO_2 catalyst. This hydrophobicity effect appeared even more visible for the silica-alumina functionalized with phenyl-sulphonic moiety (**figure 12**), confirming the crucial importance of synergism between Bronsted and Lewis acidity. Indeed, sulphonic group's addition to alumina surface in the supported aluminosilicate could decrease water adsorption by modifying surface hydrophobicity leading to increase catalyst activity.

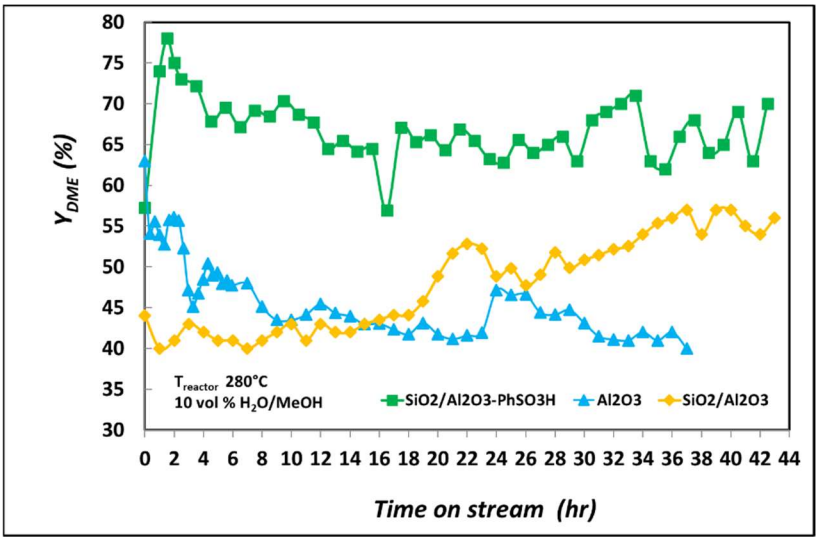

Figure 12. Comparison of the effect of water addition over γ-Al_2O_3, SiO_2/Al_2O_3 and SiO_2/Al_2O_3-$PhSO_3H$ catalysts (N_2 = 10.7 mL/min, P_{MeOH} = 81 Torr, P_{H2O}= 3 Torr; T = 280 °C).

It can be seen comparing γ-alumina and SiO_2/Al_2O_3-$PhSO_3H$ that, with a 10% vol. water/methanol fed in the stream at 280 °C, functionalized catalyst exhibited a better performance; γ-alumina was initially deactivated with water addition stabilizing its activity to 65-70 % of the initial value; this behavior is well known in literature [7]. On the other side, SiO_2/Al_2O_3-$PhSO_3H$ exhibited a great stability with cofeeding of water and methanol resulting even in a positive effect on catalyst deactivation probably due to the removal of deposited carbon from the catalyst by water (only 0.9 wt.% in carbon was detected on spent catalyst with water in feed). Bronsted acidity increased during the reaction from 0.9 mmol H^+/g to 0.93 mmol H^+/g due to partial transformation of Lewis acid sites in Bronsted acid ones; this hypothesis was also confirmed by activity of the unfunctionalized silica-alumina that increased proportionally with TOS.

3.3 Conclusion

A new catalyst for methanol dehydration has been successfully synthesized loading sulphonic acid moiety onto silica-alumina and silica. In this work, acidity came out to be the fundamental property for catalyst selectivity, activity and stability. A greater amount of strong acid sites on the catalyst leads indeed to best DME result in terms of yield. From the reported study it can be pointed out that SiO_2/Al_2O_3-$PhSO_3H$ (Si/Al = 3.2) exhibited the best catalytic performances in terms of selectivity, activity and stability at various temperatures (200-280 °C). Compared with γ-Al_2O_3, the commercial source for this reaction, the tested catalyst demonstrated a higher resistance to water deactivation.

3.4 Experimental section

3.4.1 Catalysts preparation

All the reagents were purchased and used as received without further purifications. Before functionalization the siliceous supports were dried at 120 °C for 5 hours. The amorphous silica used was the commercial one from VWR chemicals (40-63 mm). The surface acidity was determined by a reported titration method [26]. Sulphonic acid catalysts have been synthesized according to general procedures reported in literature [27-28].

3.4.1.1 Preparation of functionalized propyl-sulphonic acid anchored on silica (scheme 1)

Propyl-sulphonic acids tethered on silica-alumina and silica were named respectively SiO_2-Al_2O_3-PropSO_3H_x and SO_3Hx-SiO_2 where x is for calculated Bronsted acidity of supported catalyst.

For the three different alumina bearing propyl-sulphonic moiety *SO_3H0.51-SiO_2, SO_3H0.37-SiO_2, SO_3H0.23-SiO_2* the following procedure was used: siliceous support KG-60 silica (8g), dried for 3 hours at 120° C, was placed under reflux in Toluene (110° C) with MPTS (3-mercaptopropyl-trimethoxysilane) (8.2, 6.1 and 3 mmol respectively) under stirring for 24 hours; the resulting propylmercaptane was treated with 100 ml (1 mol) 30% aq H_2O_2 for 24 h at room temperature under stirring adding two drops of sulphuric acid after 12 hours to accomplish the oxidation to propane-sulphonic acid.

Scheme 1. Preparation of propanesulfonic acids tethered onto silica .

3.4.1.2 *Preparation of propyl-sulphonic and phenyl-sulphonic acids onto silica-alumina (SiO_2/Al_2O3-$PropSO_3H$ and SiO_2/Al_2O_3-$PhSO_3H$) (scheme 2)*

The aluminosilicate with SAR 3.2 was obtained by refluxing and mixing TEOS (tetraethyl orthosilicate, 12.5 ml, 55 mmol), aluminum triisopropoxide (35 mmol, 7.2 g) and ethanol (7.5 ml); to the homogeneous mixture H_2O (2.6 ml) and NH_4OH (30% 2.6 ml) were added slowly as gelating agents. The solution was kept under reflux for a few minutes till gelation; the gel was then dried at 100 °C and calcined at 400 °C for 70 h.

SiO_2/Al_2O_3-$PhSO_3H$ -The so obtained support (2.5 g) was stirred, under reflux, with phenyltriethoxysilane (4.15 mmol) in Toluene to give the supported phenyl; the supported phenyl material was then sulfonated by refluxing with chloro-sulphonic acid (120 mmol, 8 ml) for 4 h in 1,2 dichloroethane (30 ml). The obtained solid material was then filtrated and washed carefully with acetone (60 ml), 1,2 dichloroethane (60 ml) and water (200 ml).

SiO_2/Al_2O_3-$PropSO_3H$_0.25 and SiO_2/Al_2O_3-$PropSO_3H$_0.79 - The aluminosilicate previously obtained (2g) was refluxed, under stirring, with MPTS (3-mercaptopropyl-trimethoxysilane) (1.5 and 4.15 mmol) for 24 hours in Toluene (25 ml); obtained solid was filtered and washed; The oxidation of the

obtained thiol moiety was carried out, under stirring, in H_2O_2 (30 ml) for 24 h at room temperature adding a few drops of sulphuric acid after 12 h.

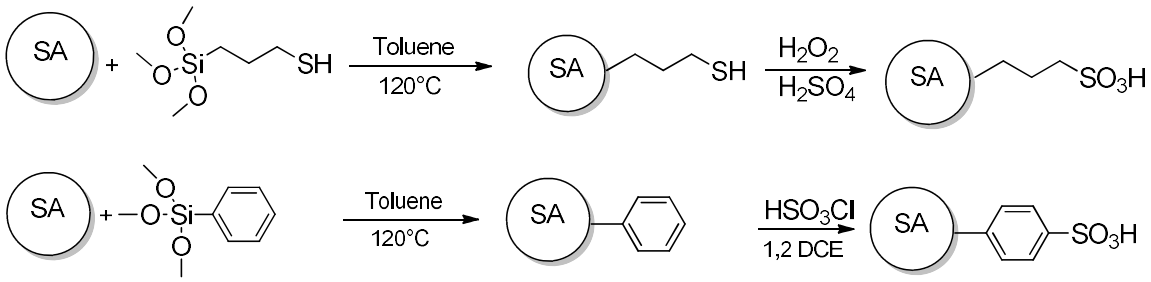

Scheme 2. Preparation of arylsulfonic and propylsulfonic acid tethered onto silica-alumina.

3.4.2 Catalyst characterization

BET analysis was carried out using Micrometrics ASAP 2020 with liquid N_2 at -196 °C. Each sample was degassed at 200 °C for 15 h before measurement to remove any impurities and moisture. The total surface area was calculated by the BET method.

XRD patterns were collected on a Rigaku Miniflex X-ray diffractometer using a Ni filtered Cu Kα source operated at 30kV at a scan rate of 0.05° s^{-1}.

The thermogravimetric analysis (TGA) technique involves thermal treatment of solid in inert atmosphere to give information about the moisture content, adsorbed gases and the thermal stability of the adsorbent. The TGA was carried out for all catalysts using Netzsch STA 409 instrument. The samples were heated in the presence of air from 30 to 1000 °C.

Inductively Coupled Plasma-Optical Emission Spectrometer (ICP-OES; Genesis by Spectro) was used for determination of sulfur elemental analyses (EA). The ion exchange capacities of the sulphonic mesoporous materials were determined using the solid acid titration technique.[29] Aqueous solutions of sodium chloride (NaCl, 2M) and tetrabutylammonium chloride (TBAC, 0.05 M) were used as ion-exchange agents to determine the acid capacities of the materials. In a typical experiment, 0.10 g of solid treated at 200 °C for one day was added to 20 ml of aqueous solution containing the corresponding salt. The resultant suspension was equilibrated for 6 h, and then filtered and washed with small amount of water and finally, the filtrate was titrated by aqueous solution of 0.01 M NaOH solution using phenolphthalein as pH indicator.

X-ray photoelectron spectroscopy (XPS) was applied to identify the oxidation state of S. A VSW HAC 5000 hemi-spherical electron energy analyzer and a non-monochromatic Mg Kα X-ray source (1253.6 eV). was used and selected catalyst samples were analyzed using both monochromatic Al Kα and achromatic Mg Kα X-ray sources.

In the SEM analysis the samples were supported on aluminum stub covered by carbon tape with gold to improve the conductivity of the electron beams, and then subjected to a vacuum condition in a chamber prior to analysis. The SEM analysis was carried out using energy dispersive x-ray analysis (EDXA) technique and a scanner (model: SEM, ZEISS EVO MA15).

3.4.3 Catalytic activity test

The catalytic activity of the prepared catalysts was evaluated in a tubular reactor with an inner diameter of 4 mm and a catalyst loading of 100 mg. The operation conditions, including the temperature/pressure in the fixed-bed reactor and the flow rates of inlet gases, were controlled by thermocouples and manometers. Gaseous methanol (purity>99.99%) was supplied at 1 sccm (standard cubic centimeter per minute, mL min^{-1}) by passing a nitrogen flow (10.7 ml/min) controlled by a MKS mass flow controller through a saturator, which held liquid methanol at 20 °C. Photo of the real working apparatus in **figure 13.** A GC-TCD-FID instrument (gas chromatography - thermal conductivity- flame ionization detector, Thermo TRACE 1300 instrument) were connected to the catalytic reactor. In order to identify the concentrations of each species, their concentration calibration curves were analyzed by GC-TCD-FID previously. In the duration of the catalytic reaction, the gaseous products were fed with an inert flowing He carrier gas at 50 sccm through the injection and a Rt-U-BOND–30 m RESTEK capillary column GC column. In the experiment to study the effect of water on the methanol consumption and DME formation, we used the previous protocol replacing methanol in the saturator by a water methanol mixture at 20 °C (10 wt% H_2O with 90 wt% MeOH). To avoid possible condensation of water, methanol, DME or hydrocarbons, the temperature of the effluent line was constantly maintained above 100 °C. Experimental results are presented in terms of methanol conversion (X_{MeOH}), DME yield (Y_{DME}) and selectivity (S_{DME}), hydrocarbons selectivity (S_{HCs}) and conversion yield to DME relative to its initial value ($Y_{DME\ relative}$) defined as it follows:

1 $$X_{MeOH} = mol_{MeOH\ converted} / mol_{MeOH\ initial} \quad (1)$$

$$Y_{DME} = 2 * mol_{DME} / mol_{MeOH\ initial} \quad (2)$$

$$S_{DME} = 2 * mol_{DME} / mol_{MeOH\ converted} \quad (3)$$

$$S_{HCs} = mol_{HCs} / mol_{MeOH\ converted} \quad (4)$$

$$Y_{DME\ relative} = Y_{DME} / Y_{DME\ initial} \quad (5)$$

Figure 13. Real experimental apparatus for DME synthesis.

3.5 References

[1] *Iwao Omae. Aspects of carbon dioxide utilization. Catalysis today 115, 2006 33-52.*

[2] *Mar Pérez-Fortes, Andrei Bocin-Dumitriu, Evangelos Tzimas. CO2 Utilization Pathways: Techno-Economic Assessment and Market Opportunities. Energy Procedia 63 (2014) 7968 – 7975.*

[3] *Rosa M. Cuellar-Franca, Adisa Azapagic. Carbon capture, storage and utilisation technologies: A critical analysis and comparison of their life cycle environmental impacts. Journal of CO2Utilization 9 (2015) 82–102.*

[4] *Yoo, J.R.; Choi H. G.; Chung, C. H.; Cho, S. M. Fuel cells using dimethyl ether. J. of Power Sources 2006, 163, 103-106.*

[5] *Cocco, D.; Tola V.; Cau G. Performance evaluation of chemically recuperated gas turbine (CRGT) power plants fuelled by di-methyl-ether (DME). Energy 2006, 31, 1446-1458.*

[6] *Arcoumanis, C.; Bae, C.; Crookes, R.; Kinoshita, E. The potential of dimethyl ether (DME) as an alternative fuel for compression-ignition engines: A review. Fuel 2008, 87, 1014 - 1030.*

[7] *Raoof, F.; Taghizadeh, M.; Eliassi, A.; Yaripour, F. Effects of temperature and feed composition on catalytic dehydration of methanol to -alumina. Fuel 2008, 87, 2967 - 2971.*

[8] *Jiang, S.; Hwang, J. S.; Jin, T.; Cai, T.; Cho, W.; Baek, Y. S.; Park, S.E. Dehydration of methanol to dimethylether over ZSM-5 zeolite. Bull. Korean Chem. Soc. 2004, 25, 185-189.*

[9] *Li, J. L.; Zhang, X. G.; Inui, T. Effect of the property of solid acid upon syngas - to-dimethyl ether conversion on the hybrid catalysts composed of Cu Zn Ga and solid acids. Appl Catal A 1996, 147, 23-33.*

[10] *Fu, Y.; Hong, T.; Chen, J.; Auroux, A.; Shen, J. Surface acidity and the dehydration of methanol to dimethyl ether. Thermochim. Acta 2005, 434, 22- 26.*

[11] *Seo, C. W.; Jung, K. D.; Lee, K. Y.; Yoo, K. S. Dehydration of methanol over Nordstrandite based catalysts for dimethyl ether synthesis. J. Ind. Eng. Chem. 2009, 15, 649 - 652.*

[12] *Mollavali, M.; Yaripour, F.; Mohammadi, F. S.; Atashi, H. Relationship between surface acidity and activity of solid-acid catalysts in vapor phase dehydration of methanol. Fuel Process. Technol. 2009, 90, 1093 - 1098.*

[13] *Yang, Q.; Kong, M.; Fan, Z.; Meng, X.; Fei, J.; Xiao, F. Aluminum Fluoride Modified HZSM-5 Zeolite with Superior Performance in Synthesis of Dimethyl Ether from Methanol. Energy Fuels 2012, 26, .*

[14] *Vishwanathan, V.; Jun, K. W.; Kim, J. W.; Roh, H. S. Vapour phase dehydration of crude methanol to dimethyl ether over Na-modified H-ZSM5 catalysts. Appl. Calal. A: General 2004, 276, 251-255.*

[15] *D. T. Production of Clean Transportation Fuel Dimethylether by Dehydration of Methanol Over Nafion Catalyst. Gazi Univ. J. Sci. 2008, 21, 37 41.*

[16] *Barbarossa, V.; Viscardi, R.; Maestri, G.; Maggi, R.; Paris, E. Sulfonated catalysts for methanol dehydration to dimethyl ether (DME). Material Research Bulletin 2019, 113, 64-69.*

[17] *R. Maggi, C. G. Piscopo, G. Sartori, L. Storaro, E. Moretti. Supported sulphonic acids: Metal-free catalysts for the oxidation of hydroquinones to benzoquinones with hydrogen peroxide", Applied Catalysis A: General 2012, 411-412, 146-152.*

[18] *Jin, H.; Ansari, M. B.; Park, S.E. Sulphonic acid functionalized mesoporous ZSM-5: Synthesis, characterization and catalytic activity in acidic catalysis. Catalysis Today 2015, 245, 116-121.*

[19] *Moralese G., Athensb G., Chmelkab B. F., van Griekena R., Melero J. A. Aqueous-sensitive reaction sites in sulphonic acid-functionalizedmesoporous silicas. Journal of Catalysis 2008, 254, 205 217.*

[20] *Wang, X.; Cheng, S.; Chan, J. C. C. Propylsulphonic Acid-Functionalized Mesoporous Silica Synthetized by in Situ Oxidation of Thiol Groups under*

Template-Free Condition. The Journal of Physical Chemistry C 2007, 111, 2156-2164.

[21] *González, M. D.; Salagre, P.; Taboada, E.; Llorca, J.; Molins, E.; Cesteros, Y. Sulphonic acid-functionalized aerogels as high resistant to deactivatio catalysts for the etherification of glycerol with isobutene. Appl. Catal. B-Environ. 2013, 136, 287 293.*

[22] *Bandiera, K.; Naccache, C. Kinetics of methanol dehydration on dealuminated H-mordenite: Model with acid and basic active centres. Appl. Catal. 1991, 69, 139-148.*

[23] *Knözinger, H.; Kochloefl, K.; Meye, W. Kinetics of the bimolecular ether formation from alcohols over alumina. J. Catal. 1973, 28, 69-75.*

[24] *Takeguchi, T.; Yanagisawa, K.I.; Inui, T.; Inoue. M. Effect of the property of solid acid upon syngas-to-dimethyl ether conversion on the hybrid catalysts composed of Cu Zn Ga and solid acids. Appl. Catal. A 2000, 192, 201-209.*

[25] *Xu, M.; Lunsford, G. H.; Goodman, D. W.; Bhattacharyya, A. Synthesis of dimethyl ether (DME) from methanol over solid-acid catalysts. Appl.Catal. A 1997, 149, 289-301.*

[26] *S. Leveneur, D. Y. Merzin, T. Salmi, J. Mol. Cat. A: Chem.,* ***2009****, 303, 148*

[27] *C.G. Piscopo, S. Buhler, G. Sartori, R. Maggi, Supported sulphonic acids: reusable catalysts for more sustainable oxidative coupling of xanthene-like compounds with nucleophiles.Catalysis Science & Technology 2012, 2, 2449-2452.*

[28] *R. Maggi, N. R. Shiju, V. Santacroce, G. Maestri, F. Bigi, G. Rothenberg, Silica-supported sulphonic acids as recyclable catalyst for esterification of levulinic acid with stoichiometric amounts of alcohols, Beilstein J. Org. Chem. 2016, 12, 2173 2180.*

[29] *R. Maggi, C. G. Piscopo, G. Sartori, L. Storaro, E. Moretti. Supported sulphonic acids: Metal-free catalysts for the oxidation of hydroquinones to benzoquinones with hydrogen peroxide", Applied Catalysis A: General 2012, 411-412, 146-152*

4) Site-selective double- and tetra-cyclization routes to fused polyheterocyclic structures by Pd-catalyzed carbonylation reactions

4.1 Introduction

Carbon monoxide is considered nowadays one of the most versatile carbon containing compound. For decades our knowledge about CO was limited to its reputation of flammable, tasteless, colourless and toxic gas [1]. In 1780 F. Fontana discovered the water gas shift reaction that was not largely utilized till '900; starting from 1920 with the Fisher and Tropsch process scientific community implemented a huge variety of methodologies to obtain syngas[2] and, starting from it, to provide a huge amount of different products. Besides syngas utilization, in recent years, several example of carbon monoxide utilization in carbonylation reaction have been developed and reported; undoubtedly carbonylation reactions catalyzed by transition metal continue to play an important role for the synthesis of chemicals bearing carbonyl group both on industrial and laboratory scale.[3] Palladium-based carbonylation techniques[4] are characterized by high versatility and great functional group tolerance and, at best, enable the synthesis of richly elaborated molecules by exquisite reaction sequences where multiple C-C and C-heteroatom bonds are assembled in a one-pot fashion.[5] The Pd-catalyzed carbonylative pentacyclization reaction reported by Negishi and coworkers is an impressive but rare example of complexity,[5] where the simultaneous presence of many competing functionalities can result in a high level of molecular sophistication. Significant examples of this idea have been recently reported by Bäckvall[6] who, for instance, described the construction of seven-membered carbocycles

through an olefin-assisted palladium-catalyzed oxidative carbocyclization–alkoxycarbonylation of bisallenes.[7] Recently, Jiang and co-workers developed a successful, ligand-controlled and palladium-catalyzed, cyclization and carbonylation reaction sequence for regioselective syntheses of indolo[3,2-*c*]coumarins and benzofuro[3,2-*c*]quinolinones starting from substrates bearing both OH and NHR moieties.[8] Obviously for this kind of reaction, good regio-, chemo- and stereoselectivities are generally difficult to achieve and a well planned and efficient catalytic control over the reaction outcome still represents a formidable challenge.[9] In addition, the tricky construction of the starting material add further concern by compromising a possible future application. Recently, prof. Della Cà and coworkers developed an efficient palladium-catalyzed method for indole-fused furanones synthesis [10] as an example of realization of molecular complexity by carbonylation of easy accessible multifunctional starting materials.

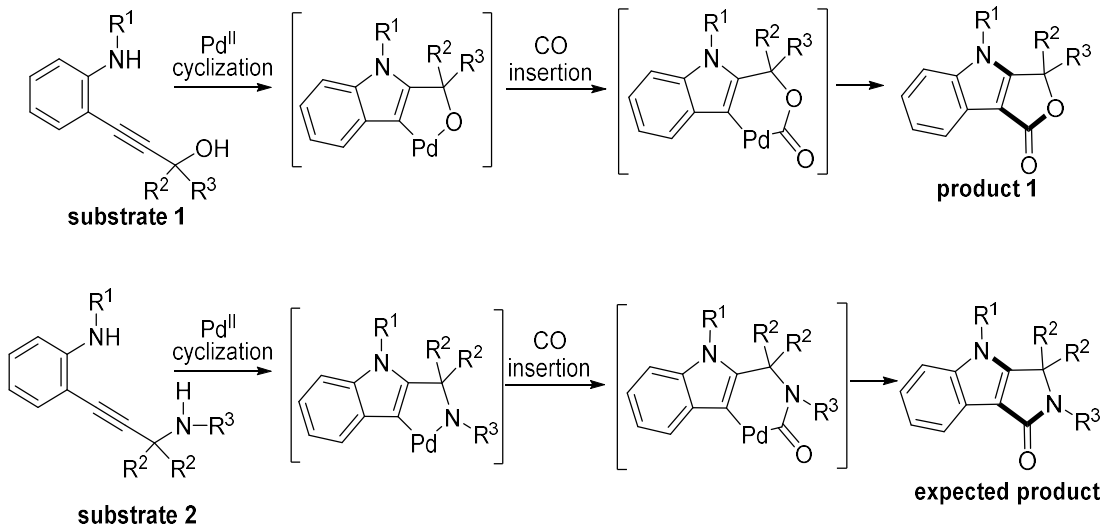

Scheme 1

In particular, anilines functionalized with propargyl alcohol moieties in *ortho* position led to a variety of polycyclic furo[3,4-*b*]indol-1-ones through a path consisting of indolization , carbonylation and lactonization reactions in presence of PdI_2/KI, as highly effective and stable catalytic system[11]. Starting from these results my work focused on the study of the reactivity of "substrate 2" type bearing amino moiety instead of the alcoholic one (**scheme 1**). It was supposed that type 2 substrates, in the same catalytic condition of type 1 substrates, should have followed the same reaction pathway. Surprisingly, a selective and efficient route to oxazino[5,6-*c*] quinolin-5-ones (**scheme 2**) when amide was present (**product 2a**), and an impressive sequence to non-symmetric fused heterocyclic structures starting from the free amino group were instead discovered (**product 3a**).

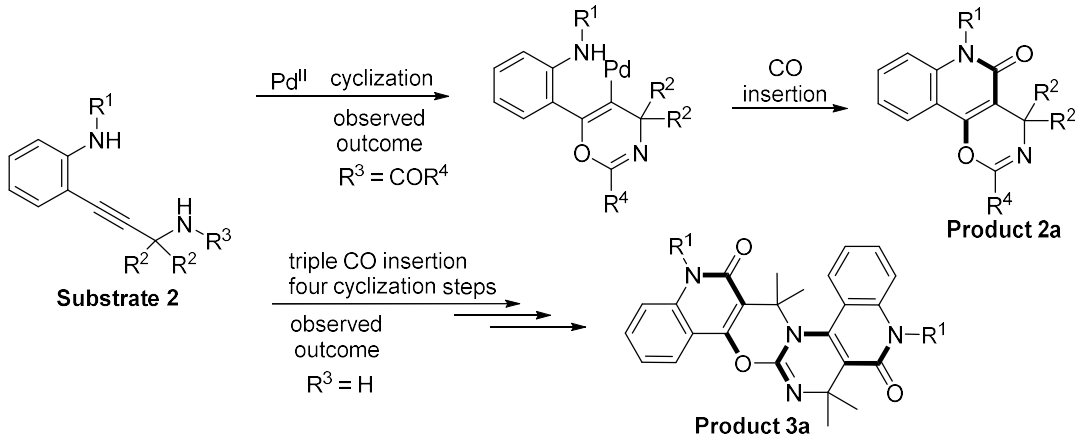

Scheme 2

4.2 Results and discussion

To prove our envisioned reactivity, we initially used the *N*-benzyl-2-(3-(benzylamino) -3-methylbut-1-yn-1-yl) aniline, bearing an alkyl substituent on the N (**scheme 3**), which is electronically similar to the hydroxyl group. However, under the original reaction conditions, which led to the formation of indole-fused furanones from anilines bearing propargyl alcohol moieties (**scheme 1** substrate 1 type), a complex mixture of unidentified organic compounds was observed. Further efforts aimed at improving the synthetic value of this reaction were totally unfruitful. We then decided to employ compound **1a** displaying a carbonyl group on the propargyl amine moiety, as model substrate. When amide **1a** (**scheme 3**) was treated with PdI_2 (1 mol%), KI (10 mol%) in the presence of CO (1.2 MPa) and air (4.8 MPa) in MeCN at 120 °C for 24 h, again the envisioned indole γ-lactam product (**scheme 1**) was not observed. Surprisingly, oxazino[5,6-*c*] quinolin-5-one **2a** was obtained in 62% yield instead (as determined by ^{1}H NMR analysis)

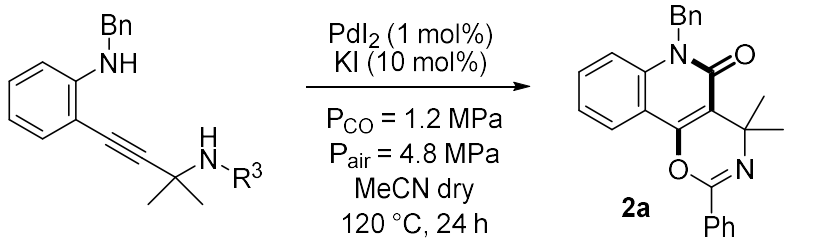

Scheme3

Probably, mechanism starts (**scheme 4**) with the nucleophilic attack of the O onto the activated triple bond by Pd (II) species leading to intermediate **I-1** (**scheme 4**). This pathway seems to be preferred with respect to the sequential indolization and CO insertion to give the expected product 1 type. As a result,

the tricyclic fused 6-membered heterocycle **2a** was produced by CO insertion and subsequent intramolecular nucleophilic amine displacement. Curiously, despite (1) Baldwin's rules allow for both types of cyclization,[12] (2) several previous examples strongly call for a 5-*exo*-dig[13] pathway over the 6-*endo*-dig one,[14] and (3) the 5-membered ring formation is often the preferred pathway when indole/indolones can be generated[15], a complete selectivity towards 6-membered rings is here observed.

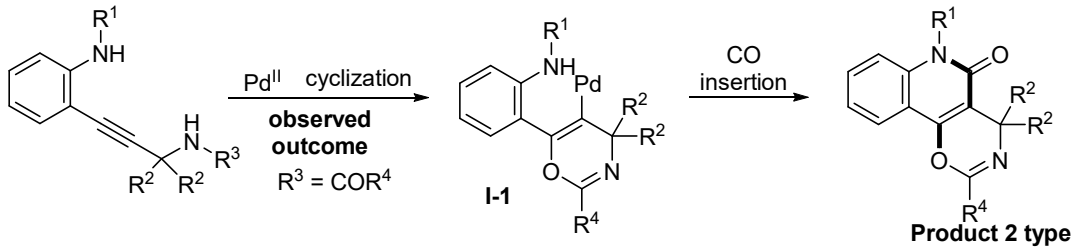

Scheme 4

With these results in hand, we set out to optimize the reaction conditions (**table 1**).

Table1

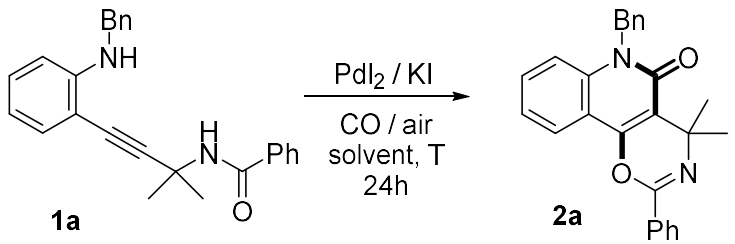

Entry	Solvent (dry)	KI (mol%)	CO/air (MPa)	T (°C)	Conv (%) **1a**[b]	Yield (%) **2a**[c,d]

1	MeCN	10	1.2/4.8	120	100	62
2	MeCN	10	0.6/2.4	120	100	28
3	MeCN	10	1.6/0.4	120	100	63
4	MeCN	10	1.6/0.4	100	100	76
5	**MeCN**	**10**	**1.6/0.4**	**80**	**100**	**86(83)**
6	MeCN	10	0.8/0.2	80	100	55
7	MeCN	10	1.6/0.4	60	100	65
8	MeCN	5	1.6/0.4	80	100	42
9	MeCN	20	1.6/0.4	80	73	56
10	1,4-Dioxane	10	1.6/0.4	80	100	15
11	DME	10	1.6/0.4	80	100	27
12	Toluene	10	1.6/0.4	80	89	6
13[e]	MeCN	10	1.6/0.4	80	100	63
14[f]	MeCN	10	1.6/0.4	80	100	32
15[g]	MeCN	10	1.6/0.4	80	100	75
16[h]	MeCN	-	1.6/0.4	80	100	58

[a] Reaction conditions: **1a** (0.5 mmol), PdI_2 (1 mol%), KI (Pd/KI molar ratio is1/10), solvent (5 mL), CO/air (reported pressure measured at 25 °C), 45 ml autoclave, 24h. [b] Conversion of **1a** was determined by ^1H NMR analysis with the internal standard method. [c] Yields were determined via ^1H NMR analysis with the internal standard method. [d] Isolated yield in brackets. [e] 10 mL of solvent. [f] 0.5 mol% of PdI_2. [g] 2.0 mol% of PdI_2. [h] 1 mol% of K_2PdI_4 in place of PdI_2/KI.

First, we noticed that decreasing the temperature was beneficial to this transformation. To our delight, yield of **2a** improved up to 86% when the reaction temperature was set at 80 °C. Different ratio CO/air and pressure were then tested, and the best results were achieved with 1.6/0.4 MPa of the CO/air mixture. Among the examined solvents, MeCN (anhydrous) clearly emerged as

a suitable reaction medium in which product **2a** was produced with higher selectivity. Amount of KI, PdI_2 and the optimal substrate concentration were further considered. Therefore, the use of PdI_2 (1 mol%), KI (10 mol%), CO (1.6 MPa), air (0.4 MPa) in anhydrous MeCN at 80 °C was defined as the optimized reaction conditions for exploring the reaction scope.

We were able to synthesize a good variety (**Table 2**) of substrates bearing EWG and EDG groups to evaluate the scope of the reaction; all the substrates were obtained in good yields using well known procedures:

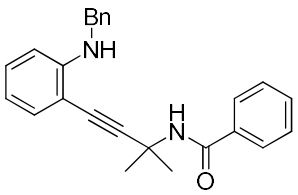

1a (65%)

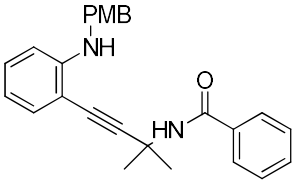

1b (73%)

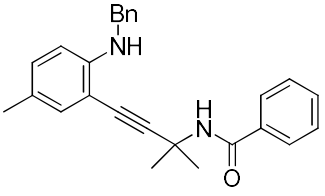

1c (47%)

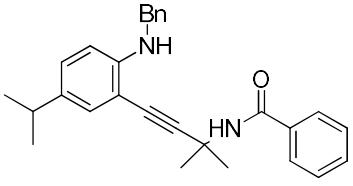

1d (62%)

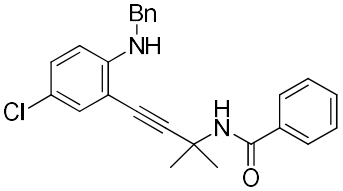

1e (41%)

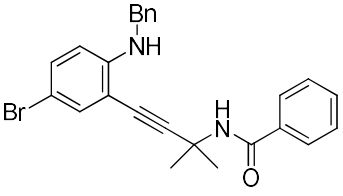

1f (71%)

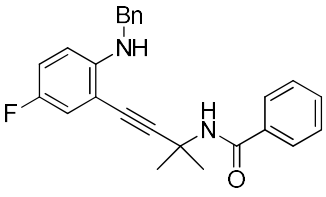

1g (67%)

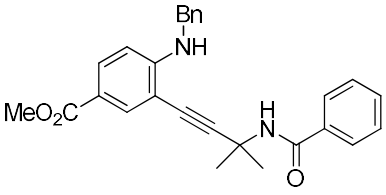

1h (70%)

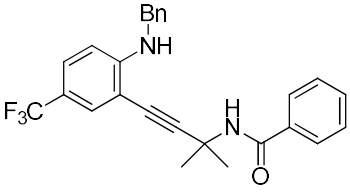

1i (65%)

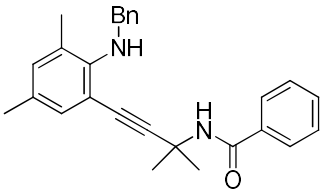

1j 50%

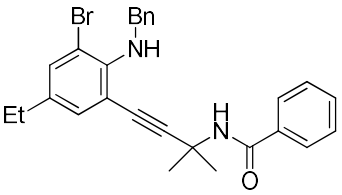

1k (80%)

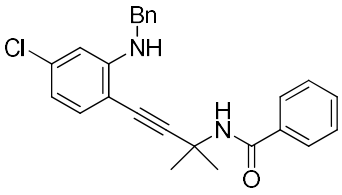

1l (65%)

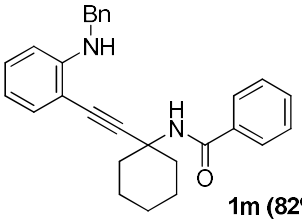

1m (82%)

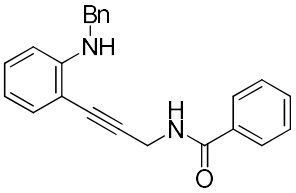

1n (44%)

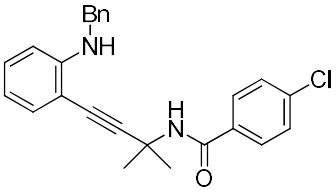

1o (60%)

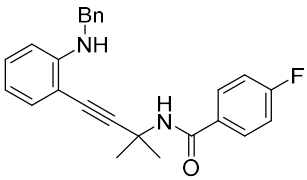

1p (60%)

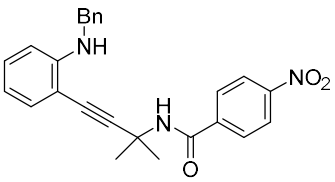

1q (70%)

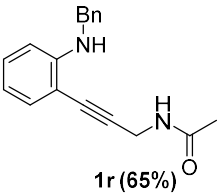

1r (65%)

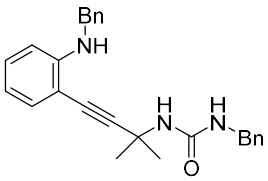

1s (84%)

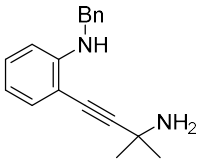

1t (67%)

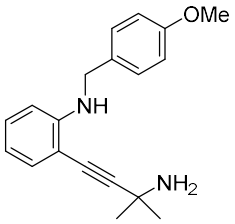

1u (84%)

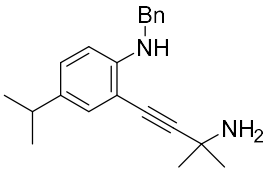

1v (74%)

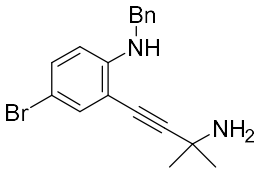

1w (89%)

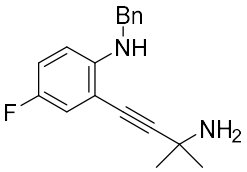

1x (72%)

All the so obtained substrates have been made to react in previous optimized carbonylative condition (**Table 1**) leading to a good number of products in satisfactory to excellent yield (**Table 3**).

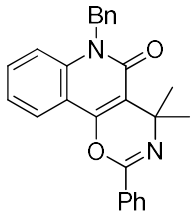

2a (83%)

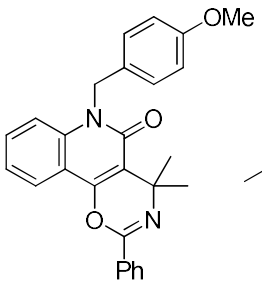

2b (80%)

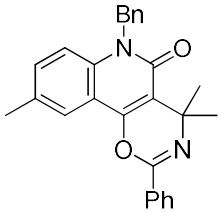

2c (88%)

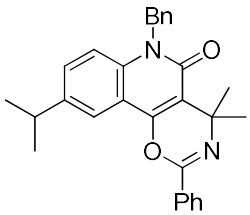

2d (93%)

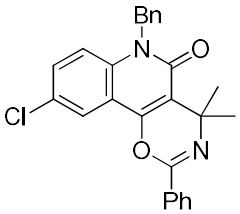

2e (72%)

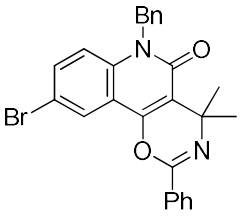

2f (81%)

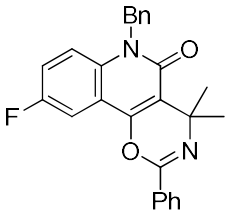

2g (89%)

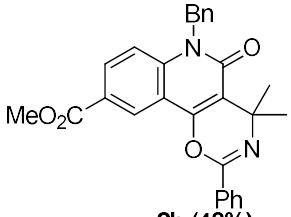

2h (48%)

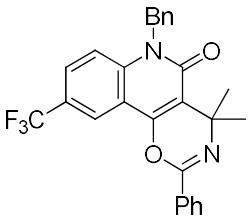

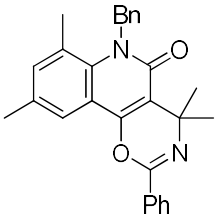

2j (62%)

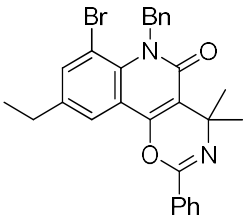

2k (12%)

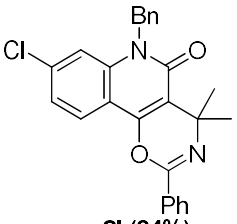

2l (84%)

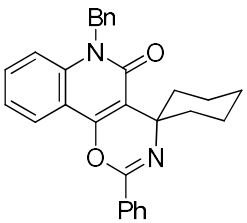

2m (73%)

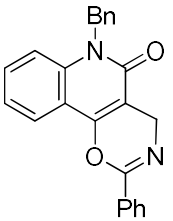

2n (58%)

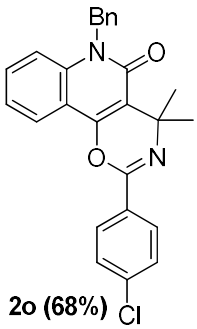

2o (68%)

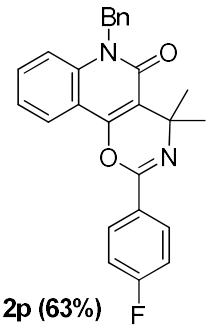

2p (63%)

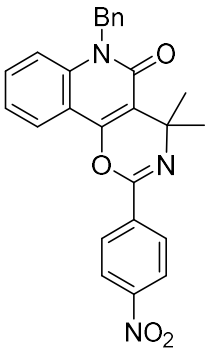

2q (82%)

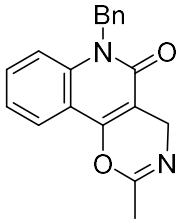

2r (38%)

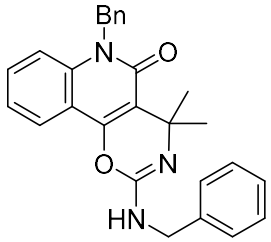

2s (80%)

Table 3 reaction scope

A range of electron-donating (ED) and electron-withdrawing (EW) groups on the aromatic ring in *para* position to the N (R^2, Table 2), including chloro, bromo, fluoro and ester, were successfully tolerated in this transformation. *Ortho* and *meta* substitutions were also demonstrated (**2j**, 62% and **2l**, 84%), even though some limitations were present (**2k**, 12%). Alkyl groups in *alpha* to the triple bond (R^3) were found to promote the sequential carbonylative cyclization, probably for *gem*-dialkyl effect (**2a-m**). However, the absence of substituents in this position afforded the corresponding product in satisfactory yield (**2n**, 58%). The R^4 group of the amide moiety was then studied. Aryl and alkyl substituents were positively tolerated (**2o-q**, **2s**). Reaction with substrate **1r** having an *ortho*-pyridine ring as R^4 was quite sluggish, providing only 15% yield of compound **2r** together with 80% of unreacted reagent. Remarkably, substrate **1u**, which contains a pendant urea moiety, gave exclusively the usual *O*-cyclization product **2u** in high yield (80%) and no products arising from a *N*-cyclization process were detected.

The reactivity of substrates bearing a free amino group on the carbon *alpha* to the triple bond was next investigated (**Table 4**). To our surprise, a totally different product arising from a completely unexpected reaction pathway was in this case observed. Under the same standard conditions employed for the synthesis of compounds **2**, the condensed polyheterocyclic structure **3a** was instead formed. Considering the many steps of this one-pot reaction, good yields were obtained with both EW and EDGs (**Table 5**). The structure of **3d** was unequivocally assigned by Single Crystal X-ray Diffraction analysis (SC-XRD). Eight new bonds and four condensed heterocycles were formed during this triple carbonylative cascade reaction.

Table 4

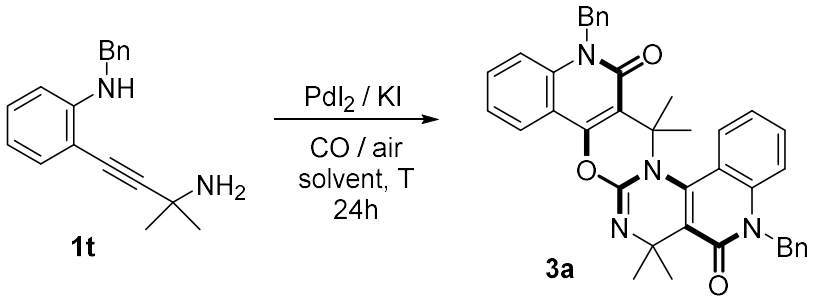

Entry	Solvent (dry)	KI (mol%)	CO/air (MPa)	T (°C)	Conv (%) **1t**[b]	Yield (%) **3a**[c,d]
1	MeCN	10	1.6/0.4	120	100	57
2	MeCN	10	1.6/0.4	100	100	73
3	**MeCN**	**10**	**1.6/0.4**	**80**	**100**	**83(81)**
4	MeCN	10	1.6/0.4	60	100	70
5	MeCN	10	1.6/0.4	40	85	20
6	MeCN	10	0.8/0.2	80	100	55

7	MeCN	5	1.6/0.4	80	100	49
8	MeCN	20	1.6/0.4	80	82	45
9	1,4-Dioxane	10	1.6/0.4	80	100	21
10	DME	10	1.6/0.4	80	100	23
11	Toluene	10	1.6/0.4	80	89	18

[a] Reaction conditions: **1t** (0.5 mmol), PdI_2 (1 mol%), KI (Pd/KI molar ratio is 1/10), solvent (5 mL), CO/air (reported pressure measured at 25 °C), 45 ml autoclave, 24h. [b] Conversion of **1t** was determined by ^1H NMR analysis with the internal standard method. [c] Yields were determined via ^1H NMR analysis with the internal standard method. [d] Isolated yield in brackets.

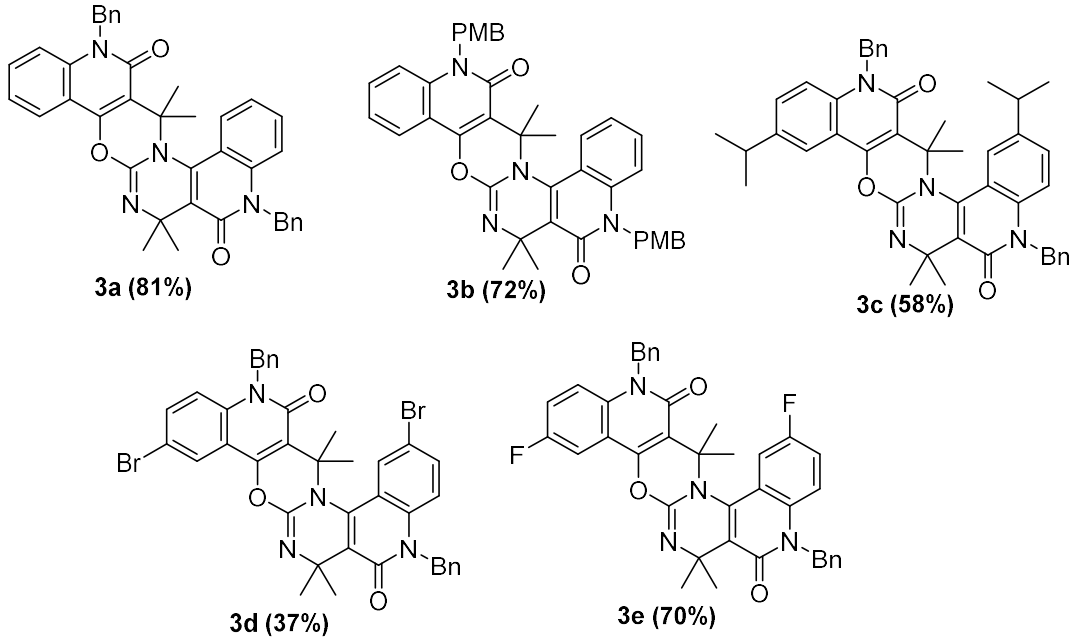

Table 5 scope of the reaction

The structure of **3d** was unequivocally assigned by Single Crystal X-ray Diffraction analysis (SC-XRD, figure 1). Eight new bonds and four condensed heterocycles were formed during this triple carbonylative cascade reaction.

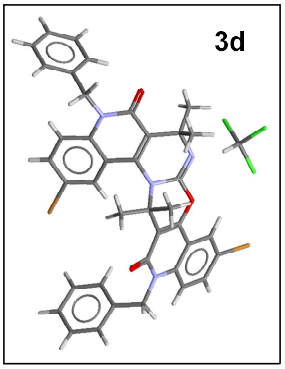

Figure 1

4.2.1 Mechanism and probes

On the base of experimental mechanistic findings (**Scheme 5**), proposed reaction pathways to compounds **2** and **3** are displayed (**Scheme 6**).

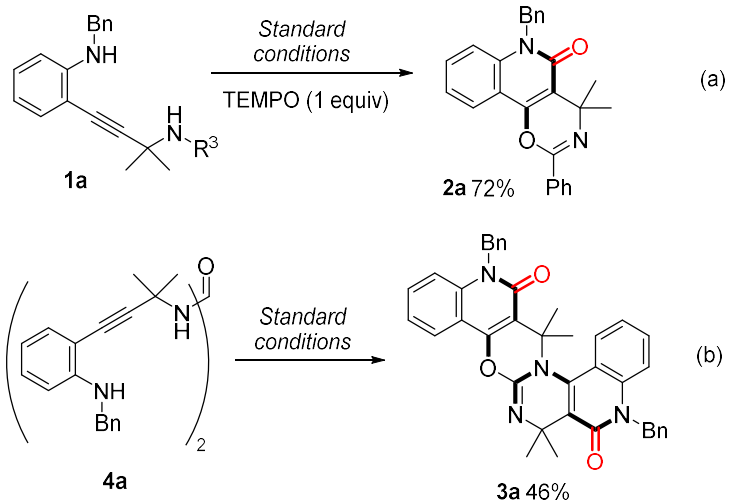

Scheme 5

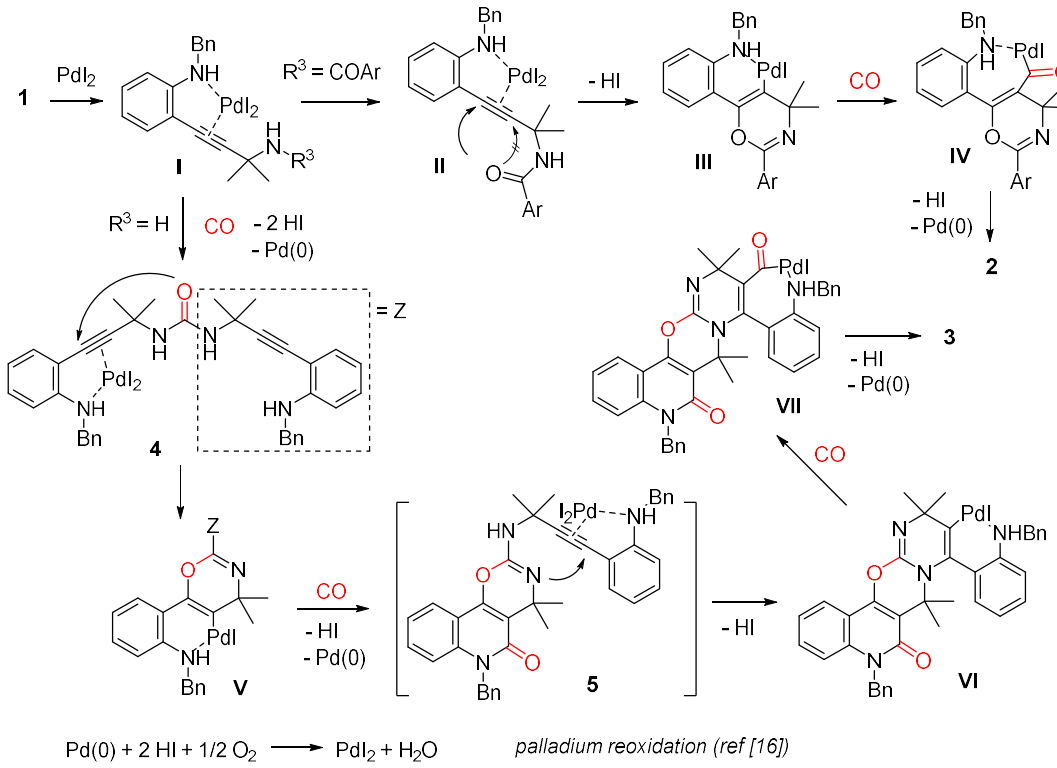

Scheme 6

The non-radical process (see the reaction carried out in the presence of TEMPO, **Scheme 5**) starts with the plausible coordination of Pd(II) species to both NHBn and the C-C triple bond to give complex **I**.[16] The amide group (R^3 = COAr) [17] attacks the activated triple bond selectively on the benzylic position, leading to σ-vinylpalladium complex **III**. The latter, after CO insertion, delivers intermediate **IV** which undergoes nucleophilic displacement by the amino group, affording product **2** and palladium (0). In a different way, when a primary amino group is present on **1** (R^3 = H), the symmetrical urea **4** is likely generated by palladium catalysis, as we have previously reported [18]. Then, organic intermediate **4** is supposed to be highly reactive under standard conditions, and, analogously to urea **1s** (**Table 2**), undergoes sequential 6-*endo*-

dig *O*-cyclization and CO insertion to compound **5**. At this point, the N atom of the newly formed heterocycle is in suitable position for a further site-selective nucleophilic attack on the proximal triple bond. The formed σ-complex **VI** incorporates the third molecule of CO leading to **VII**, which, after intramolecular palladium displacement, affords compound **3**. Both compounds **4** and **5** were never detected in the reaction mixture. In order to get further evidence of the described pathway, intermediate **4** was independently prepared and caused to react under standard conditions (**Scheme 6**).

4.3 Conclusions

In conclusion, the present study provides new attractive routes to oxazino[5,6-*c*]quinolin-5-ones and complex polyheterocyclic structures by means of palladium-catalyzed carbonylative methodology. The described transformations are extremely selective towards 6-membered cyclization products with outstanding molecular complexity achieved in a single operation: four sequential 6-*endo*-dig cyclization steps with eight new bonds (5 C-N, 2 C-C, 1 C-O) were formed in a one-pot manner. The proposed mechanistic pathways find a reasonable support in the successful conversion of a dipropargylic urea into the corresponding product.

4.4 Experimental section

4.4.1 Experimental procedures

General Procedure for alkylation of 2-haloanilines [19]

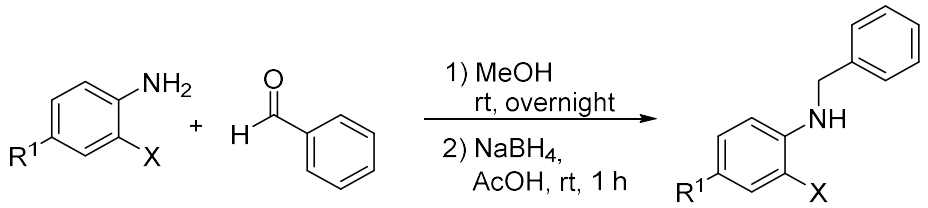

To a round-bottom flask the aniline derivative (1 equiv), the benzaldehyde derivative (1 equiv) and MeOH (2 mL/mmol of aniline) were added. The resulting mixture was stirred at rt overnight. After removal of solvent under vacuum, the residue was dissolved in AcOH (2 mL/mmol of aniline), then $NaBH_4$ (1.2 equiv) was added in portions at 0 °C. After stirring at rt for 1 h, the solvent was removed under vacuum and the residue was dissolved in EtOAc. A solution of NaOH (1N) was added to the mixture until pH 8–9. The two phases were stirred vigorously for 1 h then separated. The aqueous layer was extracted with EtOAc twice and the combined organic extracts were washed with brine, dried over anhydrous Na_2SO_4 and concentrated under vacuum to give the crude product, which was used for the next step without purification.

General Procedure for the synthesis of substrates 1 (Sonogashira coupling)

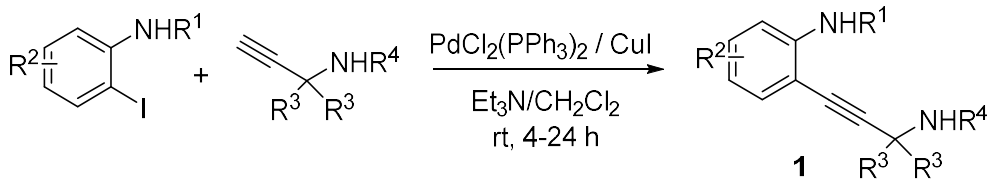

To a solution of 2-iodoaniline (1 equiv) in triethylamine (4 mL/mmol), $PdCl_2(PPh_3)_2$ (2 mol%), CuI (6 mol%) and propargylic amine/amide (1.2 equiv) were added. A proper amount of CH_2Cl_2 (1-2 mL/mmol) was added in order to obtain a homogeneous solution. The mixture was stirred at rt for 4-24 h. After filtration and evaporation of the solvent, the residue was diluted with EtOAc (40 mL) and washed with water (40 mL) and brine (30 mL). The organic layer was dried over anhydrous Na_2SO_4, filtered and the solvent was removed under reduced pressure. Products **1** were isolated by flash column chromatography on silica gel using mixtures of hexane-EtOAc as eluent.

General Procedure for the PdI_2/KI-catalyzed oxidative carbonylation of 1 to compounds 2 and 3

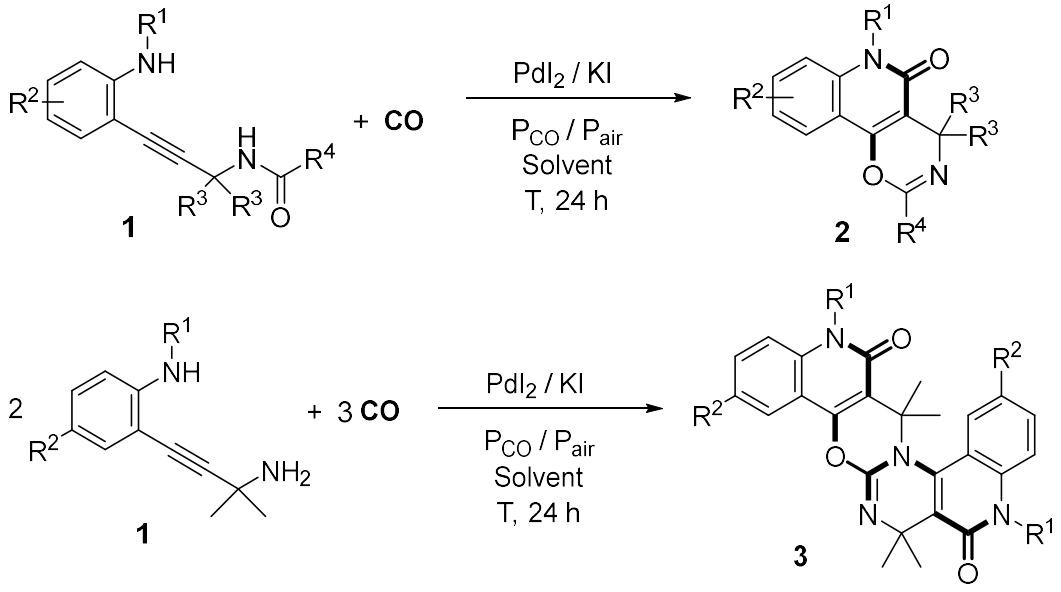

A 45 mL stainless steel autoclave was charged with substrate **1** (0.5 mmol), PdI_2 (1.8 mg, 1 mol%), KI (8 mg, 10 mol%) and the solvent (5 mL). The autoclave was sealed and pressurized with CO (1.6 MPa) and air (up to 2.0 MPa). The reaction mixture was stirred at 80-120 °C for 24 h. Then the autoclave was cooled, degassed and opened. After evaporation of the solvent, products were purified by column chromatography on silica gel using mixtures of hexane-EtOAc as eluent.

4.4.2 Substrate characterizations

N-(4-(2-(Benzylamino)phenyl)-2-methylbut-3-yn-2-yl)benzamide (1a)

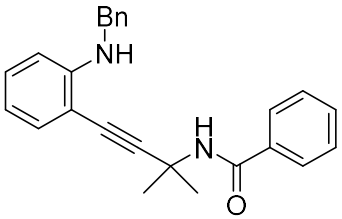

1a

pale yellow solid (m.p. 106.5-108.5 °C). ^{1}H NMR (400 MHz, $CDCl_3$): δ = 7.74–7.66 (m, 2H), 7.55–7.47 (m, 1H), 7.46–7.37 (m, 4H), 7.34–7.20 (m, 4H), 7.15–7.07 (m, 1H), 6.58 (td, *J* = 7.4, 0.9 Hz, 1H), 6.53 (d, *J* = 8.3 Hz, 1H), 6.34 (s, 1H), 6.31 (bs, 1H), 4.58 (s, 2H), 1.85 (s, 6H); ^{13}C NMR (101 MHz, $CDCl_3$): δ = 166.80, 149.88, 140.04, 134.83, 131.55, 131.19, 129.79, 128.58, 128.44, 127.07, 126.90, 126.75, 115.52, 109.60, 106.92, 98.12, 78.77, 48.43, 47.28, 29.61. HRMS (ESI+) calcd for $C_{25}H_{25}N_2O$ $(M+1)^+$ *m/z* 369.1967, found *m/z* 369.1971.

N-(4-(2-((4-Methoxybenzyl)amino)phenyl)-2-methylbut-3-yn-2-yl)benzamide (1b)

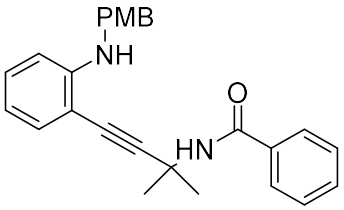

1b

brown solid (m.p. 128.5-130.0 °C). ^{1}H NMR (400 MHz, $CDCl_3$): δ = 7.73–7.67 (m, 2H), 7.51 (t, *J* = 7.4 Hz, 1H), 7.41 (t, *J* = 7.5 Hz, 2H), 7.34 (d, *J* = 8.5 Hz, 2H), 7.26 (dd, *J* = 7.5, 1.5 Hz, 1H), 7.14–7.08 (m, 1H), 6.83 (d, *J* = 8.6 Hz, 2H), 6.60–6.50 (m, 2H), 6.33 (s, 1H), 6.18 (s, 1H), 4.49 (s, 2H), 3.79 (s, 3H), 1.84 (s, 6H); ^{13}C NMR (101 MHz, $CDCl_3$): δ = 166.74, 158.50, 149.84, 134.85, 131.99, 131.53, 131.22, 129.76, 128.56, 128.29, 126.90, 115.49, 113.84, 109.61, 106.92, 98.07, 78.76, 55.25, 48.45, 46.73, 29.59. HRMS (ESI+) calcd for $C_{26}H_{27}N_2O_2$ $(M+1)^+$ *m/z* 399.2073, found *m/z* 399.2072.

N-(4-(2-(Benzylamino)-5-methylphenyl)-2-methylbu-3-yn-2-yl)benzamide (1c)

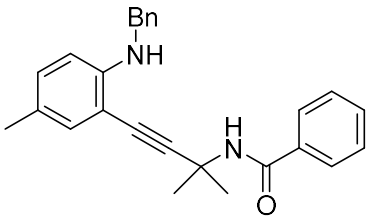

1c

brown solid (m.p. 129.5-131.0 °C). ^{1}H NMR (400 MHz, $CDCl_3$): δ = 7.72–7.67 (m, 2H), 7.53–7.47 (m, 1H), 7.44–7.37 (m, 4H), 7.32–7.26 (m, 2H), 7.25–7.18 (m, 1H), 7.09 (d, *J* = 2.0 Hz, 1H), 6.91 (dd, *J* = 8.4, 1.6 Hz, 1H), 6.43 (d, *J* = 8.4 Hz, 1H), 6.29 (bs, 1H), 6.02 (bs, 1H), 4.53 (s, 2H), 2.18 (s, 3H), 1.84 (s, 6H); ^{13}C NMR (101 MHz, $CDCl_3$): δ = 166.71, 147.69, 140.20, 134.88, 131.55, 131.50, 130.47, 128.56, 128.39, 127.05, 126.87, 126.67, 124.60, 109.75, 106.82, 97.82, 78.84, 48.49, 47.50, 29.57, 20.15;. HRMS (ESI+) calcd for $C_{26}H_{27}N_2O$ $(M+1)^+$ *m/z* 383.2123, found *m/z* 383.2120.

N-(4-(2-(Benzylamino)-5-isopropylphenyl)-2-methylbut-3-yn-2-yl)benzamide (1d)

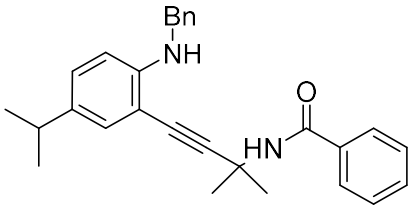

1d

yellow solid (m.p. 115.3-117.9 °C). ^{1}H NMR (400 MHz, $CDCl_3$): δ = 7.74–7.69 (m, 2H), 7.54–7.48 (m, 1H), 7.46–7.38 (m, 4H), 7.34–7.28 (m, 2H), 7.27–7.22 (m, 1H), 7.17 (d, *J* = 2.1 Hz, 1H), 7.00 (dd, *J* = 8.5, 2.1 Hz, 1H), 6.49 (d, *J* = 8.5 Hz, 1H), 6.35 (bs, 1H), 6.08 (bs, 1H), 4.55 (s, 2H), 2.78 (hept, *J* = 6.9 Hz, 1H), 1.86 (s, 6H), 1.21 (d, *J* = 6.9 Hz, 6H); ^{13}C NMR (101 MHz, $CDCl_3$): δ = 166.76, 148.07, 140.30, 135.99, 134.90, 131.52, 128.94, 128.58, 128.43, 128.10, 127.11, 126.90, 126.72, 109.66, 106.66, 97.80, 79.05, 48.53, 47.56, 33.03, 29.61, 24.20. HRMS (ESI+) calcd for $C_{28}H_{31}N_2O$ $(M+1)^+$ *m/z* 411.2436, found *m/z* 411.2431.

N-(4-(2-(Benzylamino)-5-chlorophenyl)-2-methylbut-3-yn-2-yl)benzamide (1e)

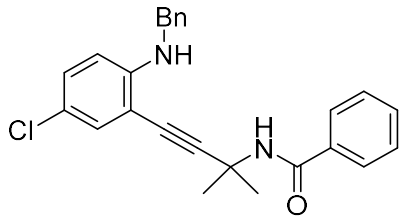

1e

brown solid (m.p. 147.3-149.0 °C). ^{1}H NMR (400 MHz, $CDCl_3$): δ = 7.72–7.67 (m, 2H), 7.51 (t, *J* = 7.4 Hz, 1H), 7.44–7.36 (m, 4H), 7.33–7.21 (m, 4H), 7.02 (dd, *J* = 8.8, 2.5 Hz, 1H), 6.43 (bs, 1H), 6.41 (d, *J* = 8.9 Hz, 1H), 6.31 (bs, 1H), 4.55 (s, 2H), 1.83 (s, 6H); ^{13}C NMR (101 MHz, $CDCl_3$): δ = 166.83, 148.57, 139.59, 134.65, 131.64, 130.44, 129.56, 128.61, 128.48, 126.99, 126.88, 126.85, 119.69, 110.63, 108.31, 98.93, 77.70, 48.21, 47.28, 29.57. HRMS (ESI+) calcd for $C_{25}H_{24}ClN_2O$ $(M+1)^+$ *m/z* 403.1577, found *m/z* 403.1579.

N-(4-(2-(Benzylamino)-5-bromophenyl)-2-methylbut-3-yn-2-yl)benzamide (1f)

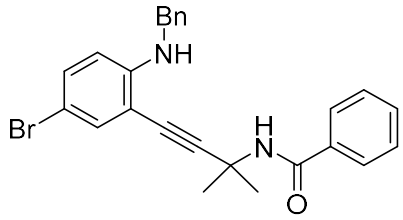

1f

brown solid (m.p. 136.8-138.5 °C). ^{1}H NMR (400 MHz, $CDCl_3$): δ = 7.72–7.67 (m, 2H), 7.54–7.48 (m, 1H), 7.44–7.34 (m, 5H), 7.32–7.23 (m, 3H), 7.15 (dd, *J* = 8.8, 2.4 Hz, 1H), 6.46 (bs, 1H), 6.37 (d, *J* = 8.9 Hz, 1H), 6.32 (bs, 1H), 4.54 (d, *J* = 2.7 Hz, 2H), 1.83 (s, 6H); ^{13}C NMR (101 MHz, $CDCl_3$): δ = 166.85, 148.95, 139.52, 134.64, 133.21, 132.35, 131.65, 128.61, 128.48, 126.98, 126.89, 126.86, 111.08, 108.88, 106.39, 99.05, 77.58, 48.20, 47.19, 29.57. HRMS (ESI+) calcd for $C_{25}H_{24}BrN_2O$ $(M+1)^+$ *m/z* 447.1072, found *m/z* 447.1078.

_N_-(4-(2-(Benzylamino)-5-fluorophenyl)-2-methylbut-3-yn-2-yl)benzamide (1g)

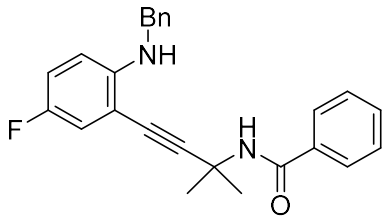

1g

pale yellow solid (m.p. 150.2-150.5 °C). ^{1}H NMR (400 MHz, $CDCl_3$): δ = 7.74–7.67 (m, 2H), 7.54–7.48 (m, 1H), 7.45–7.37 (m, 4H), 7.34–7.20 (m, 3H), 6.98 (dd, *J* = 8.9, 3.0 Hz, 1H), 6.82 (td, *J* = 8.7, 3.0 Hz, 1H), 6.41 (dd, *J* = 9.1, 4.6 Hz, 1H), 6.32 (bs, 1H), 6.22 (bs, 1H), 4.53 (s, 2H), 1.84 (s, 6H); ^{13}C NMR (101 MHz, $CDCl_3$): δ = 166.80, 153.91 (d, $J_{C,F}$ = 233.4 Hz), 146.64, 139.87, 134.69, 131.61, 128.59, 128.45, 127.04, 126.89, 126.80, 117.23 (d, $J_{C,F}$ = 23.6 Hz), 116.53 (d, $J_{C,F}$ = 22.2 Hz), 110.23 (d, $J_{C,F}$ = 7.9 Hz), 107.40 (d, $J_{C,F}$ = 9.2 Hz), 98.75, 77.95, 48.25, 47.69, 29.55. HRMS (ESI+) calcd for $C_{25}H_{24}FN_2O$ $(M+1)^+$ *m/z* 387.1873, found *m/z* 387.1874.

Methyl3-(3-benzamido-3-methylbut-1-yn-1-yl)-4(benzylamino)benzoate (1h)

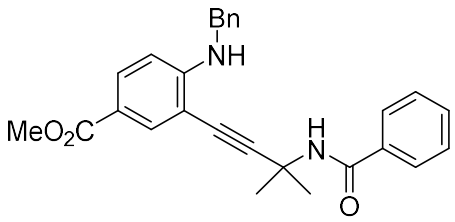

1h

pale yellow solid (m.p. 161.2-163.0 °C). ^{1}H NMR (400 MHz, $CDCl_3$): δ = 7.96 (d, *J* = 1.9 Hz, 1H), 7.77 (dd, *J* = 8.7, 1.8 Hz, 1H), 7.68 (d, *J* = 7.6 Hz, 2H), 7.49 (t, *J* = 7.1 Hz, 1H), 7.42–7.35 (m, 4H), 7.32–7.21 (m, 3H), 7.08 (b t, *J* = 5.9 Hz, 1H), 6.49 (d, *J* = 8.8 Hz, 1H), 6.42 (bs, 1H), 4.63 (d, *J* = 5.9 Hz, 2H), 3.83 (s, 3H), 1.83 (s, 6H); ^{13}C NMR (101 MHz, $CDCl_3$): δ = 166.97, 153.28, 139.09, 134.58, 133.08, 131.74, 131.65, 128.58, 128.52, 126.98, 126.96, 126.91, 116.68, 108.51, 106.65, 98.42, 77.89, 51.53, 48.15, 46.87, 29.58. HRMS (ESI+) calcd for $C_{27}H_{27}N_2O_3$ $(M+1)^+$ *m/z* 427.2022, found *m/z* 427.2026.

N-(4-(2-(Benzylamino)-5-(trifluoromethyl)phenyl)-2-methylbut-3-yn-2-yl)benzamide (1i)

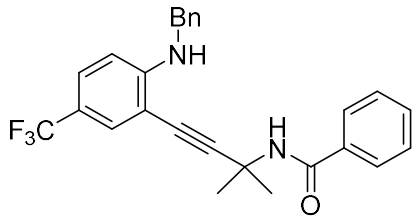

1i

pale yellow solid (m.p. 133.5-134.5 °C). ^{1}H NMR (400 MHz, $CDCl_3$): δ = 7.69 (d, *J* = 7.4 Hz, 2H), 7.55–7.47 (m, 2H), 7.45–7.37 (m, 4H), 7.33–7.21 (m, 4H), 6.93 (bs, 1H), 6.51 (d, *J* = 8.8 Hz, 1H), 6.31 (bs, 1H), 4.61 (d, *J* = 5.3 Hz, 2H), 1.84 (s, 6H); ^{13}C NMR (101 MHz, $CDCl_3$): δ = 166.92, 152.07, 139.17, 134.55, 131.70, 128.63, 128.53, 128.20 (q, $J_{C,F}$ = 3.4 Hz), 126.95, 126.87, 126.69 (q, $J_{C,F}$ = 3.3 Hz), 124.75 (q, $J_{C,F}$ = 270.3 Hz), 117.04 (q, $J_{C,F}$ = 32.8 Hz), 108.78, 106.80, 98.87, 77.71, 48.13, 46.92, 29.58. HRMS (ESI+) calcd for $C_{26}H_{24}F_3N_2O$ $(M+1)^+$ *m/z* 437.1841, found *m/z* 437.1843.

N-(4-(2-(Benzylamino)-3,5-dimethylphenyl)-2-methylbut-3-yn-2-yl)benzamide (1j)

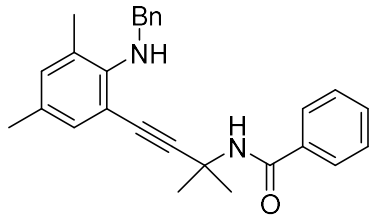

1j

pale yellow solid (m.p. 79.0-80.0 °C). ^{1}H NMR (400 MHz, $CDCl_3$): δ = 7.76–7.72 (m, 2H), 7.51–7.43 (m, 3H), 7.39 (t, *J* = 7.5 Hz, 2H), 7.34–7.27 (m, 2H), 7.26–7.22 (m, 1H), 7.11 (d, *J* = 1.6 Hz, 1H), 6.93 (d, *J* = 1.5 Hz, 1H), 6.55 (bs, 1H), 4.46 (two overlapping signals: bs and s, 3H), 2.35 (s, 3H), 2.26 (s, 3H), 1.83 (s, 6H); ^{13}C NMR (101 MHz, $CDCl_3$): δ = 166.70, 146.93, 140.89, 135.07, 132.92, 131.39, 130.56, 129.63, 128.50, 128.42, 127.96, 127.90, 127.06, 126.98, 113.50, 96.79, 79.67, 52.33, 48.78, 29.23, 20.40, 19.24. HRMS (ESI+) calcd for $C_{27}H_{29}N_2O$ $(M+1)^+$ *m/z* 397.2280, found *m/z* 397.2273.

N-(4-(2-(Benzylamino)-3-bromo-5-ethylphenyl)-2-methylbut-3-yn-2-yl)benzamide (1k)

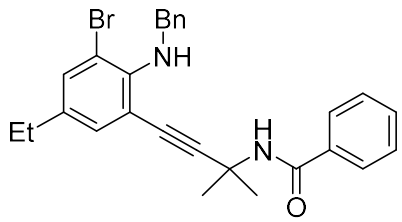

1k

pale yellow solid (m.p. 168.7-170.3 °C). ^{1}H NMR (400 MHz, $CDCl_3$): δ = 7.82–7.76 (m,1H), 7.72–7.67 (m, 2H), 7.52–7.47 (m, 1H), 7.46–7.37 (m, 4H), 7.32–7.25 (m, 2H), 7.24–7.19 (m, 1H), 7.17 (d, *J* = 1.6 Hz, 1H), 6.26 (bs, 1H), 4.73 (s, 2H), 2.52 (q, *J* = 7.6 Hz, 2H), 1.79 (s, 6H), 1.20 (t, *J* = 7.6 Hz, 3H); ^{13}C NMR (101 MHz, $CDCl_3$): δ = 166.54, 145.56, 140.32, 136.82, 134.95, 133.09, 132.43, 131.45, 128.60, 128.52, 128.38, 127.88, 127.05, 126.93, 114.33, 113.56, 97.58, 79.24, 51.51, 48.81, 29.00, 27.48, 15.43. HRMS (ESI+) calcd for $C_{27}H_{28}BrN_2O$ $(M+1)^+$ *m/z* 475.1385, found *m/z* 475.1388.

N-(4-(2-(Benzylamino)-4-chlorophenyl)-2-methylbut-3-yn-2-yl)benzamide (1l)

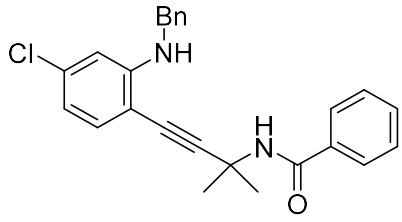

1l

pale yellow solid (m.p. 128.0-128.5 °C). ^{1}H NMR (400 MHz, $CDCl_3$): δ = 7.68 (d, *J* = 8.0 Hz, 2H), 7.51 (t, *J* = 7.4 Hz, 1H), 7.43–7.37 (m, 4H), 7.34–7.22 (m, 3H), 7.15 (d, *J* = 8.0 Hz, 1H), 6.55–6.48 (m, 3H), 6.31 (bs, 1H), 4.54 (s, 2H), 1.82 (s, 6H); ^{13}C NMR (101 MHz, $CDCl_3$): δ = 166.83, 150.85, 139.32, 135.59, 134.65, 131.86, 131.63, 128.59, 128.52, 127.05, 126.93, 126.88, 115.47, 109.43, 105.59, 98.70, 77.99, 48.25, 47.08, 29.59. HRMS (ESI+) calcd for C25H24ClN2O$C_{25}H_{24}ClN_2O$ $(M+1)^+$ *m/z* 403.1577, found *m/z* 403.1576.

N-(1-((2-(Benzylamino)phenyl)ethynyl)cyclohexyl)benzamide (1m)

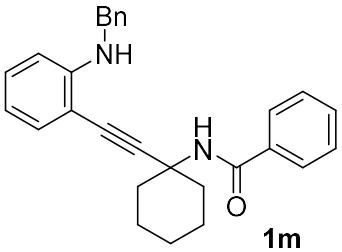

1m

pale yellow solid (m.p. 98.1-99.2 °C). ^{1}H NMR (400 MHz, $CDCl_3$): δ = 7.73–7.68 (m, 2H), 7.50 (t, *J* = 7.4 Hz, 1H), 7.44–7.37 (m, 4H), 7.33–7.21 (m, 4H), 7.13–7.08 (m, 1H), 6.58 (t, *J* = 7.4 Hz, 1H), 6.53 (d, *J* = 8.3 Hz, 1H), 6.34 (bs, 1H), 6.25 (bs, 1H), 4.56 (s, 2H), 2.47–2.35 (m, 2H), 2.97–1.77 (m, 4H), 1.76–162 (m, 3H), 1.45–1.34 (m, 1H); ^{13}C NMR (101 MHz, $CDCl_3$): δ = 166.62, 149.86, 140.05, 135.06, 131.48, 131.27, 129.67, 128.57, 128.41, 127.14, 126.89, 126.72, 115.45, 109.54, 107.22, 96.69, 80.88, 52.65, 47.30, 37.55, 25.43, 22.74. HRMS (ESI+) calcd for $C_{28}H_{29}N_2O$ $(M+1)^+$ *m/z* 409.2280, found *m/z* 409.2284.

N-(3-(2-(Benzylamino)phenyl)prop-2-yn-1-yl)benzamide (1n)

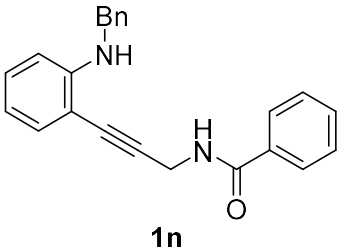

1n

pale yellow solid (m.p. 98.8-101.0 °C). ^{1}H NMR (400 MHz, $CDCl_3$): δ = 7.79 (d, *J* = 7.3 Hz, 2H), 7.53 (t, *J* = 7.4 Hz, 1H), 7.44 (t, *J* = 7.5 Hz, 2H), 7.39–7.24 (m, 6H), 7.16 (t, *J* = 7.4 Hz, 1H), 6.64 (t, *J* = 7.5 Hz, 1H), 6.57 (d, *J* = 8.3 Hz, 1H), 6.56 (bs, 1H), 4.53 (d, *J* = 5.2 Hz, 2H), 4.45 (s, 2H); ^{13}C NMR (101 MHz, $CDCl_3$): δ = 167.23, 149.14, 139.14, 133.86, 132.36, 131.78, 130.18, 128.66, 128.64, 127.17, 127.08, 127.06, 116.46, 110.01, 106.74, 90.69, 80.62, 47.60, 30.96. HRMS (ESI+) calcd for $C_{23}H_{21}N_2O$ $(M+1)^+$ *m/z* 341.1654, found *m/z* 341.1651.

N-(4-(2-(Benzylamino)phenyl)-2-methylbut-3-yn-2-yl)-4-chlorobenzamide (1o)

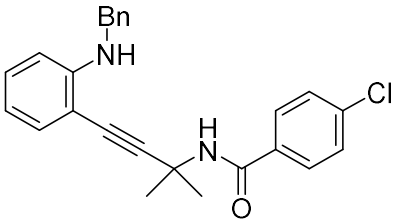

1o

pale yellow solid (m.p. 130.2-131.0 °C). ^{1}H NMR (400 MHz, $CDCl_3$): δ = 7.63–7.58 (m, 2H), 7.46–7.42 (m, 2H), 7.38–7.25 (m, 6H), 7.15 (ddd, *J* = 8.4, 7.4, 1.6 Hz, 1H), 6.62 (td, *J* = 7.5, 1.0 Hz, 1H), 6.58 (d, *J* = 8.3 Hz, 1H), 6.42 (bs, 1H), 6.25 (bs, 1H), 4.59 (s, 2H), 1.86 (s, 6H); ^{13}C NMR (101 MHz, $CDCl_3$): δ = 165.85, 149.89, 139.98, 137.72, 133.21, 131.30, 129.93, 128.78, 128.52, 128.44, 127.10, 126.89, 115.69, 109.67, 106.93, 98.07, 78.91, 48.59, 47.32, 29.60. HRMS (ESI+) calcd for $C_{25}H_{24}ClN_2O$ $(M+1)^+$ *m/z* 403.1577, found *m/z* 403.1578.

N-(4-(2-(Benzylamino)phenyl)-2-methylbut-3-yn-2-yl)-4-fluorobenzamide (1p)

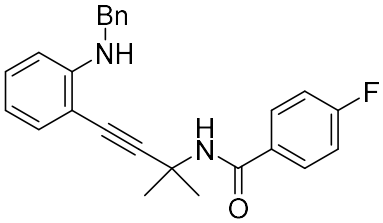

1p

brown solid (m.p. 100.1-101.0 °C). ^{1}H NMR (400 MHz, $CDCl_3$): δ = 7.73–7.67 (m, 2H), 7.45 (d, *J* = 7.2 Hz, 2H), 7.36–7.25 (m, 4H), 7.18–7.11 (m, 1H), 7.09–7.02 (m, 2H), 6.62 (td, *J* = 7.5, 0.9 Hz, 1H), 6.58 (d, *J* = 8.3 Hz, 1H), 6.48 (bs, 1H), 6.31 (bs, 1H), 4.60 (s, 2H), 1.86 (s, 6H); ^{13}C NMR (101 MHz, $CDCl_3$): δ = 165.91, 164.72 (d, $J_{C,F}$ = 251.8 Hz), 149.92, 140.03, 131.28, 131.03 (d, $J_{C,F}$ = 3.1 Hz), 129.90, 129.38 (d, $J_{C,F}$ = 8.9 Hz), 128.52, 127.10, 126.87, 115.64, 115.54 (d, $J_{C,F}$ = 24.8 Hz), 109.66, 107.00, 98.23, 78.84, 48.52, 47.30, 29.60;. HRMS (ESI+) calcd for $C_{25}H_{24}FN_2O$ $(M+1)^+$ *m/z* 387.1873, found *m/z* 387.1876.

N-(4-(2-(Benzylamino)phenyl)-2-methylbut-3-yn-2-yl)-4-nitrobenzamide (1q)

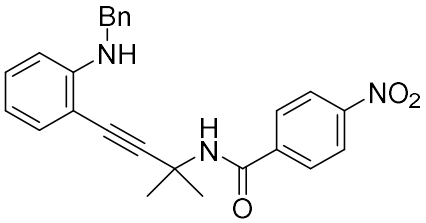

1q

yellow solid (m.p. 125.1-126.5 °C). ^{1}H NMR (400 MHz, $CDCl_3$): δ = 8.16 (d, *J* = 8.8 Hz, 2H), 7.77 (d, *J* = 8.8 Hz, 2H), 7.42 (d, *J* = 7.1 Hz, 2H), 7.37–7.23 (m, 4H), 7.18–7.11 (m, 1H), 6.65 (bs, 1H), 6.63–6.55 (m, 2H), 6.13 (bs, 1H), 4.56 (s, 2H), 1.87 (s, 6H); ^{13}C NMR (101 MHz, $CDCl_3$): δ = ^{13}C NMR (101 MHz, $CDCl_3$) δ 164.89, 149.82, 149.41, 140.35, 139.86, 131.38, 130.05, 128.54, 128.22, 127.09, 126.96, 123.68, 115.81, 109.70, 106.80, 97.68, 79.11, 48.94, 47.30, 29.49. HRMS (ESI+) calcd for $C_{25}H_{24}N_3O_3$ $(M+1)^+$ *m/z* 414.1818, found *m/z* 414.1812.

N-(3-(2-(Benzylamino)phenyl)prop-2-yn-1-yl)acetamide (1r)

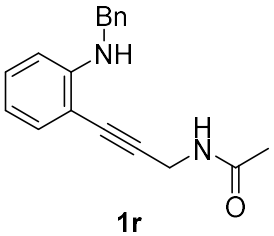

1r

pale yellow solid (m.p. 139.5-141.0 °C). ^{1}H NMR (400 MHz, $CDCl_3$): δ = 7.40–7.34 (m, 4H), 7.33–7.27 (m, 2H), 7.15 (ddd, *J* = 8.4, 7.4, 1.6 Hz, 1H), 6.63 (td, *J* = 7.5, 1.0 Hz, 1H), 6.56 (d, *J* = 8.2 Hz, 1H), 5.88 (bs, 1H), 5.13 (bs, 1H), 4.45 (s, 2H), 4.32 (d, *J* = 5.2 Hz, 2H), 2.01 (s, 3H); ^{13}C NMR (101 MHz, $CDCl_3$): δ = 169.75, 149.04, 139.13, 132.34, 130.16, 128.69, 127.21, 127.08, 116.48, 110.00, 106.72, 90.70, 80.30, 47.57, 30.41, 23.12. HRMS (ESI+) calcd for $C_{18}H_{19}N_2O$ $(M+1)^+$ *m/z* 279.1497, found *m/z* 279.1499.

1-Benzyl-3-(4-(2-(benzylamino)phenyl)-2-methylbut-3-yn-2-yl)urea (1s)

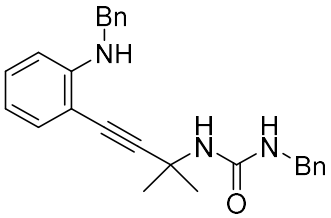

1s

pale yellow solid (m.p. 155.1-157.0 °C). ^{1}H NMR (400 MHz, $CDCl_3$): δ = 7.38–7.18 (m, 10H), 7.16 (d, *J* = 7.6 Hz, 1H), 7.10 (further split t, *J* = 7.5 Hz, 1H), 6.55 (t, *J* = 7.5 Hz, 1H), 6.48 (d, *J* = 8.3 Hz, 1H), 5.93 (bs, 1H), 5.30 (bs, 1H), 4.90 (bs, 1H), 4.42 (d, *J* = 4.2 Hz, 2H), 4.28 (d, *J* = 5.4 Hz, 2H), 1.65 (s, 6H); ^{13}C NMR (101 MHz, $CDCl_3$): δ = 157.38, 149.64, 139.80, 139.06, 131.30, 129.80, 128.59, 128.47, 127.42, 127.21, 126.95, 126.81, 115.71, 109.72, 106.80, 98.81, 79.12, 47.68, 47.25, 44.26, 30.41. HRMS (ESI+) calcd for $C_{26}H_{28}N_3O$ $(M+1)^+$ *m/z* 398.2232, found *m/z* 398.2230.

2-(3-Amino-3-methylbut-1-yn-1-yl)-N-benzylaniline (1t)

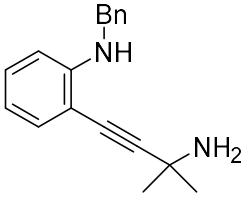

1t

brown solid (m.p. 68.5-71.0 °C). ^{1}H NMR (400 MHz, $CDCl_3$): δ = 7.43–7.35 (m, 4H), 7.34–7.27 (m, 2H), 7.16 (further split t, *J* = 7.9 Hz, 1H), 6.66 (td, *J* = 7.5, 1.0 Hz, 1H), 6.59 (d, *J* = 8.2 Hz, 1H), 4.97 (bs, 1H), 4.44 (d, *J* = 5.4 Hz, 2H), 1.84 (bs, 2H), 1.52 (s, 6H); ^{13}C NMR (101 MHz, $CDCl_3$): δ = 148.59, 139.22, 131.84, 129.57, 128.70 (2C), 127.28, 127.11, 116.57, 109.84, 107.69, 76.75, 47.83, 46.02, 32.12;. HRMS (ESI+) calcd for $C_{18}H_{21}N_2$ $(M+1)^+$ *m/z* 265.1705, found *m/z* 265.1701.

2-(3-Amino-3-methylbut-1-yn-1-yl)-N-(4-methoxybenzyl)aniline (1u)

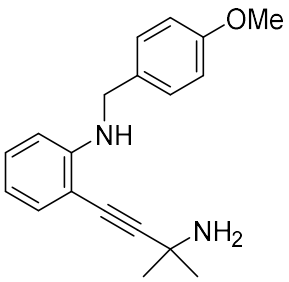

1u

pale yellow oil. ^{1}H NMR (400 MHz, $CDCl_3$): δ = 7.31 (dd, *J* = 7.6, 1.4 Hz, 1H), 7.27 (d, *J* = 8.4 Hz, 2H), 7.17–7.11 (m, 1H), 6.88 (d, *J* = 8.6 Hz, 2H), 6.63 (t, *J* = 7.3 Hz, 1H), 6.57 (d, *J* = 8.2 Hz, 1H), 4.92 (bs, 1H), 4.28 (d, *J* = 4.7 Hz, 2H), 3.73 (s, 3H), 1.79 (bs, 2H), 1.47 (s, 6H); ^{13}C NMR (101 MHz, $CDCl_3$): δ = 158.89, 148.71, 131.82, 131.16, 129.61, 128.46, 116.53, 114.11, 109.90, 107.78, 103.40, 76.80, 55.17, 47.27, 45.95, 32.12. HRMS (ESI+) calcd for $C_{19}H_{23}N_2O$ $(M+1)^+$ *m/z* 295.4060, found *m/z* 295.4063.

2-(3-Amino-3-methylbut-1-yn-1-yl)-N-benzyl-4-isopropylaniline (1v)

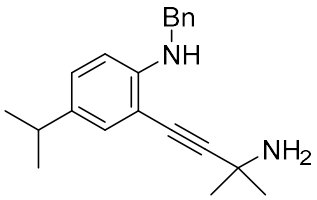

1v

pale yellow oil. ^{1}H NMR (400 MHz, $CDCl_3$): δ = 7.46–7.37 (m, 4H), 7.33 (t, *J* = 7.0 Hz, 1H), 7.25 (d, *J* = 2.1 Hz, 1H), 7.07 (dd, *J* = 8.4, 2.1 Hz, 1H), 6.58 (d, *J* = 8.4 Hz, 1H), 4.90 (bs, 1H), 4.45 (d, *J* = 4.9 Hz, 2H), 2.84 (hept, *J* = 6.9 Hz, 1H), 1.88 (bs, 2H), 1.55 (s, 6H), 1.27 (d, *J* = 6.9 Hz, 6H); ^{13}C NMR (101 MHz, $CDCl_3$): δ = 146.90, 139.57, 137.04, 129.63, 128.72, 127.84, 127.26, 127.18, 110.07, 107.64, 77.14, 48.15, 46.03, 33.13, 32.19, 24.25. HRMS (ESI+) calcd for $C_{21}H_{27}N_2$ $(M+1)^+$ *m/z* 307.2174, found *m/z* 307.2171.

2-(3-Amino-3-methylbut-1-yn-1-yl)-N-benzyl-4-bromoaniline (1w)

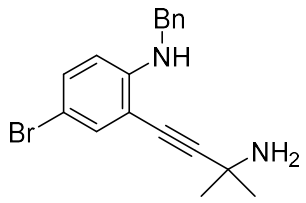

1w

pale yellow oil. ^{1}H NMR (400 MHz, $CDCl_3$): δ = 7.41 (d, *J* = 2.3 Hz, 1H), 7.39–7.26 (m, 5H), 7.19 (dd, *J* = 8.8, 2.3 Hz, 1H), 6.40 (d, *J* = 8.8 Hz, 1H), 5.01 (bs, 1H), 4.37 (d, *J* = 5.4 Hz, 2H), 1.82 (bs, 2H), 1.50 (s, 6H); ^{13}C NMR (101 MHz, $CDCl_3$): δ = 147.57, 138.70, 134.00, 132.22, 128.79, 127.45, 127.06, 111.41, 109.68, 107.63, 75.57, 47.75, 45.99, 32.11. HRMS (ESI+) calcd for $C_{18}H_{20}BrN_2$ $(M+1)^+$ *m/z* 343.0810, found *m/z* 343.0814.

2-(3-Amino-3-methylbut-1-yn-1-yl)-N-benzyl-4-fluoroaniline (1x)

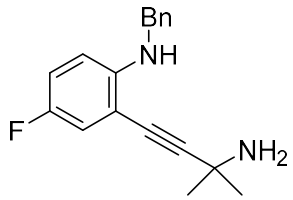

1x

white solid (m.p. 139.5-141.0 °C). ^{1}H NMR (400 MHz, $CDCl_3$): δ = 7.41–7.27 (m, 5H), 7.01 (dd, *J* = 8.9, 3.0 Hz, 1H), 6.87 (td, *J* = 8.7, 3.0 Hz, 1H), 6.48 (dd, *J* = 9.0, 4.6 Hz, 1H), 4.81 (bs, 1H), 4.40 (d, *J* = 5.3 Hz, 2H), 1.88 (bs, 2H), 1.50 (s, 6H); ^{13}C NMR (101 MHz, $CDCl_3$): δ = 154.52 (d, *J* = 234.6 Hz), 145.30 (d, *J* = 1.6 Hz), 139.05, 128.72, 127.35, 127.08, 118.00 (d, *J* = 23.7 Hz), 116.31 (d, *J* = 22.2 Hz), 110.64 (d, *J* = 7.9 Hz), 108.39 (d, *J* = 9.1 Hz), 103.89, 75.95 (d, *J* = 3.0 Hz), 48.32, 46.00, 31.92. HRMS (ESI+) calcd for $C_{18}H_{20}FN_2$ $(M+1)^+$ *m/z* 283.1611, found *m/z* 283.1609.

1,3-bis(4-(2-(Benzylamino)phenyl)-2-methylbut-3-yn-2-yl)urea (4a)

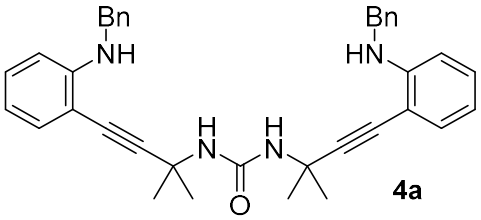

4a

white solid (m.p. 139.5-141.0 °C). ^{1}H NMR (400 MHz, $CDCl_3$): δ = 7.43–7.25 (m, 12H), 7.16 (further split t, *J* = 7.5 Hz, 2H), 6.63 (td, *J* = 7.5, 0.9 Hz, 2H), 6.52 (d, *J* = 8.2 Hz, 2H), 6.12 (b t, *J* = 5.4 Hz, 2H), 5.26 (s, 2H), 4.50 (d, *J* = 5.6 Hz, 4H), 1.66 (s, 12H); ^{13}C NMR (101 MHz, $CDCl_3$): δ = 156.69, 149.85, 139.84, 131.35, 129.88, 128.51, 126.97, 126.82, 115.78, 109.90, 106.91, 98.94, 79.17, 47.73, 47.26, 30.41. HRMS (ESI+) calcd for $C_{37}H_{39}N_4O$ $(M+1)^+$ *m/z* 555.3124, found *m/z* 555.3127.

4.4.3 Product characterizations

6-Benzyl-4,4-dimethyl-2-phenyl-4,6-dihydro-5H-[1,3]oxazino[5,6-c]quinolin-5-one (2a)

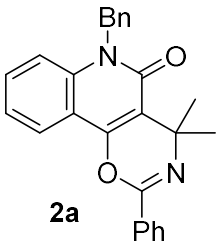

2a

white solid (m.p. 211.2-212.0 °C). ^{1}H NMR (400 MHz, $CDCl_3$): δ = 8.22 (dd, *J* = 7.9, 1.7 Hz, 2H), 8.13 (dd, *J* = 8.2, 1.4 Hz, 1H), 7.58–7.47 (m, 4H), 7.38–7.24 (m, 7H), 5.60 (bs, 2H), 1.90 (s, 6H); ^{13}C NMR (101 MHz, $CDCl_3$): δ = 161.00, 150.45, 146.06, 138.67, 136.64, 131.88, 131.20, 131.15, 128.86, 128.43, 127.48, 127.29, 126.54, 122.86, 122.11, 114.86, 113.97, 112.01, 52.95, 45.91, 30.12. HRMS (ESI+) calcd for $C_{26}H_{23}N_2O_2$ $(M+1)^+$ *m/z* 395.1760, found *m/z* 395.1762.

6-(4-Methoxybenzyl)-4,4-dimethyl-2-phenyl-4,6-dihydro-5H-[1,3]oxazino[5,6-c]quinolin-5-one (2b)

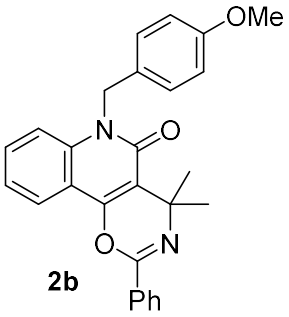

2b

white solid (m.p. 159.4-160.0 °C). ^{1}H NMR (400 MHz, $CDCl_3$): δ = 8.22 (dd, *J* = 7.8, 1.8 Hz, 2H), 8.11 (dd, *J* = 8.0, 1.3 Hz, 1H), 7.57–7.47 (m, 4H), 7.34 (d, *J* = 8.5 Hz, 1H), 7.30 (t, *J* = 7.5 Hz, 1H), 7.22 (d, *J* = 8.7 Hz, 2H), 6.89 (d, *J* = 8.7 Hz, 2H), 5.52 (bs, 2H), 3.77 (s, 3H), 1.92 (s, 6H); ^{13}C NMR (101 MHz, $CDCl_3$): δ = 160.98, 158.85, 150.37, 146.07, 138.64, 131.83, 131.24, 131.15, 128.68, 128.45, 127.96, 127.48, 122.84, 122.09, 114.86, 114.29, 113.92, 111.95, 55.26, 52.96, 45.35, 30.16. HRMS (ESI+) calcd for $C_{27}H_{25}N_2O_3$ $(M+1)^+$ *m/z* 425.1865, found *m/z* 425.1861.

6-Benzyl-4,4,9-trimethyl-2-phenyl-4,6-dihydro-5H-[1,3]oxazino[5,6-c]quinolin-5-one (2c)

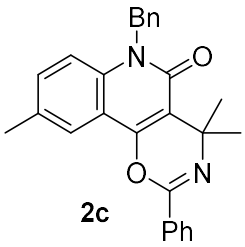

2c

white solid (m.p. 192.0-193.0 °C). ^{1}H NMR (400 MHz, $CDCl_3$): δ = 8.25–8.20 (m, 2H), 7.89 (d, *J* = 0.7 Hz, 1H), 7.60–7.51 (m, 3H), 7.37–7.17 (m, 7H), 5.58 (bs, 2H), 2.50 (s, 3H), 1.89 (s, 6H); ^{13}C NMR (101 MHz, $CDCl_3$): δ = 160.87, 150.29, 146.16, 136.75, 136.69, 132.47, 131.94, 131.74, 131.20, 128.85, 128.46, 127.48, 127.24, 126.52, 122.44, 114.85, 113.84, 111.89, 52.96, 45.85, 30.15, 21.01. HRMS (ESI+) calcd for $C_{27}H_{25}N_2O_2$ $(M+1)^+$ *m/z* 409.1916, found *m/z* 409.1916.

6-Benzyl-9-isopropyl-4,4-dimethyl-2-phenyl-4,6-dihydro-5H-[1,3]oxazino[5,6-c]quinolin-5-one (2d)

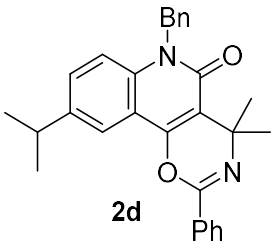

2d

white solid (m.p. 183.5-183.9 °C). ^{1}H NMR (400 MHz, $CDCl_3$): δ = 8.25–8.18 (m, 2H), 7.94 (d, *J* = 2.0 Hz, 1H), 7.61–7.52 (m, 3H), 7.40 (dd, *J* = 8.8, 2.1 Hz, 1H), 7.35 (t, *J* = 7.3 Hz, 2H), 7.31–7.24 (m, 4H), 5.59 (bs, 2H), 3.08 (hept, *J* = 6.9 Hz, 1H), 1.87 (s, 6H), 1.35 (d, *J* = 6.9 Hz, 6H); ^{13}C NMR (101 MHz, $CDCl_3$): δ = 160.94, 150.44, 146.15, 142.73, 136.96, 136.77, 131.99, 131.18, 129.86, 128.85, 128.49, 127.44, 127.24, 126.57, 119.95, 115.00, 113.77, 111.82, 52.96, 45.92, 33.66, 30.13, 24.12. HRMS (ESI+) calcd for $C_{29}H_{29}N_2O_2$ $(M+H)^+$ *m/z* 437.2229, found *m/z* 437.2233.

6-Benzyl-9-chloro-4,4-dimethyl-2-phenyl-4,6-dihydro-5H-[1,3]oxazino[5,6-c]quinolin-5-one (2e)

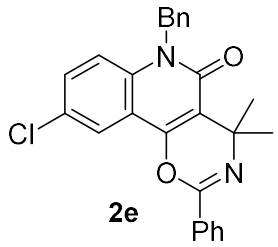

2e

white solid (m.p. 224.8-226.1 °C). ^{1}H NMR (400 MHz, $CDCl_3$): δ = 8.17 (dd, *J* = 8.0, 1.7 Hz, 2H), 8.02 (d, *J* = 2.4 Hz, 1H), 7.61–7.51 (m, 3H), 7.43 (dd, *J* = 9.0, 2.5 Hz, 1H), 7.37–7.31 (m, 2H), 7.30–7.18 (m, 4H), 5.56 (bs, 2H), 1.84 (s, 6H); ^{13}C NMR (101 MHz, $CDCl_3$): δ = 160.63, 149.50, 145.87, 137.09, 136.12, 131.47, 131.37, 131.21, 128.96, 128.52, 127.84, 127.46, 126.42, 122.28, 116.39, 115.08, 113.01, 52.97, 46.02, 29.98. HRMS (ESI+) calcd for $C_{26}H_{22}ClN_2O_2$ $(M+1)^+$ *m/z* 429.1370, found *m/z* 429.1376.

6-Benzyl-9-bromo-4,4-dimethyl-2-phenyl-4,6-dihydro-5H-[1,3]oxazino[5,6-c]quinolin-5-one (2f)

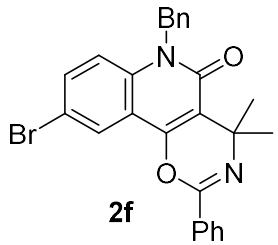

2f

white solid (m.p. 209.1-211.5 °C). ^{1}H NMR (400 MHz, $CDCl_3$): δ = 8.21–8.14 (m, 3H), 7.60–7.51 (m, 4H), 7.35 (t, *J* = 7.3 Hz, 2H), 7.28 (t, *J* = 7.2 Hz, 1H), 7.24–7.19 (m, 2H), 7.16 (d, *J* = 9.0 Hz, 1H), 5.55 (bs, 2H), 1.86 (s, 6H); ^{13}C NMR (101 MHz, $CDCl_3$): δ = 160.6, 149.4, 145.8, 137.5, 136.1, 133.9, 131.5, 131.4, 129.0, 128.5, 127.49, 127.47, 126.4, 125.3, 116.6, 115.5, 115.2, 113.0, 53.0, 46.0, 30.0. HRMS (ESI+) calcd for $C_{26}H_{22}BrN_2O_2$ $(M+1)^+$ *m/z* 473.0865, found *m/z* 473.0868.

6-Benzyl-9-fluoro-4,4-dimethyl-2-phenyl-4,6-dihydro-5H-[1,3]oxazino[5,6-c]quinolin-5-one (2g)

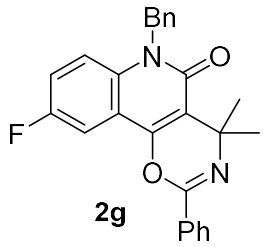

2g

white solid (m.p. 219.7-220.1 °C). ^{1}H NMR (400 MHz, $CDCl_3$): δ = 8.20–8.15 (m, 2H), 7.75 (dd, *J* = 8.6, 2.6 Hz, 1H), 7.60–7.50 (m, 3H), 7.37–7.32 (m, 2H), 7.31–7.19 (m, 5H), 5.58 (bs, 2H), 1.86 (s, 6H); ^{13}C NMR (101 MHz, $CDCl_3$): δ = 160.6, 157.9 (d, $J_{C,F}$ = 242.7 Hz), 149.7 (d, $J_{C,F}$ = 3.1 Hz), 145.8, 136.3, 135.1, 131.5, 131.3, 128.9, 128.5, 127.4, 126.4, 119.0 (d, $J_{C,F}$ = 24.0 Hz), 116.6 (d, $J_{C,F}$ = 8.0 Hz), 114.9 (d, $J_{C,F}$ = 8.5 Hz), 113.1, 108.4 (d, $J_{C,F}$ = 24.3 Hz), 53.0, 46.1, 30.0. HRMS (ESI+) calcd for $C_{26}H_{22}FN_2O_2$ $(M+1)^+$ *m/z* 413.1665, found *m/z* 413.1661.

Methyl6-benzyl-4,4-dimethyl-5-oxo-2-phenyl-5,6-dihydro-4H-[1,3]oxazino[5,6-c]quinoline-9-carboxylate (2h)

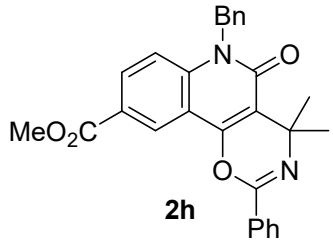

2h

white solid (m.p. 258.1-259.9 °C). ^{1}H NMR (400 MHz, $CDCl_3$): δ = 8.78 (d, *J* = 2.0 Hz, 1H), 8.23–8.18 (m, 2H), 8.12 (dd, *J* = 8.9, 2.0 Hz, 1H), 7.61–7.51 (m, 3H), 7.37–7.25 (m, 4H), 7.23 (d, *J* = 7.1 Hz, 2H), 5.60 (bs, 2H), 3.99 (s, 3H), 1.84 (s, 6H); ^{13}C NMR (101 MHz, $CDCl_3$): δ = 166.20, 161.03, 150.49, 145.91, 141.45, 136.01, 131.76, 131.50, 131.34, 128.97, 128.53, 127.51 (2C), 126.46, 125.21, 123.88, 114.87, 113.68, 112.64, 52.86, 52.42, 46.13, 29.99. HRMS (ESI+) calcd for $C_{28}H_{25}N_2O_4$ $(M+1)^+$ *m/z* 453.1814, found *m/z* 453.1812.

6-Benzyl-4,4-dimethyl-2-phenyl-9-(trifluoromethyl)-4,6-dihydro-5H-[1,3]oxazino[5,6-c]quinolin-5-one (2i)

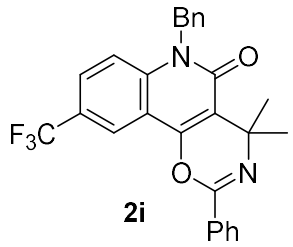

2i

white solid (m.p. 222.1-224.2 °C). ^{1}H NMR (400 MHz, $CDCl_3$): δ = 8.35 (d, *J* = 1.2 Hz, 1H), 8.19 (dd, *J* = 7.8, 1.8 Hz, 2H), 7.72 (dd, *J* = 8.9, 1.9 Hz, 1H), 7.62–7.52 (m, 3H), 7.43–7.34 (m, 3H), 7.33–7.27 (m, 1H), 7.24 (d, *J* = 7.2 Hz, 2H), 5.61 (bs, 2H), 1.87 (s, 6H); ^{13}C NMR (101 MHz, $CDCl_3$): δ = 160.9, 150.1, 145.7, 140.5, 135.9, 131.43, 131.41, 129.0, 128.6, 127.6, 127.48 (q, $J_{C,F}$ = 3.5 Hz), 127.43, 126.4, 124.34 (q, $J_{C,F}$ = 33.4 Hz), 123.96 (q, $J_{C,F}$ = 271.7 Hz), 120.54 (q, $J_{C,F}$ = 4.1 Hz), 115.4, 113.8, 113.3, 52.9, 46.1, 30.0. HRMS (ESI+) calcd for $C_{27}H_{22}F_3N_2O_2$ $(M+1)^+$ *m/z* 463.1633, found *m/z* 463.1634.

6-Benzyl-4,4,7,9-tetramethyl-2-phenyl-4,6-dihydro-5H-[1,3]oxazino[5,6-c]quinolin-5-one (2j)

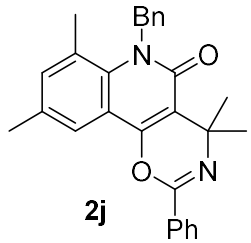

2j

white solid (m.p. 188.2-189.5 °C). ^{1}H NMR (400 MHz, $CDCl_3$): δ = 8.24–8.19 (m, 2H), 7.84 (s, 1H), 7.60–7.50 (m, 3H), 7.34 (t, *J* = 7.3 Hz, 2H), 7.25 (t, *J* = 7.3 Hz, 1H), 7.20 (s, 1H), 7.11 (d, *J* = 7.6 Hz, 2H), 5.70 (bs, 2H), 2.56 (s, 3H), 2.48 (s, 3H), 1.83 (s, 6H); ^{13}C NMR (101 MHz, $CDCl_3$): δ = 162.5, 150.6, 146.4, 138.8, 138.0, 137.7, 132.0, 131.8, 131.2, 128.7, 128.5, 127.5, 126.7, 125.4, 124.4, 121.0, 115.7, 111.4, 52.9, 49.9, 30.0, 24.1, 20.8. HRMS (ESI+) calcd for $C_{28}H_{27}N_2O_2$ $(M+1)^+$ *m/z* 423.2073, found *m/z* 423.2077.

6-Benzyl-7-bromo-9-ethyl-4,4-dimethyl-2-phenyl-4,6-dihydro-5H-[1,3]oxazino[5,6-c]quinolin-5-one (2k)

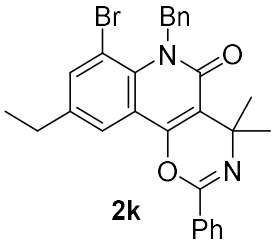

2k

pale yellow solid (m.p. 185.6-186.1 °C). ^{1}H NMR (400 MHz, $CDCl_3$): δ = 8.16 (dd, *J* = 7.9, 1.6 Hz, 2H), 7.91 (d, *J* = 2.0 Hz, 1H), 7.70 (d, *J* = 2.1 Hz, 1H), 7.61–7.51 (m, 3H), 7.33–7.27 (m, 2H), 7.22 (t, *J* = 7.3 Hz, 1H), 7.11 (d, *J* = 7.3 Hz, 2H), 6.00 (s, 2H), 2.77 (q, *J* = 7.6 Hz, 2H), 1.77 (s, 6H), 1.34 (t, *J* = 7.6 Hz, 3H); ^{13}C NMR (101 MHz, $CDCl_3$): δ = 162.34, 149.69, 146.14, 139.47, 138.75, 138.61, 136.43, 131.71, 131.29, 128.49, 128.30, 127.43, 126.52, 126.00, 121.34, 117.51, 112.52, 107.61, 52.90, 49.58, 29.87, 27.73, 15.34. HRMS (ESI+) calcd for $C_{28}H_{26}BrN_2O_2$ $(M+1)^+$ *m/z* 501.1178, found *m/z* 501.1171.

6-Benzyl-8-chloro-4,4-dimethyl-2-phenyl-4,6-dihydro-5H-[1,3]oxazino[5,6-c]quinolin-5-one (2l)

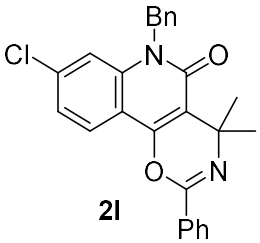

2l

pale yellow solid (m.p. 245.1-247.0 °C). ^{1}H NMR (400 MHz, $CDCl_3$): δ = 8.18–8.13 (m, 2H), 8.01 (d, J = 8.5 Hz, 1H), 7.59–7.49 (m, 3H), 7.40–7.22 (m, 7H), 5.53 (bs, 2H), 1.83 (s, 6H); ^{13}C NMR (101 MHz, $CDCl_3$): δ = 160.88, 150.12, 145.81, 139.45, 137.33, 135.98, 131.63, 131.27, 128.98, 128.44, 127.50, 127.42, 126.52, 124.12, 122.58, 114.75, 112.47, 112.13, 52.87, 46.03, 29.97. HRMS (ESI+) calcd for $C_{26}H_{22}ClN_2O_2$ $(M+1)^+$ *m/z* 429.1370, found *m/z* 429.1367.

6'-Benzyl-2'-phenylspiro[cyclohexane-1,4'-[1,3]oxazino[5,6-c]quinolin]-5'(6'H)-one (2m)

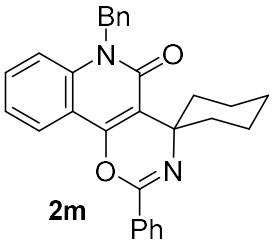

2m

pale yellow solid (m.p. 198.1-200.0 °C). ^{1}H NMR (400 MHz, $CDCl_3$): δ = 8.24 (d, J = 7.9 Hz, 2H), 8.13 (d, J = 8.1 Hz, 1H), 7.56–7.47 (m, 4H), 7.35–7.22 (m, 7H), 5.58 (bs, 2H), 2.94 (td, *J* = 13.2, 3.8 Hz, 2H), 2.25–2.13 (m, 2H), 1.85 (d, *J* = 13.1 Hz, 1H), 1.73 (d, *J* = 12.9 Hz, 2H), 1.65–1.56 (m, 3H); ^{13}C NMR (101 MHz, $CDCl_3$): δ = 161.08, 151.34, 143.99, 138.79, 136.62, 132.14, 131.05, 128.82, 128.72, 128.35, 127.45, 127.21, 126.47, 122.85, 122.03, 114.75, 114.10, 111.68, 55.29, 45.94, 36.45, 25.77, 20.84. HRMS (ESI+) calcd for $C_{29}H_{27}N_2O_2$ $(M+1)^+$ *m/z* 435.2073, found *m/z* 435.2074.

6-Benzyl-2-phenyl-4,6-dihydro-5H-[1,3]oxazino[5,6-c]quinolin-5-one (2n)

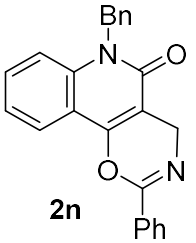

2n

pale yellow solid (m.p. 209.0-210.5 °C). ^{1}H NMR (400 MHz, $CDCl_3$): δ = 8.18–8.12 (m, 2H), 8.05 (dd, *J* = 7.9, 1.4 Hz, 1H), 7.59–7.48 (m, 4H), 7.35–7.22 (m, 7H), 5.56 (bs, 2H), 4.76 (s, 2H); ^{13}C NMR (101 MHz, $CDCl_3$): δ = 161.21, 152.04, 150.12, 138.68, 136.41, 131.59, 131.30, 128.98, 128.93, 128.55, 127.51, 127.45, 126.69, 122.41, 122.18, 115.29, 114.11, 104.17, 45.92, 41.99. HRMS (ESI+) calcd for $C_{24}H_{19}N_2O_2$ $(M+1)^+$ *m/z* 367.1447, found *m/z* 367.1452.

6-Benzyl-2-(4-chlorophenyl)-4,4-dimethyl-4,6-dihydro-5H-[1,3]oxazino[5,6-c]quinolin-5-one (2o)

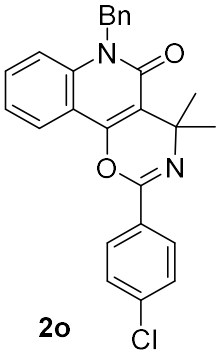

2o

white solid (m.p. 195.6-197.3 °C). ^{1}H NMR (400 MHz, $CDCl_3$): δ = 8.15–8.10 (m, 2H), 8.07 (dd, *J* = 8.1, 1.4 Hz, 1H), 7.54–7.47 (m, 3H), 7.37–7.20 (m, 7H), 5.59 (bs, 2H), 1.84 (s, 6H); ^{13}C NMR (101 MHz, $CDCl_3$): δ = 160.91, 150.24, 145.31, 138.62, 137.40, 136.50, 131.25, 130.28, 128.87, 128.82, 128.69, 127.30, 126.49, 122.73, 122.16, 114.91, 113.79, 111.91, 53.03, 45.91, 30.02. HRMS (ESI+) calcd for $C_{26}H_{22}ClN_2O_2$ $(M+1)^+$ *m/z* 429.9240, found *m/z* 429.9243.

6-Benzyl-2-(4-fluorophenyl)-4,4-dimethyl-4,6-dihydro-5H-[1,3]oxazino[5,6-c]quinolin-5-one (2p)

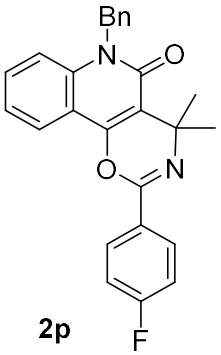

2p

pale yellow solid (m.p. 225.7-226.8 °C). ^{1}H NMR (400 MHz, $CDCl_3$): δ = 8.24–8.15 (m, 2H), 8.08 (dd, *J* = 8.2, 1.4 Hz, 1H), 7.55–7.47 (m, 1H), 7.38–7.16 (m, 9H), 5.59 (bs, 2H), 1.84 (s, 6H); ^{13}C NMR (101 MHz, $CDCl_3$): δ = 164.70 (d, $J_{C,F}$ = 251.4 Hz), 160.94, 150.29, 145.25, 138.62, 136.52, 131.21, 129.66 (d, $J_{C,F}$ = 8.8 Hz), 128.86, 127.97 (d, $J_{C,F}$ = 3.0 Hz), 127.29, 126.49, 122.73, 122.13, 115.49 (d, $J_{C,F}$ = 21.9 Hz), 114.90, 113.84, 111.95, 52.93, 45.90, 30.03. HRMS (ESI+) calcd for $C_{26}H_{22}FN_2O_2$ $(M+1)^+$ *m/z* 413.1665, found *m/z* 413.1665.

6-Benzyl-4,4-dimethyl-2-(4-nitrophenyl)-4,6-dihydro-5H-[1,3]oxazino[5,6-c]quinolin-5-one (2q)

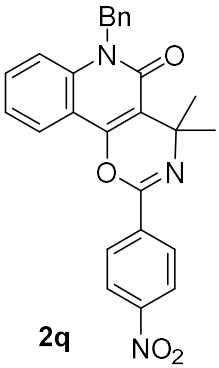

2q

yellow solid (m.p. 204.2-206.4 °C). ^{1}H NMR (400 MHz, $CDCl_3$): δ = 8.44–8.31 (m, 4H), 8.08 (dd, *J* = 8.2, 1.4 Hz, 1H), 7.56–7.50 (m, 1H), 7.37–7.30 (m, 4H), 7.29–7.22 (m, 3H), 5.59 (bs, 2H), 1.87 (s, 6H); ^{13}C NMR (101 MHz, $CDCl_3$): δ = 160.7, 150.0, 149.5, 144.7, 138.7, 137.5, 136.4, 131.5, 128.9, 128.5, 127.3, 126.5, 123.6, 122.6, 122.3, 115.0, 113.5, 111.8, 53.5, 46.0, 30.0. HRMS (ESI+) calcd for $C_{26}H_{22}N_3O_4$ $(M+1)^+$ *m/z* 440.1610, found *m/z* 440.1612.

6-Benzyl-2-methyl-4,6-dihydro-5H-[1,3]oxazino[5,6-c]quinolin-5-one (2r)

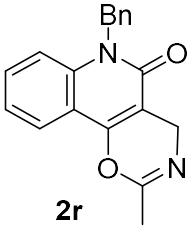

2r

white solid (m.p. 255.2-257.0 °C). ^{1}H NMR (400 MHz, $CDCl_3$): δ = 7.98–7.94 (m, 1H), 7.48–7.42 (m, 1H), 7.41–7.31 (m, 5H), 7.22–7.17 (m, 2H), 5.34 (s, 2H), 4.57 (s, 2H), 2.65 (s, 3H); ^{13}C NMR (101 MHz, $CDCl_3$): δ = 171.1, 163.8, 153.0, 142.0, 134.6, 129.3, 128.7, 127.3, 123.9, 122.6, 122.2, 120.7, 111.4, 110.8, 49.0, 43.6, 24.3. HRMS (ESI+) calcd for $C_{19}H_{17}N_2O_2$ $(M+1)^+$ *m/z* 305.1290, found *m/z* 305.1286.

6-Benzyl-2-(benzylamino)-4,4-dimethyl-4,6-dihydro-5H-[1,3]oxazino[5,6-c]quinolin-5-one (2*s*)

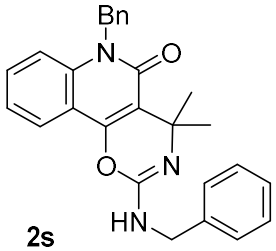

2s

pale yellow solid (m.p. 144.2-146.0 °C). ^{1}H NMR (400 MHz, $CDCl_3$): δ = 7.84 (dd, *J* = 8.0, 1.3 Hz, 1H), 7.49–7.36 (m, 5H), 7.36–7.15 (m, 8H), 5.56 (bs, 2H), 4.54 (s, 2H), 4.26 (s, 1H), 1.78 (s, 6H); ^{13}C NMR (101 MHz, $CDCl_3$): δ =161.0, 150.5, 143.2, 139.1, 138.5, 136.7, 130.9, 128.8, 128.6, 127.9, 127.4, 127.2, 126.5, 122.6, 121.9, 114.7, 113.8, 113.5, 52.5, 45.9, 45.8, 30.7. HRMS (ESI+) calcd for $C_{27}H_{26}N_3O_2$ $(M+1)^+$ *m/z* 424.2025, found *m/z* 424.2028.

5,14-Dibenzyl-7,7,16,16-tetramethyl-5H,14H-benzopyrido[3'',4'':5',6']pyrimido[2',1':2,3][1,3]oxazino[5,6-c]quinoline-6,15-dione (3a)

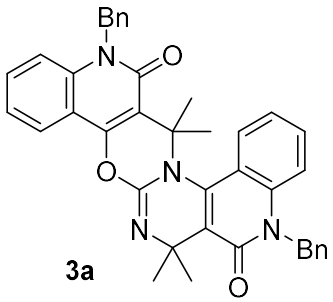

3a

pink solid (m.p. 213.8-213.5 °C). ^{1}H NMR (400 MHz, $CDCl_3$): δ = 8.24 (dd, *J* = 8.0, 1.2 Hz, 1H), 7.85 (dd, *J* = 8.0, 1.0 Hz, 1H), 7.51 (further split t, *J* = 7.6 Hz, 1H), 7.41–7.16 (m, 14H), 7.07 (t, *J* = 7.4 Hz, 1H), 5.75 (d, *J* = 16.1 Hz, 1H), 5.67–5.47 (m, 2H), 5.40 (d, *J* = 16.1 Hz, 1H), 1.98 (s, 3H), 1.85 (s, 3H), 1.83 (s, 3H), 1.76 (s, 2H); ^{13}C NMR (101 MHz, $CDCl_3$): δ = 160.51, 160.00, 153.39, 148.67, 141.63, 138.94, 138.03, 136.38 (2C), 131.87, 130.27, 129.63, 128.92 (2C), 127.38, 127.32, 126.80, 126.50, 126.45, 123.76, 122.38, 120.79, 119.43, 114.83, 114.73, 114.20, 114.03, 64.59, 57.50, 46.27, 46.11, 31.60, 28.77, 28.12, 26.96. HRMS (ESI+) calcd for $C_{39}H_{34}N_4O_3$ $(M+1)^+$ *m/z* 607.2709, found *m/z* 607.2711.

5,14-Di-4-methoxybenzyl-7,7,16,16-tetramethyl-5H,14H-benzopyrido[3'',4'':5',6']pyrimido[2',1':2,3][1,3]oxazino[5,6-c]quinoline-6,15-dione (3b)

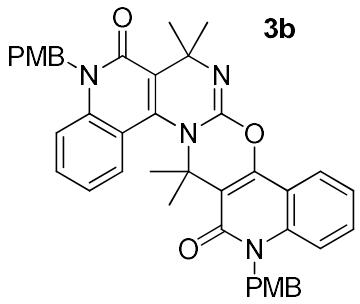

white solid (m.p. 158.9-160.5 °C). ^{1}H NMR (400 MHz, $CDCl_3$): δ = 8.20 (dd, *J* = 8.1, 1.4 Hz, 1H), 7.79 (dd, *J* = 8.1, 1.3 Hz, 1H), 7.52 (ddd, *J* = 8.6, 7.2, 1.5 Hz, 1H), 7.34 (d, *J* = 8.5 Hz, 2H), 7.26 (d, *J* = 8.2 Hz, 2H), 7.21–7.13 (m, 4H), 7.05 (further split t, *J* = 8.3 Hz, 1H), 6.89–6.83 (m, 4H), 5.74–5.22 (m, 4H), 3.77 (s, 3H), 3.76 (s, 3H), 1.93 (s, 3H), 1.80 (s, 3H), 1.77 (s, 3H), 1.71 (s, 3H); ^{13}C NMR (101 MHz, $CDCl_3$): δ = 160.51, 160.00, 158.86, 158.82, 153.31, 148.69, 141.52, 138.93, 138.03, 131.78, 130.18, 129.65, 128.41, 127.88, 127.83, 126.76, 123.75, 122.31, 120.70, 119.43, 114.78, 114.68, 114.30 (2C), 114.23, 114.13, 114.03, 64.54, 57.48, 55.28 (2C), 45.71, 45.58, 31.54, 28.73, 28.08, 26.91. HRMS (ESI+) calcd for $C_{41}H_{38}N_4O_5$ $(M+1)^+$ *m/z* 667.2920, found *m/z* 667.2922.

5,14-Dibenzyl-2,11-diisopropyl-7,7,16,16-tetramethyl-5H,14H-benzopyrido[3'',4'':5',6']pyrimido[2',1':2,3][1,3]oxazino[5,6-c]quinoline-6,15-dione (3c)

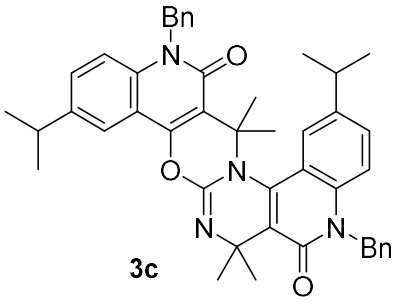

3c

white solid (m.p. 178.5-180.0 °C). ^{1}H NMR (400 MHz, $CDCl_3$): δ = 8.10 (s, 1H), 7.62 (s, 1H), 7.43 (d, *J* = 8.7 Hz, 1H), 7.38–7.32 (m, 4H), 7.31–7.22 (m, 8H), 7.19 (d, *J* = 8.7 Hz, 1H), 5.76–5.65 (m, 2H), 5.48–5.35 (m, 2H), 3.02 (hept, *J* = 6.9 Hz, 1H), 2.88 (hept, *J* = 6.8 Hz, 1H), 1.98 (s, 3H), 1.85 (s, 3H), 1.82 (s, 3H), 1.76 (s, 3H), 1.30 (d, *J* = 6.9 Hz, 6H), 1.20 (t, *J* = 7.9 Hz, 6H); ^{13}C NMR (101 MHz, $CDCl_3$): δ = 160.46, 159.84, 153.51, 148.92, 143.25, 141.65, 140.90, 137.25, 136.58, 136.33, 130.62, 129.42, 129.11, 128.89, 127.34, 127.28, 126.53, 126.47, 124.05, 121.01, 119.17, 114.90, 114.71, 114.24, 114.02, 64.38, 57.53, 46.27, 45.94, 33.77, 33.38, 31.58, 28.84, 28.16, 27.01, 24.07, 23.50. HRMS (ESI+) calcd for $C_{45}H_{46}N_4O_3$ $(M+1)^+$ *m/z* 691.3648, found *m/z* 691.3651.

5,14-Dibenzyl-2,11-dibromo-7,7,16,16-tetramethyl-5H,14H-benzopyrido[3'',4'':5',6']pyrimido[2',1':2,3][1,3]oxazino[5,6-c]quinoline-6,15-dione (3d)

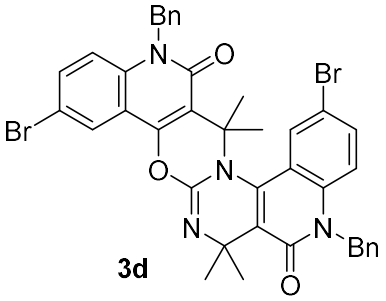

3d

white solid (m.p. 96.8-98.2 °C). ^{1}H NMR (400 MHz, $CDCl_3$): δ = 8.38 (d, *J* = 2.3 Hz, 1H), 7.91 (d, *J* = 2.3 Hz, 1H), 7.60 (dd, *J* = 9.0, 2.3 Hz, 1H), 7.44 (dd, *J* = 9.0, 2.3 Hz, 1H), 7.39–7.33 (m, 4H), 7.32–7.25 (m, 2H), 7.25–7.17 (m, 5H), 7.12 (d, *J* = 9.0 Hz,

1H), 5.73 (d, *J* = 16.2 Hz, 1H), 5.64–5.50 (m, 2H), 5.34 (d, *J* = 16.0 Hz, 1H), 1.94 (s, 3H), 1.81 (s, 3H), 1.80 (s, 3H), 1.74 (s, 3H); ^{13}C NMR (101 MHz, $CDCl_3$): δ = 160.10, 159.61, 152.17, 148.05, 140.43, 137.76, 136.90, 135.87, 135.84, 134.71, 133.01, 131.01, 129.03 (2C), 128.87, 127.58, 127.55, 126.39, 126.36, 126.19, 120.95, 116.55, 116.51, 115.59, 115.42, 114.78, 114.04, 65.09, 57.66, 46.40, 46.15, 31.51, 28.52, 27.82, 26.89. HRMS (ESI+) calcd for $C_{39}H_{32}Br_2N_4O_3$ $(M+1)^+$ *m/z* 763.0919, found *m/z* 763.0917.

5,14-Dibenzyl-2,11-difluoro-7,7,16,16-tetramethyl-5H,14H-benzopyrido[3'',4'':5',6']pyrimido[2',1':2,3][1,3]oxazino[5,6-c]quinoline-6,15-dione (3e)

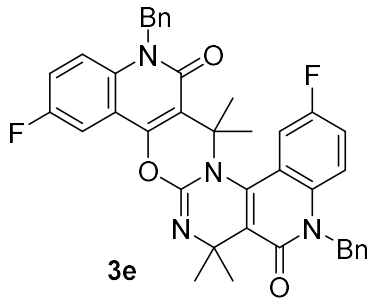

3e

white solid (m.p. 230.5-232.0 °C). ^{1}H NMR (400 MHz, $CDCl_3$): δ = 7.90 (dd, *J* = 8.7, 2.5 Hz, 1H), 7.51 (dd, *J* = 9.3, 2.9 Hz, 1H), 7.40–7.32 (m, 4H), 7.31–7.18 (m, 9H), 7.13–7.06 (m, 1H), 5.75 (d, *J* = 16.1 Hz, 1H), 5.61 (d, *J* = 16.3 Hz, 1H), 5.52 (d, *J* = 15.8 Hz, 1H), 5.36 (d, *J* = 16.1 Hz, 1H), 1.96 (s, 3H), 1.83 (s, 2H), 1.82 (s, 3H), 1.75 (s, 3H); ^{13}C NMR (101 MHz, $CDCl_3$): δ = 160.15, 159.62, 158.00 (d, $J_{C,F}$ = 243.5 Hz), 156.94 (d, $J_{C,F}$ = 241.8 Hz), 152.48 (d, $J_{C,F}$ = 3.1 Hz), 148.22, 140.74 (d, $J_{C,F}$ = 2.8 Hz), 136.04, 135.46, 134.55, 131.24, 129.01, 127.51 (d, $J_{C,F}$ = 4.2 Hz), 126.38 (d, $J_{C,F}$ = 5.0 Hz), 120.68 (d, $J_{C,F}$ = 8.2 Hz), 119.91 (d, $J_{C,F}$ = 24.0 Hz), 118.08 (d, $J_{C,F}$ = 23.8 Hz), 116.68 (d, $J_{C,F}$ = 7.9 Hz), 116.46 (d, $J_{C,F}$ = 7.9 Hz), 115.0, 114.96 (d, $J_{C,F}$ = 9.3 Hz), 112.21 (d, $J_{C,F}$ = 24.9 Hz), 109.24 (d, $J_{C,F}$ = 24.8 Hz), 64.98, 57.72, 46.54, 46.37, 31.50, 28.58, 27.83, 26.70. HRMS (ESI+) calcd for $C_{39}H_{32}F_2N_4O_3$ $(M+1)^+$ *m/z* 643.2521, found *m/z* 643.2524.

4.5 References

[1] *Jin-Bao Peng, Hui-king Geng and Xiao-Feng Wu Chem volume 5, issue 3, 14 march 2019, pages 526-552*

[2] *Mariano MartínMartín Industrial Chemical Process Analysis and Design 2016, Pages 199-297*

[3] *J.-B.Peng, F.-P. Wu, X.-F. Wu, Chem. Rev.* ***2018****, DOI 10.1021/acs.chemrev.8b00068.*

[4] *Shen, X.-F. Wu, Chem. Eur. J.* ***2017****, 23, 2973–2987.*

[5] *R. C. Carmona, O. D. Köster, C. R. D. Correia, Angew. Chem. Int. Ed.* ***2018****, 57, 12067–12070; R. Mancuso, I. Ziccarelli, A. Chimento, N. Marino, N. Della Ca', R. Sirianni, V. Pezzi, B. Gabriele, iScience* ***2018****, 3, 279–288*

[6] *C. Zhu, B. Yang, J.-E. Bäckvall, J. Am. Chem. Soc.* ***2015****, 137, 11868–11871.*

[7] *C. Zhu, B. Yang, Y. Qiu, J.-E. Bäckvall, Angew. Chem. Int. Ed.* ***2016****, 55, 14405–14408.*

[8] *D. Ding, G. Zhu, X. Jiang, Angew. Chem. Int. Ed.* ***2018****, 57, 9028–9032.*

[9] *J.-B. Peng, X.-F. Wu, Angew. Chem. Int. Ed.* ***2018****, 57, 1152–1160*

[10] *A. Acerbi, C. Carfagna, M. Costa, R. Mancuso, B. Gabriele, N. Della Ca', Chem. Eur. J.* ***2018****, 24, 4835–4840*

[11] *B. Gabriele, R. Mancuso, G. Salerno, Eur. J. Org. Chem.* ***2012****, 6825–6839*

[12] *I. V. Alabugin, K. Gilmore, Chem. Commun.* ***2013****, 49, 11246–11250.*

[13] *V. H. L. Wong, S. V. C. Vummaleti, L. Cavallo, A. J. P. White ,S. P. Nolan, K. K. M.Hii, Chem. Eur. J.* ***2016****, 22, 13320–13327*

[14] *A.Urbanaite, M. Jonusis, R.Buksnaitiene, S. Balkaitis, I. Cikotiene, Eur. J. Org. Chem.* ***2015****, 7091–7113*

[15] *S. Cacchi, G. Fabrizi, Chem. Rev.* ***2005****, 105, 2873–2920; b) B. Gabriele, L. Veltri, G. Salerno, R. Mancuso, M. Costa, Adv. Synth. Catal.* ***2010****, 352, 3355–3363.*

[16] *S. Cacchi, G. Fabrizi, Chem. Rev.* ***2005****, 105, 2873–2920*

[17] *M. Costa, N. Della Ca', B. Gabriele, C. Massera, G. Salerno, M. Soliani, J. Org. Chem.* ***2004****, 69, 2469–2477.*

[18] *N. Della Ca', P. Bottarelli, A. Dibenedetto, M. Aresta, B. Gabriele, G. Salerno, M. Costa, J. Catal.* ***2011****, 282, 120–127*

[19] *M. Jiang, J. Li, F. Wang, Y. Zhao, F. Zhao, X. Dong, W. Zhao, Org. Lett.* ***2012****, 14, 1420–1423.*